

UNIVERSITÉ DU QUÉBEC À MONTRÉAL

CLINICAL VALIDATION OF [18F]-FLUOROETHOXYBENZOVESAMICOL USED WITH POSITRON  
EMISSION TOMOGRAPHY IMAGING FOR THE DETECTION AND QUANTIFICATION OF  
ALZHEIMER'S DISEASE ON THE BASIS OF CORTICAL CHOLINERGIC DENERVATION

THESIS

PRESENTED

IN PARTIAL FULFILLMENT OF REQUIREMENT

DOCTOR OF PSYCHOLOGY

BY

MEGHMIK AGHOURIAN-NAMAGERDY

DECEMBER 2022

UNIVERSITÉ DU QUÉBEC À MONTRÉAL

VALIDATION CLINIQUE DU [18F]-FLUOROETHOXYBENZOVESAMICOL UTILISÉ AVEC L'IMAGERIE  
CÉRÉBRALE PAR TOMOGRAPHIE D'ÉMISSION DE POSITONS POUR DÉTECTER ET QUANTIFIER LA  
MALADIE D'ALZHEIMER À PARTIR DE LA DÉNERVATION CHOLINERGIQUE

THÈSE

PRÉSENTÉE

COMME EXIGENCE PARTIELLE

DOCTORAT EN PSYCHOLOGIE

PAR

MEGHMIK AGHOURIAN-NAMAGERDY

DÉCEMBRE 2022

UNIVERSITÉ DU QUÉBEC À MONTRÉAL  
Service des bibliothèques

Avertissement

La diffusion de cette thèse se fait dans le respect des droits de son auteur, qui a signé le formulaire *Autorisation de reproduire et de diffuser un travail de recherche de cycles supérieurs* (SDU-522 – Rév.04-2020). Cette autorisation stipule que «conformément à l'article 11 du Règlement no 8 des études de cycles supérieurs, [l'auteur] concède à l'Université du Québec à Montréal une licence non exclusive d'utilisation et de publication de la totalité ou d'une partie importante de [son] travail de recherche pour des fins pédagogiques et non commerciales. Plus précisément, [l'auteur] autorise l'Université du Québec à Montréal à reproduire, diffuser, prêter, distribuer ou vendre des copies de [son] travail de recherche à des fins non commerciales sur quelque support que ce soit, y compris l'Internet. Cette licence et cette autorisation n'entraînent pas une renonciation de [la] part [de l'auteur] à [ses] droits moraux ni à [ses] droits de propriété intellectuelle. Sauf entente contraire, [l'auteur] conserve la liberté de diffuser et de commercialiser ou non ce travail dont [il] possède un exemplaire.»

## ACKNOWLEDGMENT

Who knew this day would finally come! This journey has thought me a great deal about myself as a person and as a scientist. I could have never overcome to the challenges without the help and moral support of everyone around me. I would like to extend my gratitude and appreciation to everyone who has been a part of my journey: Everyone at UQÀM, the McConnell Brain Imaging Centre, the McGill Centre for Studies in Aging, and especially those in my personal life.

I would like to express my gratitude to my supervisor Dr. Marc-André Bédard. Thank you for giving me a chance to work at your lab and to take part in the realization of your research objectives. I appreciate the support and guidance over the years, and I am grateful for everything you have done for me.

I would like to thank my lab members (present and past) Camille, Étienne, Rebekah, Maxime, Marilyn, and Guillaume for their contribution and support. Each one of you has taught me something about being a scientist. I would specially like to thank Camille for all her help regarding patient recruitment and PET data analysis. We made a great team, and I could have not done it without you.

I would also like to acknowledge all the precious support and technical experience that I acquired from Dr. Pedro Rosa-Neto and his lab. I would specially like to thank Peter, Sulantha, Tharick, and Andréa. Without your help I could not have published my first article.

Of course, none of this would have been possible without my family (including Brucie and Gypsie), Samuel and friends outside of the laboratory. Everyone who has come in my life, especially during my years as a graduate student, has shaped me in a way. Special shout out to Alexandra, Catherine, Taline, Raluca, Marie as well as to the many CSP friendships that I hold very dear. You came in my life for a reason. Each of you have taught me something and have helped me evolve and become the person that I am today. I thank you all for the encouraging words, for believing in me, and for being patient with me.

Lastly, I would also like to thank my committee members Dr. Christian Bocti, Dr. Marc Lussier and Dr. François Richer for their time and effort in reviewing my dissertation and their precious contribution.

## DEDICATION

I would like to dedicate this work to my family, mom, dad, Meghedi, and Maral, and to the memory of my grandparents, Siran, Marthan, Hagop and Vartan.

Dedicated to the 5000+ Armenian soldiers who in 2020 and 2022, at the prime age of 18 to 20, lost their lives protecting their motherland.

In memory of my late grandparents. Although they left us too early, they are forever in our hearts.

To my family, for their continuous support of my personal and academic endeavors.

To my friends and colleagues, for their consistent encouragement throughout the last 8 years.

## TABLE OF CONTENTS

ACKNOWLEDGMENT .....	iii
DEDICATION .....	iv
LIST OF FIGURES .....	viii
LIST OF TABLES.....	ix
LIST OF ABBREVIATIONS AND ACRONYMS.....	x
LIST OF SYMBOLS AND UNITS .....	xiv
RÉSUMÉ.....	xv
ABSTRACT.....	xvii
CHAPITRE 1 LITERATURE REVIEW AND BACKGROUND.....	19
1.1 Epidemiology and clinical presentation of Alzheimer’s Disease (AD).....	19
1.2 Neuropathology of AD .....	21
1.2.1 Tau, amyloid, and neurodegeneration in AD.....	21
1.2.2 Cholinergic dysfunction in AD.....	23
1.3 The Basal Forebrain Cholinergic System .....	25
1.3.1 The cholinergic systems of the brain .....	25
1.3.2 Nucleus basalis of Meynert and its cortical projections .....	26
1.3.3 Neuronal vulnerability of nucleus basalis of Meynert and their fate in AD.....	28
1.4 The basal forebrain cholinergic system and cognitive functioning.....	29
1.5 The current biomarkers of AD .....	31
1.6 The in vivo quantification of brain cholinergic denervation in AD.....	36
1.6.1 PET neuroimaging.....	36
1.6.2 Cholinergic PET biomarkers .....	37
1.6.3 [ <sup>18</sup> F]-FE0BV as a reliable cholinergic PET radioligand.....	39
CHAPITRE 2 RESEARCH QUESTION, OBJECTIVES AND RATIONALE .....	42
2.1 General question and aim.....	42
2.2 Study 1 .....	42
2.2.1 Study 1 - Objectives: .....	43
2.2.2 Study 1- Hypotheses: .....	43
2.3 Study 2 .....	44
2.3.1 Study 2 - Objectives: .....	44
2.3.2 Study 2 - Hypotheses: .....	44

2.4	Rationale for the methods used .....	45
2.4.1	PET neuroimaging.....	45
2.4.2	MRI .....	46
2.4.3	Cognitive measures .....	46
CHAPITRE 3 STUDY 1 - QUANTIFICATION OF BRAIN CHOLINERGIC DENERVATION IN ALZHEIMER'S DISEASE USING PET IMAGING WITH [ <sup>18</sup> F]-FEOBV .....		47
3.1	Introduction.....	50
3.2	Method .....	51
3.2.1	Subjects.....	51
3.2.2	Imaging data acquisition.....	52
3.2.3	Image processing and analyses.....	53
3.3	Results.....	54
3.3.1	PET imaging in AD and control subjects.....	54
3.3.2	FEOBV correlations with FDG and NAV .....	58
3.3.3	Correlations between FEOBV and cognitive scales.....	59
3.4	Discussion .....	59
3.4.1	FEOBV and the cholinergic systems in AD .....	59
3.4.2	FEOBV amongst AD biomarkers.....	61
3.5	Author contributions .....	64
3.6	References .....	65
3.7	Conclusion of the first study and the conception of the subsequent study .....	70
CHAPITRE 4 STUDY 2 – FEOBV-PET TO QUANTIFY CORTICAL CHOLINERGIC DENERVATION IN AD : RELATIONSHIP TO BASAL FOREBRAIN VOLUMETRY .....		71
4.1	Introduction.....	74
4.2	Method .....	74
4.2.1	Participants.....	74
4.2.2	PET and MRI data processing.....	75
4.2.3	Statistical analyses.....	76
4.3	Results.....	76
4.3.1	Between groups differences of [ <sup>18</sup> F]-FEOBV uptake and ChBF volumes .....	77
4.3.2	Correlations between [ <sup>18</sup> F]-FEOBV uptake and ChBF volumes.....	78
4.4	Discussion .....	79
4.5	Author contribution .....	81
4.6	References .....	82
4.7	Conclusion of the second study .....	84
CHAPITRE 5 GENERAL DISCUSSION AND CONCLUSION .....		85
5.1	Recapitulation of the two studies.....	85

5.2 Reliability of the current findings.....	86
5.2.1 The representativeness of the current results .....	86
5.2.2 Potential nonspecific FEOBV binding.....	88
5.3 Implications of the current findings.....	89
5.3.1 Using PET-FEOBV as a tool for differential diagnosis of AD.....	89
5.3.2 Using PET-FEOBV as an AD biomarker .....	91
5.3.3 FEOBV and cognition .....	93
5.4 Conclusion.....	95
APPENDIX A ETHICS CERTIFICATE-UQÀM .....	96
APPENDIX B ETHICS CERTIFICATE- MCGILL UNIVERSITY .....	99
APPENDIX C CONSENT FORM.....	103
APPENDIX D REPRINT OF ARTICLE BY TAYLOR SCHMITZ AND COLLEAGUES 2018.....	110
REFERENCES .....	121



## LIST OF FIGURES

Figure 1.1 Cortical cholinergic neurotransmission.....	24
Figure 1.2 Basal forebrain cholinergic systems.....	26
Figure 1.3 NBM/Ch4 subdivisions with corresponding cortical topographic projections.....	27
Figure 3.1 FEOBV SUVR in three different participants with AD.....	55
Figure 3.2 Average SUVRs for the three PET radiotracers (FEOBV, FDG and NAV).....	56
Figure 3.3 Brain mapping showing significant radiotracer uptake differences in AD compared to control. .....	57
Figure 3.4 Brain mapping showing significant positive and negative correlations between the radiotracers. .....	57
Figure 4.1 Spatial location and extent of the cholinergic forebrain nuclei.....	76

## LIST OF TABLES

Table 1.1 Cholinergic nuclei, efferent projections and interneurons .....	25
Table 1.2 Different AD biomarkers.....	32
Table 1.3 Current PET imaging biomarkers in AD .....	33
Table 1.4 Cholinergic PET radiotracers.....	38
Table 1.5 Main PET radiotracers for VAcHT .....	39
Table 2.1 Description of the different cognitive scales used in this thesis. ....	46
Table 3.1 Sample characteristics.....	54
Table 4.1 Sociodemographic and clinical features.....	77
Table 4.2 Between group comparisons of [18F]-FEOBV SUVRs for each hemisphere. ....	77
Table 4.3 Between group comparisons of ChBFs volumetric values* .....	78
Table 4.4 Partial correlations, controlling for age.....	78

## LIST OF ABBREVIATIONS AND ACRONYMS

A $\beta$	Amyloid beta protein
ACh	Acetylcholine
AChE	Acetylcholinesterase
ACHEI	Acetylcholinesterase inhibitor
AD	Alzheimer's disease
ANCOVA	One-way analysis of covariance
APOE	Apolipoprotein E
apoE	Apolipoprotein-E lipid transport protein
APP	Amyloid precursor protein
BDNF	Brain Derived Neurotrophic Factor
BF	Basal forebrain
Ch1	Cholinergic neurons of Medial septum
Ch2	Cholinergic neurons of Vertical limb of the diagonal band of Broca
Ch3	Cholinergic neurons of Horizontal limb of the diagonal band of Broca
Ch4	Cholinergic neurons of Cholinergic neurons of the NBM
Ch4a-i	Cholinergic neurons of anterior and intermediate Ch4
Ch4am	Cholinergic neurons of anteromedial Ch4
Ch4al	Cholinergic neurons of Intermediodorsal Ch4
Ch4id	Cholinergic neurons of Intermediodorsal Ch4
Ch4iv	Cholinergic neurons of Intermedioventral Ch4
Ch4p	Cholinergic neurons of Posterior Ch4
Ch5	Pedunclopontine nucleus
Ch6	Laterodorsal tegmental nucleus
Ch7	Medial habenular nucleus

Ch8	Parabigeminal nucleus
ChAT	Choline Acetyltransferase
ChBF	Cholinergic systems of basal forebrain
Cho	Choline
CDK5	Cyclin Dependent Kinase 5
CSF	Cerebrospinal fluid
FDG	[ <sup>18</sup> F]Fluorodeoxyglucose
FEOBV	[ <sup>18</sup> F]Fluoroethoxybenzovesamicol
FTD	Frontotemporal dementia
GABA	Gamma-Aminobutyric acid
GDS	Geriatric Depression Scale
GI	Gastrointestinal tract
GM	Grey matter
GSK-3	Glycogen synthase kinase 3
HRRT	High Resolution Research Tomograph
IPL	Inferior parietal lobule
LBD	Lewy body dementia
LDT	Laterodorsal tegmental complex
mAChR	Muscarinic acetylcholine receptors (M1-M5)
MAP	Microtubule-associated protein
MCI	Mild cognitive impairment
mi	Myo-inositol
MMSE	Mini-Mental State Examination
MoCA	Montreal Cognitive Assessment
[ <sup>11</sup> C]MP4A	[ <sup>11</sup> C]Methyl-4-piperidyl acetate
MRI	Magnetic resonance imaging

MRS	Proton magnetic resonance spectroscopy
MSA	Multiple Systems Atrophy
NAA	N-acetylaspartate
NAV	[ <sup>18</sup> F]-NAV4694
nAChR	Nicotinic acetylcholine receptors ( $\alpha$ 4 $\beta$ 2-nAChRs - $\alpha$ 7-nAChRs)
NBM	Nucleus basalis of Meynert
NFT	Neurofibrillary tangles
NGF	Nerve growth factor
OP-OSEM	Ordinary Poisson-Ordered Subset Expectation Maximization
p75NTR	Nerve growth factor receptor
PET	Positron Emission Tomography
PD	Parkinson's disease
PKA	protein Kinase A
[ <sup>11</sup> C]PIB	[ <sup>11</sup> C]Pittsburgh compound B
[ <sup>11</sup> C]PMP	[ <sup>11</sup> C]Methyl-piperidin-4-yl propionate
PPN	Pedunclopontine nucleus
PSP	Progressive Supranuclear Palsy
P-tau	Phosphorylated tau
PVE	Partial volume effect
ROI	Region of interest
SCI	Subjective cognitive impairment
SPECT	Single-photon emission computed tomography
SUV	Standard uptake values
SUVR	Standardized uptake value ratio
SV2A	Synaptic vesicle glycoprotein 2A
TIV	Total intracranial volume

T-tau	Total tau
VAcHT	Vasicalr acetylcholine transporter
VD	Vascular dementia
WM	White matter

## LIST OF SYMBOLS AND UNITS

MBq	Megabecquerel (unit of radioactivity)
keV	kilo-electron-Volts
$\mu\text{g}$	microgram
$\text{mm}^3$	millimeter cube

## RÉSUMÉ

La mesure de la perte cholinergique cérébrale pourrait être la meilleure façon d'identifier et quantifier l'évolution de la maladie d'Alzheimer. Le [<sup>18</sup>F]-fluoroéthoxybenzovesamicol (FEOBV) est un nouveau radiotracer utilisé avec l'imagerie cérébrale par tomographie d'émission de positons (TEP) qui se lie au transporteur vésiculaire de l'acétylcholine. Chez l'animal et l'humain, le FEOBV s'est révélé sensible et fiable pour caractériser les terminaisons nerveuses cholinergiques présynaptiques. Dans le cadre de cette thèse, le FEOBV a été utilisé pour la première fois chez des patients atteints de la maladie d'Alzheimer (MA), afin de mieux en connaître son potentiel comme biomarqueur.

L'échantillon comprend 12 participants répartis également entre un groupe de sujets contrôle et de patients atteints de la MA. Chaque participant a été évalué à l'aide des échelles cognitives « Mini-Mental State Examination » (MMSE) et « Montreal Cognitive Assessment » (MoCA). Ils ont aussi subi trois séances d'imagerie cérébrale par TEP avec (1) le FEOBV comme traceur des terminaisons cholinergiques, (2) le [<sup>18</sup>F]-NAV4694 (NAV) comme traceur de la protéine bêta-amyloïde et (3) le [<sup>18</sup>F]-Fluorodéoxyglucose (FDG) comme traceur du glucose et indice métabolique. Le ratio de la valeur de fixation standard normalisée (SUVR) a ensuite été calculé pour chaque traceur et comparé entre les deux groupes à l'aide de tests-t voxel-à-voxel. Des corrélations ont également été calculées entre chaque traceur et les échelles cognitives, ainsi qu'entre le FEOBV et les deux autres radiotraceurs. Les résultats ont montré des réductions importantes de l'activité du FEOBV dans de multiples zones corticales connues pour être touchées dans la MA. Ces réductions étaient non seulement détectées dans le groupe MA, mais chez chacun des patients pris individuellement. Les traceurs FDG et NAV ont également permis de distinguer les deux groupes, mais avec une plus faible sensibilité que le FEOBV. De plus, l'activité du FEOBV était positivement corrélée à l'activité du FDG dans de nombreuses régions corticales, et négativement corrélées à l'activité du NAV dans certaines zones restreintes. Les échelles cognitives MMSE et MoCA présentaient aussi des corrélations significatives avec l'activité du FEOBV et du FDG. Ainsi, nos résultats confirment une sensibilité et fiabilité optimale du traceur FEOBV pour identifier la MA et en quantifier la sévérité. La mesure de la perte neuronale cholinergique chez l'humain représente donc un excellent biomarqueur de la MA.

Dans le but de vérifier si la perte des terminaisons cholinergiques corticales, telle que mesurée par le FEOBV, concorde bien avec la mort neuronale des cellules cholinergiques, une seconde étude fut mise sur pied. Celle-ci s'intéressait aux corrélations entre, d'une part, l'intensité du signal FEOBV au niveau du cortex et, d'autre part, le degré d'atrophie des noyaux cholinergiques du prosencéphale basal (ChBF). Ces analyses ont été réalisées à partir du même échantillon de participants décrit plus haut. Des régions d'intérêts (RI) corticales ont été définies à partir des résultats obtenus avec le FEOBV dans la première étude. Une segmentation du ChBF a aussi été effectuée à partir des images IRM de chaque participant. Des comparaisons ont alors été réalisées entre les deux groupes, ainsi que des corrélations chez les patients atteints de la MA entre l'activité du FEOBV dans des RI corticales et le volume des noyaux du ChBF, comprenant le noyau basal de Meynert (Ch4) et le septum médial/médian verticale de la bande diagonale de Broca (Ch1/2). Les patients atteints de la MA ont montré à la fois des volumes du ChBF-Ch4 et une activité du FEOBV plus faible que les sujets sains. De plus, les volumes de la subdivision du noyau Ch4 étaient significativement corrélés à l'activité du FEOBV observée dans les RI. Par ailleurs, les volumes de la subdivision du noyau Ch1/2, qui reste relativement intacte dans la MA, n'étaient pas corrélés à l'activité du FEOBV dans l'hippocampe, ni dans aucune zone corticale. Ces résultats suggèrent que la dénervation cholinergique corticale mesurée par le FEOBV est proportionnelle à l'atrophie du ChBF mesurée par IRM,



ce qui confirme la fiabilité et la validité du traceur FEOBV pour quantifier la dégénérescence cholinergique dans la MA. Cette conclusion est également celle formulée par une équipe de chercheurs canadiens qui ont utilisé nos données avec le FEOBV dans la MA, pour illustrer les fortes corrélations avec les mesures du ChBF obtenus dans un vaste échantillon issu de l'Alzheimer's Disease Neuroimaging Initiative (ADNI). Leurs résultats ont montré que la topographie de dénervation cholinergiques telle que mesurée par le FEOBV dans la MA est concordante avec les patrons de dégénérescence du ChBF, ce qui renforce la consistance de nos propres résultats.

Mots clés : Maladie d'Alzheimer (MA); Démence; Biomarqueur; Noyaux cholinergiques du prosencéphale basal; Tomographie d'émission de positons (TEP); [<sup>18</sup>F]-fluoroéthoxybenzovesamicol (FEOBV)

## ABSTRACT

Measuring brain cholinergic degeneration might be considered as the best approach to identify and quantify Alzheimer's disease (AD). The [ $^{18}\text{F}$ ]-fluoroethoxybenzovesamicol (FEOBV) is a new radiotracer used with positron emission tomography (PET) neuroimaging technique. This radiotracer binds to the vesicular acetylcholine transporter and was previously found reliable to characterize presynaptic cholinergic nerve terminals in both animals and humans. It has been used in the current study to quantify brain cholinergic loss in AD, for the first. Twelve subjects were included in this thesis project, divided equally in healthy subjects and patients with probable AD, all assessed with the Mini-Mental State Examination (MMSE) and Montreal Cognitive Assessment (MoCA) cognitive scales. In this thesis, the 12 participants underwent three consecutive PET imaging sessions with (1) [ $^{18}\text{F}$ ]-FEOBV (FEOBV) as a tracer of the cholinergic terminals, (2) [ $^{18}\text{F}$ ]-NAV4694 (NAV) as an amyloid-beta tracer, and (3) [ $^{18}\text{F}$ ]-Fluorodeoxyglucose (FDG) as a glucose tracer and brain metabolic measurement. Standardized uptake value ratios (SUVRs) were computed for each tracer and compared between the two groups using voxel wise t-tests. Correlations were also computed between each tracer and the cognitive scales, as well as between FEOBV and the two other radiotracers. Results showed major reductions of FEOBV uptake in multiple cortical areas known to be affected in AD. These reductions were seen both in the AD group as a whole when compared to the control group, and in each individual AD subject. FDG and NAV were also able to distinguish the two groups, but with lower sensitivity than FEOBV. FEOBV uptake values were positively correlated with FDG in numerous cortical areas, and negatively correlated with NAV in some restricted areas. The MMSE and MoCA cognitive scales were found to correlate significantly with FEOBV and FDG, but not with NAV. These results suggest optimal sensitivity and reliability of the FEOBV radiotracer to identify AD and quantify its severity. Measuring cholinergic neuronal loss in human with FEOBV is therefore as an excellent surrogate biomarker for AD.

In order to verify whether cortical cholinergic denervation, as measured with FEOBV, correlated well with cholinergic cell death, a second study was conducted with the data set obtained from the first study. This second study aimed at correlating the FEOBV cortical uptake with the degree of atrophy of the cholinergic nuclei of the basal forebrain (ChBF). Cortical regions of interest (ROIs) were defined from the results obtained with FEOBV in the first study. ChBF segmentation was also performed using MRI images of each participant. These variables were compared between the two groups, and partial correlations were performed in the AD patients between FEOBV uptake in specific ROIs and volumetry of the corresponding ChBF subareas, which include the nucleus basalis of Meynert (Ch4), and the medial septum/vertical limb of the diagonal band of Broca (Ch1/2). Patients with AD showed both lower ChBF-Ch4 volumetric values and lower FEOBV cortical uptake than healthy volunteers. Volumes of the Ch4 subdivisions correlated significantly with the FEOBV uptake values observed in the relevant ROIs. Volume of the Ch1/2, which remains relatively unaffected in AD, did not correlate with FEOBV uptake in the hippocampus, nor with any cortical area. We concluded that cortical cholinergic denervation as measured with FEOBV-PET is proportional to ChBF atrophy measured with MRI-based volumetry, further supporting the reliability and validity of FEOBV-PET to quantify cholinergic degeneration in AD. Such a conclusion was also obtained by a team of Canadian researchers who used our data with FEOBV in AD, to illustrate the strong correlations with the ChBF volumetry obtained in a large sample from the AD Neuroimaging Initiative (ADNI). Their results showed that the cholinergic denervation topography as measured by FEOBV in AD was consistent with the patterns of ChBF degeneration, reinforcing therefore the consistency of our own results.

Keywords : Alzheimer Disease (AD); Dementia; Biomarker; Basal forebrain Cholinergic nuclei; Positron Emission Tomography (PET); [<sup>18</sup>F]-fluoroethoxybenzovesamicol (FEOBV)

## CHAPITRE 1

### LITERATURE REVIEW AND BACKGROUND

#### 1.1 Epidemiology and clinical presentation of Alzheimer's Disease (AD)

Alzheimer's disease (AD) is a progressive neurodegenerative disease and the leading cause of dementia (Hebert et al., 2003). According to World Health Organization, AD accounts for more than half of the dementia cases and affects more than 47 million people worldwide. This number is increasing with the ageing population, and it is predicted to reach 66 million by year 2030, and 115 million by 2050 (Wortmann, 2012). In Canada, it is estimated that the prevalence of AD will double by 2038 to more than 770,000 people, placing a heavy burden on the Canadian society (Herrmann et al., 2015).

AD may be present as an inherited form in a small percentage of patients (less than 5% of cases) aged 65 or younger (early-onset AD), however the majority of AD cases are sporadic (late-onset AD), with an increase in prevalence with the advancing age. Indeed, age is commonly considered as the strongest risk factor for developing AD (Hebert et al., 2001; Liu et al., 2013), doubling the incident rate every five years after the age of 65 (Lindsay et al., 2002). Other risk factors include female sex, genetic and environmental risk factors. Women are at a greater risk of developing AD, almost a twofold increased risk compared to men (Farrer et al., 1997; Zhao et al., 2016). A sudden drop in sex hormones during the fifth decade and a longer life span are speculated to explain this increased susceptibility (Seshadri et al., 1997; Pike, 2017). AD has also been linked to certain genetic predisposition. The variation in Apolipoprotein E (APOE) genotype is a well-established risk factor for AD (Liu et al., 2013; Husain et al., 2021). In human, the APOE gene encodes for the apolipoprotein-E lipid transport protein (apoE), with three major isoforms (E2, E3, E4) that regulate lipid metabolism and redistribution. Carriers of the APOE4 allele are known to present with an increased predispositions to AD and an earlier age of onset, compared to non-carriers (Borgaonkar et al., 1993; Sando et al., 2008; Liu et al., 2013; Husain et al., 2021). Cardiovascular risk factors (diabetes, hypertension, and obesity) or unhealthy lifestyle habits such as smoking, sedentary life, decreased social and mental activity, have also been associated with an increased AD risk (de Bruijn & Ikram, 2014; Crous-Bou et al., 2017). Conversely, some protective factors have been identified to reduce the risk of developing AD. Cognitive, social and intellectual activity together with higher education and occupational attainment have shown to decrease the risk of cognitive decline and AD by increasing cognitive reserve, the capacity of the brain to resist the effects of neuropathological damage (Stern, 2012; Martorana et al., 2021).

The clinical symptomatology of AD is characterized by an insidious onset and progressive cognitive decline, interfering with independence in everyday activities. According to the DSM-5 diagnostic criteria, the cognitive decline must be significant and affect one or more of cognitive domains (complex attention, executive function, learning and memory, language, perceptual-motor, or social cognition) (American Psychiatric Association, 2013). In addition, the observed deficits must not be explainable by any other medical or psychiatric conditions (American Psychiatric Association, 2013). The earliest and the most distinguishable cognitive feature in typical AD is an impairment in episodic memory and learning, which is present in more than 71% of confirmed post-mortem cases (Reed et al., 2007; Baker et al., 2018). Other cognitive functions may also be affected with the progression of the disease, but are generally of lesser magnitude, such as attention, working memory, executive function, and language (Dubois et al., 2007; McKhann et al., 2011). It must be mentioned that an atypical clinical presentation of AD may also arise, where memory impairment is not the principal feature. The atypical or non-amnesic presentation could present prominent deficits in domains such as language, visuospatial and executive functioning (McKhann et al., 2011). Furthermore, concurrent neuropsychiatric symptoms such as behavioral disorders, depression, and personality changes may also be present early on and worsen over the course of the disease. With the evolution of the disease, the neurodegeneration progressively affects the whole central and peripheral nervous systems, causing motor, autonomic and systemic complications such as a dehydration, malnutrition or infection which lead to incapacitation and ultimately death. Currently, there is no curative treatment or disease-modifying medication in AD.

It is generally assumed that AD evolves over decades before the onset of the first noticeable cognitive symptoms. Compensatory processes are therefore thought to occur during the preclinical or asymptomatic phase despite the initial neuropathological changes (Albert et al., 2011; Sperling et al., 2011; Gaubert et al., 2019). The Mild Cognitive Impairment (MCI) phase is thought to occur as a transitional or prodromal phase of AD. Although the MCI does not affect daily activities, it can be detected and objectified using cognitive testing batteries. The MCI can be categorized further as an amnesic or a non-amnesic type, the former being at highest risk to evolve towards an AD diagnosis within three to five years (McKhann et al., 2011).

Currently, the clinical diagnosis of AD is principally based on the progressive deterioration of cognitive and behavioral functions, and the presence of some risk factors such as being a carrier of APOE4 allele. The cognitive symptoms are mainly measured using standardized neuropsychological scales in clinical settings.

However, these symptoms are not always specific to AD and cannot identify or measure the biological processes underlying the disease, nor detect the disease at its preclinical stage. Other forms of dementias with different neuropathologies such as Lewy body dementia (LBD), and frontotemporal dementia (FTD) could present comparable and overlapping clinical symptoms to AD, making the differential diagnosis challenging (Weintraub et al, 2012; Rascovsky et al., 2011; McKeith et al., 2017). Furthermore, it is not uncommon to have a mixed presentation, that is a combination of two or more types of dementias, posing further difficulty in the differential diagnosis. For instance, co-occurrence of AD and vascular dementia (VD) is estimated at 30% of the diagnoses in clinical settings (Matej et al., 2019). Given the complexity in differential diagnosis and the need to detect AD very early on, even at a preclinical stage, effort has been made to shift from the clinical diagnosis towards a biological diagnosis based on an AD neuropathology (Perrin et al., 2009; Jack et al., 2010, 2018).

## 1.2 Neuropathology of AD

The exact etiopathology of AD remains unknown, but it is believed to be multifactorial, involving an interplay of several degenerative pathways, leading to synaptic loss and neurodegeneration with disease progression (Chen & Mobley, 2019). Although several neuropathological hallmarks have been characterized in AD, the most studied are the brain aggregation of amyloid beta ( $A\beta$ ) and tau proteins, leading respectively to the accumulation of the senile plaques and intracellular neurofibrillary tangles (NFT), which ultimately lead to neuronal death (Hardy & Higgins, 1992; Braak & Braak, 1991; Naseri et al., 2019; Hampel et al., 2021).

### 1.2.1 Tau, amyloid, and neurodegeneration in AD

Amyloid plaques are formed from aggregation of  $A\beta$  peptides which are produced by the enzymatic cleavage of the amyloid precursor protein (APP) (Hardy & Selkoe, 2002). In a normal, “non-amyloidogenic” metabolic pathway, APP is successively cleaved by the  $\alpha$ -secretase and  $\gamma$ -secretase enzymes, resulting in a soluble extracellular segment, which gets cleared in the cerebrospinal fluid (CSF). The purpose of APP and its metabolism are not very well understood, but there is some evidence showing that it plays a neurotrophic role (Meziane et al., 1998; Roch et al., 1994; Tan & Gleeson, 2019). For reasons yet unclear, APP is sometimes “dys-metabolized”, starting with a cleavage by a different enzyme,  $\beta$ -secretase, which produce extracellular insoluble segments of either 40 or 42 amino acids-long ( $A\beta$ 40 and  $A\beta$ 42). Unlike the larger and soluble APP segments, these  $A\beta$  fragments are hydrophobic and lipophilic, so instead of being cleared in the CSF, they tend to get trapped in the extracellular space and accumulate together, forming

fibrillar aggregates called amyloid plaques. The non-aggregated A $\beta$  monomers are not toxic, and may even have neuroprotective properties (Giuffrida et al., 2009). Indeed, it has been shown that A $\beta$  is modulated in response to a variety of environmental stressors (exposure to microorganisms, viral challenges, infectious agents) and is able to induce pro-inflammatory activities. There is evidence indicating that A $\beta$  can act as an antimicrobial peptide, that is, it can bind directly to pathogens and eliminate them, highlighting its protective role in the immune system of the brain (Soscia et al., 2010; Bourgade et al., 2015; Gosztyla, Brothers & Robinson, 2018). However, in their oligomeric form, A $\beta$  exert neurotoxic effects on the surrounding neurons (Goodman & Mattson, 1994). The toxic outcome of oligomeric A $\beta$  might be mediated by several different pathways, including disruption of mitochondrial function (Lustbader et al., 2004), formation of extraneous ion channels that disrupt homeostasis (Kagan, 2012), and inhibition of the Wnt signaling pathways (required for synaptic plasticity), eventually triggering cell death by apoptosis (Caricasole et al., 2003).

The amyloid cascade hypothesis, which assumed cortical accumulation of A $\beta$  as the primary driving force of AD pathogenesis, dominated the field of AD research for the past two decades. However, the validity of this hypothesis has been questioned. Mainly because therapeutic approaches targeting to clear A $\beta$  failed to show any amelioration in cognition, and longitudinal studies showed that there was an uncoupling of amyloid concentration with disease progression very early on in the disease (Drachman, 2014; Mullane & Williams, 2013, 2018). Focus thus shifted towards the detection and characterization of tau protein.

Tau proteins are well-known components of the neuronal cytoskeleton, serving mainly as stabilizers of the microtubules involved in axonal guidance and intracellular transport. The phosphorylation of tau depends on several kinases including GSK-3, CDK5, MAP and PKA which together control its function (Iqbal et al., 2005; Pei et al., 1999; Lindwall & Cole, 1984). In AD, however, this regulatory mechanism is disrupted, and levels of phosphorylated tau (p-tau) are much higher than in healthy brains (Khatoon et al., 1992). This hyperphosphorylation leads to the polymerization of tau into paired helical filaments, which forms complex neurofibrillary tangles (NFTs). These intraneuronal NFTs interfere with the normal function of tau and other microtubule-associated proteins, resulting in cytoskeletal disruption that eventually leads to cell death by apoptosis (Alonso et al., 1994; Iqbal et al., 2010; Kametani & Hasegawa, 2018).

Like amyloid plaques, NFTs accumulation follows a specific spatial pattern in the brain, appearing first in the transentorhinal cortex, then progressively spreading to the limbic region and neocortical areas (Braak

& Braak, 1991; Braak & Del Tredici, 2018). However, recent findings have challenged the cortical origin of AD, as they show an early subcortical tau pathology (Braak & Del Tredici, 2011; Arendt et al., 2015; Geula et al., 2021). These studies suggest that AD tauopathy may begin earlier than previously thought as it is detectable in subcortical nuclei projecting to the cerebral cortex, such as the cholinergic neurons of the basal forebrain (ChBF) (Arendt et al., 2015; Stratmann et al., 2016; Tiernan et al., 2018). Although Schliebs & Arendt (2011) had previously shown that there was an early cholinergic dysfunction in the ChBF rather than cell death in MCI, their subsequent findings actually showed an early neuronal loss in this region, which became detectable at preclinical stage and was clearly manifested at the prodromal MCI stage (Arendt et al., 2015; Richter et al., 2022).

### 1.2.2 Cholinergic dysfunction in AD

The central cholinergic system is the most affected neurochemical system in AD showing the earliest neuropathological changes in the evolution of the disease (Geula & Mesulam, 1999). This cholinergic loss is the most clinically relevant event in AD as it is closely coupled with the decline in cognitive functioning and disease severity (Mesulam et al., 2004, 2013). It is noteworthy to mention that other systems such as the noradrenergic, glutamatergic, dopaminergic and serotonergic systems also undergo pathological remodeling in AD, although these are generally much less affected than the cholinergic cells (Dringenberg, 2000; Garcia-Alloza et al., 2005; Grudzien et al., 2007; Lai et al., 2002; Nazarali & Reynolds, 1992). In this thesis the focus will be on the cholinergic system.

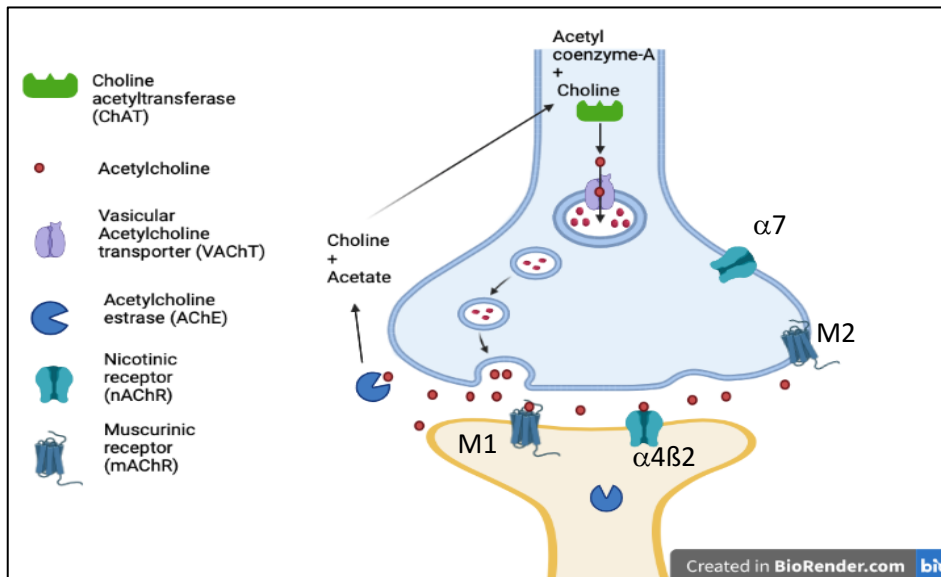
Cholinergic neurons of the basal forebrain provide the primary source of the neurotransmitter Acetylcholine (ACh) to the cortex and the hippocampus (Mesulam, 1990). ACh is considered as a primary neuromodulator in the brain. Indeed, the neocortex is densely innervated by cholinergic projections and the ACh release regulates the activity of efferent circuitry involved in higher-order cognitive functions such as attention and memory (Hasselmo & Sarter, 2011; Colangelo et al., 2019). Because of its prominent role in regulating such functions, deficits in cholinergic transmission could potentially influence all aspects of cognition (Sarter & Bruno, 1999; Hasselmo & Sarter, 2011; Ballinger et al., 2016). In AD, there is a progressive degeneration of cholinergic neurons of the ChBF and their projections (Mesulam & Geula, 1988; Teipel et al., 2011; Grothe et al., 2012; Kilimann et al., 2014). As a result, there is a reduction in the enzymatic activity of choline acetyltransferase (ChAT) and acetylcholinesterase (AChE), the enzymes responsible for ACh synthesis and degradation, respectively. There is also a decline in the vesicular acetylcholine transporter (VACHT) located in the presynaptic cholinergic terminals (Wenzel et al., 2021),



which is responsible for the transport of cytoplasmic ACh into the presynaptic vesicles (See Figure 1.1 for an overview of the central cholinergic transmission).

As part of the cholinergic dysfunction, pre and post synaptic ACh receptors such as ionotropic nicotinic receptors (nAChRs) and metabotropic muscarinic receptors (mAChRs) also undergo changes. The brain nicotinic receptors have at least six  $\alpha$  subunits ( $\alpha 2$ - $\alpha 7$ ), and three  $\beta$  subunits ( $\beta 2$ - $\beta 4$ ) that together make the different subtypes. The presynaptic  $\alpha 7$ -nAChRs and the pre and post synaptic  $\alpha 4\beta 2$ -nAChRs are the most abundant subtypes of nicotinic receptors expressed in the human cortex and undergo substantial decline in AD (Hernandez & Dineley, 2012). Muscarinic receptors consist of many subtypes (M1-M5), of which M1 and M2 subtypes are mainly expressed in the brain and considered the most relevant in AD (Caulfield & Birdsall, 1998). The presynaptic M2 subtype, expressed in the basal forebrain/septum, is shown to decrease in AD (Caulfield & Birdsall, 1998; Flynn et al., 1995), while the postsynaptic M1 subtype, which is expressed throughout the cortex and hippocampus is believed to be preserved (Terry & Buccafusco, 2003; Overk et al., 2010). This M2/M1 distribution pattern in AD is thought to reflect a reduction of the presynaptic terminals, caused by a significant loss of neurons arising from the ChBF and projecting to the cortex (Whitehouse et al., 1982; Hampel et al., 2018).

Figure 1.1 Cortical cholinergic neurotransmission



This figure demonstrates cortical cholinergic neurotransmission. ACh is synthesized in the cytoplasm of the nerve terminal from choline and acetylcoenzyme-A, by the synthesis enzyme, choline acetyltransferase (ChAT). ACh is then transported into the presynaptic vesicles via the vesicular Acetylcholine transporter (VACHT) and stored there. When released in the synaptic cleft, ACh binds to nicotinic (nAChR) and muscarinic receptors (mAChR). The degradation enzyme, Acetylcholinesterase

(AChE), present in the synaptic cleft breaks down Ach upon release into choline and acetate. The liberated choline in this reaction is captured and re-enters the nerve terminal and is again used for the synthesis of Ach. ( Figure created using [www.Biorender.com](http://www.Biorender.com))

### 1.3 The Basal Forebrain Cholinergic System

#### 1.3.1 The cholinergic systems of the brain

Cholinergic innervation is widely distributed and includes multiple nuclei located in the central and peripheral nervous systems. These nuclei can be distinguished according to their projection sites as shown in Table 1.1.

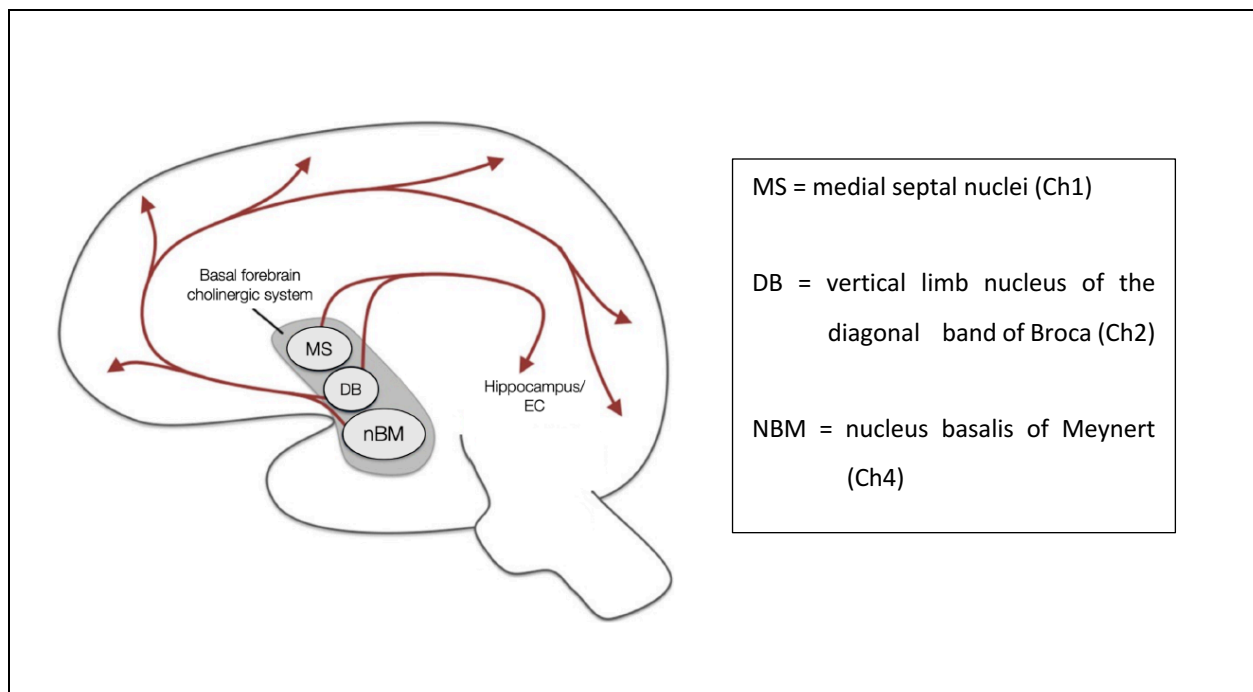
Table 1.1 Cholinergic nuclei, efferent projections and interneurons

Basal forebrain Cholinergic system
<ul style="list-style-type: none"> <li>○ Ch1 (medial septal nuclei) projecting to hippocampus;</li> <li>○ Ch2 (vertical limb nucleus of the diagonal band of Broca) projecting to the hippocampus and hypothalamus;</li> <li>○ Ch3 (horizontal limb nucleus of the diagonal band of Broca) projecting to the olfactory bulb and piriform cortex;</li> <li>○ Ch4 (nucleus basalis of Meynert) projecting to the cortical mantle, and amygdala.</li> </ul>
Cholinergic nuclei of the brainstem
<ul style="list-style-type: none"> <li>○ Ch5 (pedunculo-pontine nucleus (PPN)) projecting to the thalamic complex and partially the medial dorsal striatum; basal forebrain, brainstem, and spinal cord;</li> <li>○ Ch6 (laterodorsal tegmental complex (LDT)) projecting to the thalamic complex and partially the anteroventral striatum; basal forebrain, brainstem, and spinal cord;</li> <li>○ Ch7 (medial habenula in the epithalamus) projecting to the interpeduncular nucleus of the mesencephalon;</li> <li>○ Ch8 (parabigeminal nucleus of the mesencephalon) projecting to the superior colliculus ;</li> <li>○ Medial vestibular nucleus (pons) projecting to the cerebellum and the basal interstitial nucleus of the cerebellum;</li> <li>○ The dorsal motor nucleus of the vagus and vagus nerve efferents that provide parasympathetic innervation to the GI tract.</li> </ul>
Other cholinergic nuclei
<ul style="list-style-type: none"> <li>○ Striatal cholinergic interneuron;</li> <li>○ Cholinergic enteric neurons and glial cells;</li> <li>○ The descending and sigmoid colon receive parasympathetic innervation from sacral cholinergic preganglionic neurons;</li> <li>○ Interomediolateral preganglionic sympathetic neurons;</li> <li>○ Spinal cord cholinergic interneurons.</li> </ul>

This table summarizes the different cholinergic nuclei and interneurons in the central nervous system and their projection sites (From Mesulam, 1990, 2004, 2013).

Not all of these cholinergic systems have a prominent role in AD pathology as most of the literature in this field is concerned with Ch1 to Ch4. These nuclei correspond to the ChBF as a whole, and they are distributed in a series of heterogeneous areas without clear borders projecting to the entire cortical mantle, the hippocampal complex, and the amygdala (Mesulam, 2004) (See Figure 1.2). Among them, Ch4, also called nucleus basalis of Meynert (NBM), has been described as the most severely affected in AD and will be discussed in detail below.

Figure 1.2 Basal forebrain cholinergic systems.



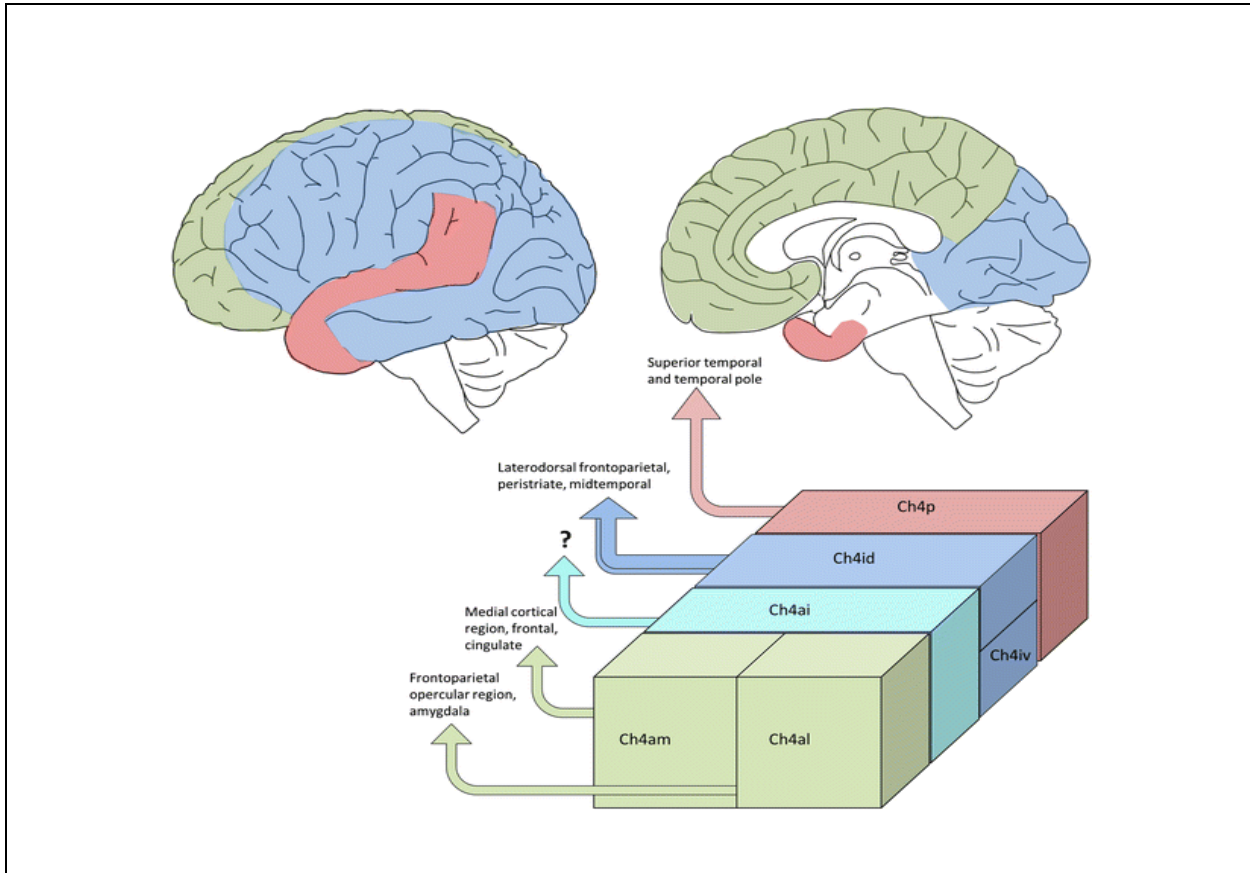
Schematic representation of the main basal cholinergic nuclei and their projection sites in the brain. NBM or the Ch4 projects to the cortical mantle, MS and BD (Ch1/Ch2) project mainly to the hippocampus (Adapted from Newman et al., 2012, p.2).

### 1.3.2 Nucleus basalis of Meynert and its cortical projections

Detailed human anatomical studies show that NBM is a flat nearly horizontal structure extending from the olfactory tubercle anteriorly to the level of the uncus hippocampus, spanning 13-14 mm in the sagittal plane (Mesulam & Geula, 1988). In humans, NBM has around 210,000 neurons in each hemisphere of which 90% are cholinergic and interspersed with smaller GABAergic neurons (Gilmor et al., 1999; Mufson et al., 2003). NBM or the Ch4 is the largest nucleus of the basal forebrain, and its cholinergic neurons can be further subdivided into five subsectors based on their cortical topographical projections (based on the topography of their cortical projections) (see figure 1.3). These include the anterior part of Ch4 which

subdivides this into anteromedial (Ch4am) and anterolateral (Ch4al) subsectors; the intermediate part which subdivides into intermediodorsal (Ch4id) and intermedioventral (Ch4iv) subsectors, and the most posterior part (Ch4p) (Mesulam & Geula, 1988; Mesulam et al., 1983, Mesulam, 2004).

Figure 1.3 NBM/Ch4 subdivisions with corresponding cortical topographic projections.



Schematic representation of the five subdivisions of the NBM (Ch4) and their corresponding cortical projection sites visualized by different colors. These include the anterior part of Ch4 which subdivides this into anteromedial (Ch4am) and anterolateral (Ch4al) subsectors; the intermediate part which subdivides into intermediodorsal (Ch4id) and intermedioventral (Ch4iv) subsectors, and the most posterior part (Ch4p). Cortical projections of the Ch4ai are not currently known (From Liu et al., 2015, p. 530).

These cholinergic nuclei are oriented in a caudal-rostral axis and are known to innervate the cortex in a concordant posterior-anterior pattern (Liu et al., 2015). The anterior part of the Ch4 innervates more anterior parts of the cortex and the posterior part innervates more posterior areas. Indeed, the Ch4am and Ch4al provide the major cholinergic projection to medial aspects of frontal, parietal and cingulate cortices, and frontoparietal opercular and amygdalar regions, respectively (Mesulam, 2013; Liu et al., 2015). Whereas, the Ch4p subsector has a more restricted projection site which is the superior temporal

gyrus and the temporal pole (Mesulam, 2013; Liu et al., 2015). The intermediate NBM (Ch4id and Ch4iv) subsectors have similar projection patterns and innervate the remainder of the cortical mantle. Prominent projections are sent to ventrolateral orbital, insular, periarculate, peristriate areas as well as to the inferior parietal lobule (Mesulam, 2013; Liu et al., 2015). Alongside their principal projections, each Ch4 subsector sends lesser projections innervating adjacent and non-ascent cortical areas, except for the Ch4p which has a more restricted projection site (Mesulam & Geula, 1988; Mesulam et al., 1983). Overall, those cortical innervations are not uniform, as there are differences in the regional density of projections, with limbic and paralimbic areas receiving substantially higher levels of cholinergic input than adjacent neocortical association areas (Mesulam, 2013).

Despite the widespread Ch4 cortical efferent, the afference towards Ch4 is not reciprocal or symmetrical as it is restricted mainly to fibers originating in the limbic and paralimbic areas (Mesulam & Geula, 1988; Russchen et al., 1985). Subcortical structures such as thalamus, amygdala, hypothalamus, and other neurotransmitter systems originating in the brainstem (substantia nigra, raphe nuclei nucleus locus coeruleus) also provide additional input to the Ch4 (Mesulam, 2013; Jones & Cuello, 1989). Given the extensive anatomical connections with various cortical and subcortical areas, and the distal locations of these areas, the long cholinergic fibers arising from the NBM are more susceptible than any other CNS neurons to be affected by changes occurring at any place along their course.

### 1.3.3 Neuronal vulnerability of nucleus basalis of Meynert and their fate in AD

Post-mortem data from Whitehouse and colleagues (1982), demonstrated for the first time a profound loss of NBM cholinergic neurons (Ch4) in patients with AD, and a severe denervation of the cortex. Indeed, the loss of Ch4 neurons appears to be selective in AD as the other cholinergic nuclei (Ch1,2,3,5,6) remain relatively preserved (Mesulam, 2013 ; Liu et al., 2015). Recent in vivo neuroimaging studies also confirmed the selective vulnerability and early NBM (Ch4) degeneration in AD patients (Hanyu et al., 2002; Teipel et al., 2011, 2018). Furthermore, longitudinal voxel-based morphometric analyses showed that progressive atrophy of NBM follows a posterior to anterior pattern, with the posterior Ch4 showing smaller volumes already detectable in preclinical and MCI stages compared to the anterior part (Grothe et al., 2010, 2012). Most importantly, recent in vivo longitudinal structural imaging studies show early volumetric reductions and pathological changes (pretnagles, changes in gene expression and dysregulation of neurotropic and neurotransmitter signaling) in the cholinergic neurons of NBM as this precedes the cortical spreading of AD pathology and memory impairment, emphasizing the selective vulnerability of the NBM cholinergic

neurons early on in AD entorhinal (Fernández-Cabello et al., 2020; Tiernan et al., 2018a, 2018b; Schmitz & Spreng, 2016).

Cholinergic neurons of NBM have very specific morphological and metabolic properties rendering them susceptible, more than any other type of neurons, to early neurofibrillary tangle formation and neurodegeneration in AD (Mufson et al., 1989; Mesulam, 2013; Tiernan et al., 2018a). Indeed, post-mortem studies have shown that the loss of cortical cholinergic innervation is associated with and is probably caused by the neurofibrillary tangles that accumulate primarily in the NBM (Braak & Del Tredici, 2013; Cantero et al., 2020). The NBM cholinergic neurons are among the largest and most complex neurons with very long axonal length, spreading throughout the cortical mantle with more than 1000 branches per neuron, requiring therefore a very high demand in energy and trophic factors such as the nerve growth factor (NGF) (Szutowicz et al., 2014; Wu et al., 2014; Chen & Mobley, 2019). Evidence indicates that  $\beta$ -amyloid and NFT formations may ultimately disrupt NGF metabolism, causing the degeneration of the NBM cholinergic neurons early on, while sparing the other cholinergic nuclei which express no specific NGF receptors (Cuello et al., 2019; Fahnstock & Shekari, 2019).

Non-pathological aging has also been shown to negatively impact the ChBF (Schliebs & Arendt, 2011). Aging is associated with reduced neurotrophic factors in the ChBF, accompanied by a gradual cell loss and diminished projection to the cortex and the hippocampus (Shekari & Fahnstock, 2019). In vivo MRI volumetric studies also confirm this selective involvement by showing ChBF atrophy in advancing aging in humans (Grothe et al., 2013). The NGF induced shrinkage of the cholinergic neurons of NBM and medial septal region of the basal forebrain neurons may account for the decline of cholinergic innervation that occurs with aging, leading to the known age-related cognitive and memory decline (Mesulam & Mufson, 1983; Bartus et al., 1982). However, the cholinergic changes seen in AD are more severe when compared to non-pathological aging, which is thought to be exacerbated by the presence of amyloid and tau pathology (Schliebs & Arendt, 2011; Chen & Mobley, 2019).

#### 1.4 The basal forebrain cholinergic system and cognitive functioning

Since the 70s, there has been a continuous interest towards the role of the central cholinergic system in cognition, as it was shown that cholinergic markers in the cerebral cortex were reduced in patients with AD and that these reductions correlated with both cortical pathology and the degree of cognitive impairment (Bowen et al., 1976; Perry et al., 1978). A vast number of experimental studies showed

learning and memory impairments after compromising the cholinergic system using pharmacological or lesion methods. The first experimental studies that evaluated the effects of Scopolamine (non-selective muscarinic receptor antagonist) on cognitive functions showed that when given to healthy volunteers, Scopolamine mimicked many of the cognitive dysfunctions (learning and memory deficits) that could be observed in aging or in AD (Crow & Grove-White, 1973; Drachman & Leavitt, 1974). Additionally, when given to AD patients, Scopolamine seemed to exacerbate their cognitive dysfunctions (Sunderland et al., 1987). Conversely, cognitive performances were increased with cholinergic enhancers such as acetylcholinesterase inhibitor (AChEI), which works by partially blocking the degradation of acetylcholine in the synapse and enabling more of the neurotransmitter to reach and activate cholinergic receptors (Fibiger, 1991; Mohammed, 1993). These studies further reinforced the cholinergic hypothesis of memory dysfunction in geriatric aging and in AD, inciting the development of cholinergic enhancers for treating such cognitive deficits (Bartus et al., 1982).

During the last decades, the role of the central cholinergic system in cognition has been refined. The development of the selective cholinergic immunotoxin 192-IgG-saporin (eliminates cells expressing nerve growth factor receptor ) was a breakthrough in this field (Wiley, 1992). This selective toxin binds to specific receptors expressed on the ChBF neurons and can induce specific cholinergic lesions when injected in discrete parts of the brain (cortical vs hippocampal). Animal behavioral studies using this method provided support for the role of cortical ACh in attentional processes, where ACh plays a vital role in the top-down control of attentional orienting, working memory and stimulus discrimination (Klinkenberg et al., 2011). As such, deficits in its transmission could impair learning and memory processes (Everitt & Robbins, 1997; Ballinger et al., 2016). In contrast, cholinergic signaling in the septal-hippocampal system is suggested to be involved in the encoding of new information, as a modulator of hippocampal networks (Everitt & Robbins, 1997).

More recent experiments focus on the role of the cholinergic receptors in mediating the effects of acetylcholine on cognition. There is an emerging unanimity that blocking the postsynaptic M1 receptor is particularly associated with memory impairment, as this subtype is highly involved in memory and learning processes, and that the use of M1 agonists ameliorate cognitive decline in preclinical and clinical AD (Eglen, 2006; Terry & Buccafusco, 2003; Hasselmo & Sarter, 2011). It is also shown that the presynaptic M2 receptor (autoreceptor) antagonists may be associated with improvements in memory, perhaps by increasing acetylcholine release (Baratti et al 1993, Hasselmo & Sarter, 2011). Results regarding nicotinic

AChR subtypes, however, have been less consistent. It has been shown that nicotine (a non-selective nAChR agonist) can improve attentions in individuals with early-stage AD, through the activation of  $\alpha 4\beta 2$ -nAChR (Sahakian & Coull, 1994). The effect of  $\alpha 7$ -nAChRs on attention is still conflicting as pharmacological studies have failed to implicate this receptor in such functions (Grottick & Higgins, 2000; Hasselmo & Sarter, 2011). Thus, it appears that the role of ACh in cognition is different per brain region and per cholinergic receptor subtypes, emphasizing the complex role of the cholinergic system as an important neuromodulator of the brain.

Currently, the most widely prescribed treatment for AD are the AChE inhibitors, such as donepezil. However, the success of these treatments has been very limited. Despite statistically significant improvements in cognitive tests and dementia scales observed in multiple clinical trials, the impact of these treatments in real life situations is modest at best. Moreover, these treatments remain symptomatic as they do not stop or reduce the AD neurodegenerative process. Consequently, the scientific and pharmaceutical communities have reoriented the focus of their works and investments during the last twenty years toward other therapeutic avenues, such as disease modifying drugs that may reduce Tau or A $\beta$  aggregations. This reorienting of research strategies produced a great enthusiasm for new diagnostic tools that are based on Tau and amyloid proteins detection in the brain of patients with AD. However, it is still not known whether these proteins aggregations are the cause or the consequence of AD, and as such we might again be on a wrong track to find reliable biomarkers for this disease. Perhaps, the best approach would be to measure neuronal loss, irrespective of the pathophysiology. In this respect, measuring cholinergic cell death could be a gold standard, if a reliable marker could be found.

### 1.5 The current biomarkers of AD

A biomarker is a biological molecule in a given tissue that provides an objective and measurable indicator of a normal condition or of a disease state in a living individual. These molecules can be identified using various methods, such as detection in the blood, in the cerebrospinal fluid (CSF), or via imaging tools. In the field of neurodegenerative disorders, such as AD, a biomarker should reflect a pathological process that is specific to AD, in order to distinguish this disease from other forms of dementias. It should also be highly sensitive to detect the disease early on and to follow the progression in a given individual. Biomarkers specific to a neuropathological process in AD are sought after not only for detection but most importantly for the assessment of efficacy of a potential therapeutic treatment.



Several potential AD biomarkers have been explored during the last decades such as the detection of tau/A $\beta$  proteins and quantification of neuronal loss using various methods. The field of neuroimaging has seen the fastest growth as a preferred tool for the development of a biomarker as it provides a visual map of these changes in the brain. Techniques such as brain magnetic resonance imaging (MRI) and positron emission tomography (PET) are commonly used in AD to measure brain atrophy and functional alterations. PET imaging is more prolific as it can be used to quantify synaptic/metabolic activity and detect various proteins in the brain (receptors, enzymes, transporters). PET imaging is described in detail in the following subchapter. The search for the ideal biomarker, however, has not been fruitful as there are limitations with the currently used biomarkers. See table 1.2 and 1.3 for a list of different biomarkers, their characteristics, and limitations as a reliable tool for AD.

Table 1.2 Different AD biomarkers

Biomarkers	Characteristics	Limitations
CSF biomarkers	<p>This method is used for the detection of tau and A<math>\beta</math> proteins in the CSF. An elevated (P-tau) or total tau (T-tau) level and a decreased A<math>\beta</math><sub>42</sub> / A<math>\beta</math><sub>40</sub> ratio are found in patients with AD and MCI who progress to AD (Buerger et al., 2006; Palmqvist et al., 2015; Santangelo et al., 2020).</p> <p>These biomarkers are found to correlate with A<math>\beta</math> or tau levels detected by in vivo brain imaging or by post-mortem quantifications (Strozyk et al., 2003; Gordon et al., 2016).</p>	<p>the variation in these indices is very low and it is almost impossible, in a given individual, to distinguish the different degree of severity evolving over a period of one or two years (De Leon, et al., 2006; Stomrud et al., 2015).</p> <p>The margin of error is very wide between the various laboratories that test for these CSF proteins, making this approach less reliable (Hansson et al., 2018).</p> <p>There are also novel fluid biomarkers (neuroinflammation proteins) but their validity as AD biomarkers have yet to be validated (Molinuevo et al., 2018).</p>
MRI biomarkers	<p>MRI volumetry is used to quantify brain atrophy. It can characterize hippocampal atrophy with high specificity in AD (González et al., 2016). 3% reduction in hippocampal volume in patient with MCI, 10-30% reduction in patients with mild-to-moderate AD, and close to 40% loss in the most severe cases of AD are reported (Khan et al.,</p>	<p>Hippocampal atrophy is not exclusive to AD, and also observed in many other degenerative dementias (Elder et al., 2017; Patel et al., 2017).</p> <p>This method cannot detect the exact tissue type affected by the hippocampal atrophy (gliosis vs. neuronal loss), which could explain</p>

	<p>2015; Westman et al., 2011a, 2011b; Josephs et al., 2017).</p> <p>There is significant correlation between hippocampal volume and AD cognitive severity (Jack et al., 1999, 2002). Higher annual rate of hippocampal atrophy in AD patients (2-6%) than in the normal aging population is demonstrated (0.2-1.7%) (Cover et al., 2016).</p>	<p>Inconsistent results between hippocampal atrophy measured by MRI and post-mortem neuropathological measures (amyloid plaques and tangles) (Burton et al., 2012).</p>
--	--	---

MRS biomarkers		
	<p>Proton magnetic resonance spectroscopy (MRS) is used for the analysis of brain metabolites, such as N-acetylaspartate (NAA), choline (Cho) and myo-inositol (ml), which are associated with neuronal loss and gliosis (Kantarci et al., 2000, 2005). Results have shown a decrease in NAA and an increase in ml in amnesic MCI who convert to AD (Glodzik et al., 2015; Fayed et al., 2017), and a significant decrease in NAA and an increase in ml and Cho in AD (Wang et al., 2015).</p>	<p>The MRS findings are not exclusive to AD, and also reported in patients with VD, and hypertensive subjects without dementia (Graff-Radford et al., 2013). MRS data is significantly affected by the AChE inhibitors used in the symptomatic treatment of AD (Modrego et al., 2006).</p>

This table summarizes the characteristics and limitations of different types of AD biomarkers such as those related to CSF, MRI and MRS.

Table 1.3 Current PET imaging biomarkers in AD

PET biomarkers	Characteristics	Limitations
<p>Biomarker of hypometabolism</p> <p>[<sup>18</sup>F]FDG</p>	<p>[<sup>18</sup>F]fluorodeoxyglucose (FDG) is used for quantification of metabolic dysfunction. It is a marker of cellular glucose uptake, which is closely correlated with tissue metabolism and synaptic dysfunction. Reduction of FDG uptake in certain brain areas (temporal and parietal lobes) is considered as a hallmark of AD pathology, resulting in 90% correct classification of these patients (Chetelat et al., 2003; Rocher et al., 2003; Mosconi et al., 2013; Brown et al., 2014).</p>	<p>FDG provides only an indirect functional assessment of neuronal activity, and cannot be considered as a direct biomarker per se, as it does not directly quantify a neuropathological substrate specific to AD. Uptake by other cell types such as astrocytes, which could bias FDG results (Zimmer et al., 2017).</p>

	<p>FDG-PET can predict the conversion of MCI to AD, and facilitate the differential diagnosis of AD, hence its widespread use as a supporting diagnostic tool (Minoshima et al., 2001;McKhann et al., 2011; Pagani et al., 2017).</p>	
<hr/>		
<p>Biomarker of Synaptic density</p>		
<hr/>		
[ <sup>11</sup> C]UCB-J	<p>Most successful and suitable PET ligand so far has been [<sup>11</sup>C]UCB-J, which binds to a ubiquitous synaptic vesicle glycoprotein 2 A (SV2A) found in synaptic vesicles of any neuron, independent of its neurotransmitter or neuron type (Nabulsi et la., 2016; Becker et al., 2020). Useful indicator of direct synaptic density in AD, as opposed to FDG. Widespread reductions of SV2A binding in medial temporal and neocortical brain regions in early AD/MCI compared to control participants (Chen et al., 2021; Mecca et al., 2020). More sensitive than MRI volumetry to indicate cognitive severity. Significant association between synaptic density (hippocampus) and cognitive performance (episodic memory) in MCI and early stages of AD, better than volumetry (Mecca et al., 2022).</p>	<p>However, despite being a direct marker of synaptic integrity, it is still considered as a non-specific biomarker for neurodegeneration in AD, as (SV2A) is not directly linked to a specific pathology of AD. This also means that the synaptic changes of selectively vulnerable neurotransmitter systems, such as the cholinergic system, cannot be accurately assessed using UCB-J. Furthermore, SV2A proteins are not exclusive to synaptic vesicles, as they are also expressed in mitochondria (Stockburger et al., 2016).</p>
<hr/>		
<p>Biomarkers of amyloid deposition</p>		
<hr/>		
[ <sup>11</sup> C] Pittsburgh compound B (PIB) [ <sup>18</sup> F]NAV4694 (NAV) [ <sup>18</sup> F]Florbetapir	<p>These amyloid PET tracers are very sensitive to detect the presence of amyloidosis at the pre-clinical stage (asymptomatic subjects) or at the MCI stages (Cselényi et al., 2012; Hatashita &amp; Wakebe, 2017; Rowe &amp; Villemagne, 2013). Brain distribution of these radiotracers in AD are found to be concordant with senile plaques observed at autopsy (Ikonovic et al., 2008; Rowe et al., 2013; Seo et al., 2017).</p>	<p>These tracers have limited ability to quantify amyloid in the progression of AD, as amyloidosis reaches a maximum level and plateaus in later disease stages (Jack et al., 2010; Chételat et al., 2020). Amyloid deposition does not show a close correlation with symptom severity in AD (Landau et al., 2012). Amyloid imaging alone is considered insufficient to predict clinical conversion in prodromal and asymptomatic stages of AD (Chételat et al., 2020).</p>
<hr/>		

		Amyloid imaging is thus uninformative to quantifying AD progression or measure the efficacy of disease modifying treatments.
<hr/>		
Biomarkers of Tau proteins:		
[ <sup>18</sup> F]-THK-5117 [ <sup>18</sup> F]-THK-5351 [ <sup>18</sup> F]-AV-1451	The second-generation tau radioligands show better sensitivity to tau than amyloid deposits, and there seems to be a more linear relationship between Tau radioligands and disease severity (Zhang et al., 2012; Chiotis et al., 2016).	There is still off target binding with the newest tau PET tracers, which could preclude accurate in vivo quantification, and limiting their selectivity as a tracer (Lemoine et al., 2018; McClauskey et al., 2020). The type of tau deposits (conformation, maturation stage, isoform) and their specific binding sites are not yet fully known in AD which could affect the binding intensity of tau tracers currently used (Saint-Aubert et al., 2017; Lowe et al., 2016). The added challenge of tau deposition in normal aging must be addressed to provide a reliable threshold and avoid false positives (McClauskey et al., 2020). Further work is required to fully characterize tau and the binding properties of the tau PET tracers (Zimmer et al., 2014).

This table summarizes the characteristics and limitations of different types of PET biomarkers in AD such as those developed for quantifying metabolic activity, synaptic density, and detection of amyloid and Tau proteins.

As shown above, the current AD biomarkers have several shortcomings, as some of the targets are not directly anchored into the AD neuropathology, while others lack sensitivity and reliability to identify and quantify AD. Using a theoretical model of the current AD biomarkers, Jack and colleagues have demonstrated that an approach sensitive to neuronal loss, irrespective of the pathophysiological process, is ideal for identifying and quantifying AD severity, from the pre-symptomatic stage up to the most severe AD stages, as such measures are closely coupled with symptom severity (Jack et al., 2010; Jack & Holtzman 2013). It has been shown that synaptic loss is an important structural correlate of cognitive impairment in AD (DeKosky et al., 1996; Mecca et al., 2022), however, as a general measure of neurodegeneration, it is not specific to any neuronal type or neurochemical system and as such it is probably not a hallmark specific

to AD (Scheff et al., 2014). As a biomarker that is specific to a hallmark of AD and which also encompasses neuronal death, irrespective of the underlying neuropathology, the cholinergic degeneration could indeed be a more suitable target. As discussed earlier, the degeneration of cholinergic neurons in AD is one of the earliest and most prevalent features in AD, as a specific neuromodulator which is selectively impacted in AD, that has a prominent role in cognition, its decline is more closely coupled to cognitive deficits compared to other neurochemical systems (monoaminergic) or other neuropathological features (Bierer et al., 1995; Dournaud et al., 1995; Shinotoh et al., 2000; Schliebs & Arendt, 2011; Ballinger et al., 2016). Even though these neurochemical systems probably have a role in cognition, directly or indirectly, their individual/distinctive dysfunction is more correlated with non-cognitive symptoms such as changes in mood, behaviors and vegetative functions (Wang et al., 2009; Šimić et al., 2017). Compared to these systems, cholinergic changes have a more direct relationship with cognitive function and are shown to progress with the disease (Mesulam, 2004). Also, the fact that some cognitive improvement is obtained by specifically targeting the cholinergic system is also indicative that the cholinergic dysfunction is more tightly linked to the cognitive decline seen in AD. Thus, an in vivo biomarker sensitive to cholinergic cell denervation would be a specific surrogate marker of neurodegeneration, as compared to quantification of synaptic density or a specific pathology such as amyloid or tau proteins.

## 1.6 The in vivo quantification of brain cholinergic denervation in AD

In the past, methods relied on postmortem identification and quantification of the cholinergic depletion in AD. However, there are now different methods to quantify these changes in vivo in human. Amongst these, positron emission tomography (PET) remains the most prolific and promising one for the development of in vivo biomarkers in AD.

### 1.6.1 PET neuroimaging

PET is an imaging technique derived from nuclear medicine that is vastly used in the field of neurodegenerative disorders for the examination of metabolism, enzyme activity, protein accumulation, etc. It allows the visualization of positron emissions produced by the decay of a radioactive agent previously injected in very small quantities into the systemic circulation (Wernick & Aarsvold, 2004). PET imaging relies on the injection of a radiotracer molecule (also called a radioligand), which is “tagged” with a positron-emitting isotope (usually Carbon-11, Oxygen-15 or Fluorine-18) that binds to a specific target in the brain. A positron emitted during the  $\beta^+$  decay of these isotopes, travels a short distance before being attracted to an electron of the surrounding tissue, at which point both particles annihilate, emitting two

perpendicular gamma rays (photons) at a 511 keV energy. The PET detector ring (scanner) records coincident events of these pairs of photons; the sum of these events can be computerized and reconstructed into images representing the spatial distribution and intensity of radiotracer concentrations in the tissue, from which the binding or uptake parameters can be derived. Since these radioactive molecules are bound to a ligand that specifically binds to a given target, PET can be used to localize the distribution of a radiotracer in the body that has a specific affinity for that target. For example, one of the most widely used radiotracers is FDG, which is a radioactive substitute for glucose, and thus makes it possible to define the sites in the body that consume the most energy. FDG is therefore widely used in the detection of cancer cells, which consume a lot of energy, or to determine the brain areas most involved in various cognitive, motor or sensory tasks, as they consume more glucose.

#### 1.6.2 Cholinergic PET biomarkers

Currently, there are three classes of cholinergic PET biomarkers, i.e., radioligands binding to three different components of the cholinergic transmission. These are radioligands specific for 1) AChE 2) cholinergic receptors (nicotinic or muscarinic subtypes) and 3) VAcHT. The synthesis enzyme of ACh (ChAT) has often been used *in vitro* for the identification of cholinergic neurons, although no successful *in vivo* PET radiotracer has yet been developed (Tiepol et al., 2019).

Radiotracers for AChE and cholinergic receptors are generally considered to be an indirect cholinergic measure and less accurate than VAcHT radiotracers, since the binding sites of the first two categories are found extracellularly in the pre and post synapse (Pappata et al., 1996; Hillmer et al., 2012; Ravasi et al., 2012; Mulholland et al., 1998). As such, both categories are strongly influenced by extracellular metabolism and by commonly used prescription drugs in AD (Ryu & Chen, 2008; Shinotoh et al., 2004). The selectivity of the AChE tracers has also been questioned as it is shown that significant concentrations of AChE are also found in non-cholinergic neurons (Mesulam & Geula, 1992). Furthermore, the majority of these radiotracers are Carbon-11 labeled which has a short half-life (20 minutes), as opposed to fluorine-18 (half life of 110 mins), limiting their use in clinical settings where no radio-synthesizing cyclotron is housed. See table 1.4 for the characteristics of AChE and cholinergic receptor radiotracers.

Table 1.4 Cholinergic PET radiotracers

Radiotracers	Characteristics	Limitations
[ <sup>11</sup> C]PMP/ [ <sup>11</sup> C]MP4A	These tracers bind to the the enzyme AChE. Reduction in binding of these tracers in AD (Bohnen et al., 2005; Hirano et al., 2018).	No correlation with PMP and hypometabolism in AD (Kuhl et al., 1999). MP4A barely distinguishes MCI patients from control subjects, and no correlation with cognitive scores (MMSE) are obtained (Rinne et al., 2003). Significantly influenced by AChE inhibitors such as Donepezil. AChE enzyme surrogate biomarker show poor reliability and specificity (Bohnen et al., 2005; Roy et al., 2016; Van Waarde et al., 2021). Both have short half-life ([ <sup>11</sup> C ] labelled).
[ <sup>18</sup> F]ASEM	Highly specific to nicotinic $\alpha$ 7-nAChRs. Increased cortical binding over the course of healthy aging. Higher binding in MCI patients than in controls (Coughlin et al., 2018, 2020).	Not yet characterized in AD. Significantly influenced by commonly prescribed medications in AD (neuroleptics) and by smoking (nicotine intake), in addition to variable results due to the different quantification methods used (Tiepol et al., 2019).
[ <sup>18</sup> F]-Flubatine	Binds to nicotinic $\alpha$ 4 $\beta$ 2-nAChRs. Reduction mainly present within the basal forebrain-cortical and septohippocampal cholinergic projections in mild AD. Positive correlation with cognitive impairment (Sabri et al., 2018).	Significantly influenced by commonly prescribed medications in AD (neuroleptics) and by smoking (nicotine intake) (Tiepol et al., 2019).
[ <sup>11</sup> C]-LSN3172176	Binds to muscarinic M1 subtype radiotracer. Recently translated to human PET imaging (Naganawa et al., 2021).	Not yet characterized in MCI or AD.

This table summarizes the characteristics and limitation of the main cholinergic PET tracers used to quantify the cholinergic system of the brain.

The third category of cholinergic PET radiotracers, the VAChT binding ligands, are believed to be more reliable than the previously mentioned classes. This category is predominantly composed of derivatives of

the molecule vesamicol, a selective inhibitor that binds non-competitively to the intracellular VAcHT, making it a direct pre-synaptic measure of cholinergic terminals (Efange, 2000).

### 1.6.3 [<sup>18</sup>F]-FEOBV as a reliable cholinergic PET radioligand

Many PET radioligands have been developed for VAcHT imaging, but only a few have proven useful for clinical use in humans. Indeed, most of them have shown poor selectivity for VAcHT, a slow uptake and distribution, and a fast metabolism in the brain (see Table 1.5 for a list of various VAcHT radiotracers).

Table 1.5 Main PET radiotracers for VAcHT

Radiotracers	Characteristics/Limitations
(-)-[ <sup>3</sup> H]vesamicol	Low selectivity for VAcHT (Altar & Marien, 1988)
[ <sup>11</sup> C]MABV	Short half-life ([ <sup>11</sup> C] labelled) limiting use in PET (Kilbourn et al., 1990)
[ <sup>18</sup> F]FMV	Kinetics profile not suitable for PET scanner Imprecise quantification of VAcHT (Rogers et al., 1994; Widen et al., 1992)
[ <sup>18</sup> F]FAA	Very rapid metabolism (Rogers et al., 1994)
(+)-[ <sup>18</sup> F]FBT	Low selectivity for VAcHT; rapid metabolism. (Efange et al., 1994; Gage et al., 2000; Mach et al., 1997)
(+)-[ <sup>18</sup> F]SpiroFBT	Very rapid metabolism (Efange et al., 1994, 1999)
(-)-[ <sup>18</sup> F]NEFA	Very rapid metabolism with no uptake in the cortex (Rogers et al., 1994)
(-)-[ <sup>11</sup> C]OMV	Short half-life ([ <sup>11</sup> C] labelled) limiting use in PET , Low selectivity for VAcHT (Kuhl et al., 1994; Mazere et al., 2013; Van Dort et al., 1993)
[ <sup>18</sup> F]FPO-BV	Low brain absorption and significant defluorination. (Giboureau et al., 2007)
[ <sup>18</sup> F]FAMV	Low lipophilicity, very rapid metabolism and accumulation of metabolites in brain and blood (Sorger et al., 2008)
[ <sup>18</sup> F]FBVM	Good selectivity for VAcHT and metabolism, further studies needed (Sorger et al., 2009).
(-)-[ <sup>18</sup> F]FEOBV*	Seems to be the best candidate for cholinergic PET imaging in humans. It shows high selectivity for VAcHT, and its safety is approved in humans. (Kilbourn et al., 2009; Landry et al., 2008a, 2008b; Mulholland et al., 1998; Mzengeza et al., 2007; Rosa-Neto et al., 2007; Soucy & Bedard, 2007; Petrou et al., 2014)

This table summarizes the main PET radiotracers developed for the VAcHT.

[<sup>18</sup>F]fluoroethoxybenzovesamicol (FEOBV) has been recently developed and investigated in Canada by our team and is the most promising PET radioligand for brain imaging of cholinergic terminals to date



(Mzengeza, et al., 2007; Cyr et al., 2015; Landry et al., 2008a; 2008b; Parent et al., 2011; 2012; 2013; Rosa-Neto et al., 2007; Soucy et al., 2010). FEOBV exhibits a very high binding affinity and an excellent specificity for VAcHT and is an excellent biomarker for cholinergic system (Landry et al., 2008a, 2008b; Mulholland et al., 1998; Rosa-Neto et al., 2007). FEOBV provides an estimate of the presynaptic neuronal integrity and is thought to remain unaffected by the post-synaptic activity of enzymes such as AChE, although this has yet to be demonstrated in vivo. This demonstrates clear advantages over other existing cholinergic radiotracers that essentially target AChE in the synaptic cleft, or the pre-post synaptic receptors, hence making FEOBV a reliable method for quantifying cerebral cholinergic nerve terminals.

Animal studies in rats have confirmed the high sensitivity of FEOBV in quantifying the severity of cholinergic degeneration in the brain (Cyr et al., 2015; Parent et al., 2012, 2013). More specifically a reduced FEOBV uptake was observed in older rats (18 months), which was limited to the hippocampus, a finding that supports current data in the literature in non-pathological aging (Canas et al., 2009). A similar reduction in binding distribution was also seen in rats with selective lesions of the cholinergic systems. Excellent correlations ( $r = .88$  to  $.97$ ) were observed between the binding potential of FEOBV, and the extent of the lesions measured ex vivo by choline acetyltransferase (ChAT) immunocytochemistry (Cyr et al., 2015; Parent et al., 2011, 2013). In addition to the high sensitivity and specificity, FEOBV is found to be selective to the location of the cholinergic lesions. Brain mapping reveals a different distribution pattern of the tracer depending on whether the lesions involve the NBM, whose cholinergic projections are essentially cortical, or whether the lesions exclusively involve the pedunclopontine nucleus (PPN), whose cholinergic projections are mainly thalamic. This is particularly important in humans when establishing a differential diagnosis using FEOBV, given that the cholinergic lesions seen in AD affect the NBM but not the PPN, whereas the reverse is observed in other neurodegenerative diseases. For example, in Parkinson's disease (PD), Multiple Systems Atrophy (MSA), Progressive Supranuclear Palsy (PSP) and dementia with Lewy body (DLB) that mainly affect the brainstem cholinergic systems, there is a significant subcortical cholinergic reduction along with some cortical involvement but in patterns that differ from the denervation in AD (Warren et al., 2007; Schmeichel et al., 2008; Mazère et al., 2012; Nejad-Davarani et al., 2019). Similar findings also apply to VD which has a prominent subcortical involvement (Mesulam, 2003).

Recent studies in humans have shown the safety of this tracer when used in humans, and its distribution in the healthy brain which corresponds to the known anatomical distribution of cholinergic terminals (Kilbourn et al., 2009; Landry et al., 2008b; Rosa-Neto et al., 2007, Petrou et al., 2014). The greatest specific

activity of FEOBV is seen in the striatum, followed by the thalamus, the temporo-parietal cortex, the hippocampus, and the cerebellar hemispheres concordant with the known distribution pattern of brain cholinergic density (Parent et al., 2012; Petrou et al., 2014). Furthermore, an autoradiographic study in AD brain tissue using FEOBV was able to detect reduced VAcHT in the same brain regions documented in AD, which reflects the degeneration of the NBM cortical cholinergic pathways (Parent et al., 2013). Such results, thus indicate that FEOBV is indeed a promising PET radioligand to explore cholinergic abnormalities in vivo in humans.

## CHAPITRE 2

### RESEARCH QUESTION, OBJECTIVES AND RATIONALE

#### 2.1 General question and aim

There is currently a lack of data on the ability of FEOBV-PET to detect in vivo cholinergic degeneration or denervation in humans presenting with a cholinergic degeneration such as AD. Therefore, validating this approach for the quantification of cholinergic integrity would be a substantial contribution to the field of AD biomarkers. Given the recent promising results obtained with FEOBV-PET in animals and cognitively normal humans, this radiotracer might represent the best candidate for such a purpose. Thus far (at the time of this research project) FEOBV has never been used with PET imaging in humans with a degenerative disorder.

The general aim of this thesis project is to characterize FEOBV used with PET imaging for the first time in a cohort of patients with AD, and to show its sensitivity and reliability to detect and quantify cholinergic denervation in these patients. We will conduct two studies within the scopes of this thesis project. The first one focuses on the quantification of cholinergic loss with FEOBV-PET and its sensitivity compared to other commonly used PET biomarkers of AD. The second study explores the concordance between cortical cholinergic denervation, as measured with FEOBV-PET, and cholinergic cell death in the cholinergic basal forebrain of AD as assessed with MRI volumetry.

#### 2.2 Study 1

The first study aims to verify for the first time in humans with AD the sensitivity and reliability with which FEOBV could quantify the cholinergic denervation in AD, and to compare this imaging method with those currently used for the diagnosis and follow up of patients with AD: PET imaging for hypometabolism (FDG) and amyloid deposition (NAV). PET imaging with FDG is a gold standard in AD diagnosis. It is considered as an indirect measure of synaptic loss, hence the interest in comparing it with FEOBV that is believed to reflect cholinergic denervation.

Imaging of A $\beta$  plaques has been extensively studied in the last decades, and the current best surrogate marker of this is the NAV PET radiotracer. We will use this tracer to confirm amyloid accumulation in our participants, and to compare its sensitivity with that of FEOBV. We chose NAV as an amyloid surrogate

biomarker, as this tracer shows the highest specificity to A $\beta$  sheets compared to other amyloid tracers and has a longer half-life (~110 minutes) given that it is a F-labeled radiotracer.

General cognitive measures such as the Mini-Mental State Examination (MMSE) and Montreal Cognitive Assessments (MoCA) will be used to quantify cognitive impairment in our sample and to explore associations with FEOBV and the other two tracers in AD.

#### 2.2.1 Study 1 - Objectives:

1. To demonstrate in cognitively normal control subjects that the brain distribution of FEOBV corresponds to the known distribution of cholinergic terminals documented in the literature.
2. To verify the sensitivity of FEOBV as a cholinergic biomarker, in comparison with that of FDG (metabolism) and NAV (amyloid) to distinguish between AD and control subjects.
3. To identify the relationship between AD severity measured by the cognitive scales and each of the three PET radioligands (FEOBV, NAV, and FDG).

#### 2.2.2 Study 1- Hypotheses:

- 1- Since FEOBV has shown high specificity to cholinergic terminals in previous animal and human studies, its distribution in healthy control subjects is expected to correspond to the known topography of brain cholinergic innervation: the highest concentration is expected in the striatum, thalamus, cerebral cortex, hippocampus and cerebellum.
- 2- Given the substantial cholinergic denervation revealed in post-mortem studies in AD, there is an expected significant reduction of FEOBV uptake in the whole cortical mantle of the AD group compared to control.
- 3- Cholinergic system is heavily depleted in AD and is suggested to be a direct indicator of AD pathology compared to amyloid or metabolic biomarkers. As such, the group difference obtained with FEOBV is expected to be more sensitive to distinguish the AD subjects from control, when compared to NAV or FDG.
- 4- Additionally, the cholinergic system is shown to be the best correlate of cognitive decline in AD. Thus, FEOBV uptake is expected to show the strongest positive correlation with scores obtained on the cognitive measures, as compared to FDG. No correlation is expected with cognitive measures and NAV, as there is an uncoupling between amyloid deposition and cognition early in AD.

## 2.3 Study 2

In order to verify the concordance between the cortical cholinergic denervation, as measured with FEOBV, with cholinergic cell death, a second study is conducted with the imaging data obtained from the first study. The second study aims at correlating the FEOBV uptake in brain areas affected vs. nonaffected in AD with the degree of atrophy of the corresponding cholinergic nuclei of the basal forebrain (Ch4 and Ch1/2), using MRI volumetry, in the AD subjects.

### 2.3.1 Study 2 - Objectives:

1. To demonstrate, using in vivo MRI-based volumetry, the topography of atrophy in different nuclei of the ChBF (Ch4 and Ch1/2), in AD subjects compared to control.
2. To demonstrate differential FEOBV uptake in cortical areas affected in AD and those areas that are relatively preserved, compared to control.
3. To identify in the AD subjects the relationship between ChBF (Ch4 and Ch1/2) volumes and FEOBV uptake in the cortical areas that are affected vs. those that are unaffected in AD.

### 2.3.2 Study 2 - Hypotheses:

1. Given the selective vulnerability of the NBM cholinergic neurons in AD, the AD subjects are expected to have smaller Ch4 (NBM) than control, and lower cortical FEOBV uptake in specific cortical regions usually affected in AD. No reduction is expected for the volume of Ch1/2 and the hippocampal FEOBV uptake, which are shown to be relatively preserved in mild-moderate AD.
2. As the Ch4 supplies cholinergic input to the cortex in a specific topographical pattern, positive correlations are expected between the Ch4 volumes and FEOBV uptake in the corresponding cortical areas that are affected in AD. As such, the posterior Ch4 is expected to correlate with the FEOBV uptake in the superior temporal areas and the more anterior portions of the Ch4 with the more anterior/frontal cortical areas.
3. Given that the cholinergic Ch1/2 is relatively preserved in AD and no cholinergic reduction is assumed in hippocampus, no relationship is expected between the Ch1/2 volume and FEOBV uptake in the hippocampus nor in any cortical area affected in AD.

## 2.4 Rationale for the methods used

### 2.4.1 PET neuroimaging

In this thesis project we used the newly developed [<sup>18</sup>F]fluoroethoxybenzovesamicol (FEOBV) radioligand, as this has been shown to be the most promising vesamicol derivative to be used with PET. It is highly sensitive and specific to VAcHT and as such, FEOBV fulfills all the requirements to be a reliable PET radioligand.

First and foremost, FEOBV is a fluorine-18 labeled radioligand, which is inherently superior to the other isotopes, as this has a much longer half-life and can be synthesized off location and be transported. FEOBV easily crosses the blood-brain barrier, and binds with high affinity to its target, the VAcHT. The kinetic profile of FEOBV is fast enough to allow short and accurate image acquisition (Mulholland et al., 1998). Furthermore, the metabolism of FEOBV reveals no radioactive metabolites capable of penetrating the CNS, in addition to exhibiting a transformation and elimination rate that is ideal for PET imaging (Landry et al., 2008a, 2008b). FEOBV is stable in the plasma and does not generate significant amounts of [18F] radicals (Kilbourn et al., 2009; Soucy et al., 2010), unlike several other vesamicol derivatives (Giboureau et al., 2007). Finally, its use in rodents, primates and humans suggests good safety when used at the microdoses required for PET (Kilbourn et al., 2009; Soucy et al., 2010, Petrou et al., 2014). While PET imaging following 240 MBq of FEOBV was sufficient to produce excellent quality PET images, human dosimetry calculations demonstrate that up to 450 MBq could be administered while keeping radiation doses below regulatory limits (Petrou et al., 2014). Moreover, no sign of toxicity was observed with this radio-compound, nor any alterations in vital signals a result of FEOBV administrations in humans at doses of  $0.7 \pm 0.3 \mu\text{g}$  (Petrou et al., 2014).

Studies using high-performance liquid chromatography were able to rule out the existence of any lipophilic metabolite capable of penetrating the blood-brain barrier and interfering with the binding of FEOBV in the brain (Landry et al., 2008b). Based on a Simplified Reference Tissue Model, it was possible to determine the binding potential of FEOBV, thus making it more accessible for routine PET scans performed in clinical settings. Additionally, FEOBV reversibly binds to VAcHT and this has been demonstrated in both rats, primates and humans (Cyr et al., 2015; Landry et al., 2008a; Rosa-Neto et al., 2007; Parent 2012; 2013; Soucy et al., 2010, Petrou et al., 2014). Furthermore, rapid penetration to and subsequent elimination from the brain is observed within the first 20 minutes following an IV administration of FEOBV, with localization observed mainly in the regions rich in cholinergic nerve terminals (Parent et al., 2012; Petrou

et al., 2014). The greatest specific activity of FEOBV is seen in the neostriatum and the frontal cortex, followed by the thalamus, the temporo-parietal cortex, the hippocampus, and the cerebellar hemispheres concordant with the known distribution pattern of brain cholinergic density (Parent et al., 2012; Petrou et al., 2014). Such data clearly suggest that FEOBV can be used safely and reliably as a PET radiotracer for the purpose of imaging brain cholinergic integrity.

#### 2.4.2 MRI

A structural MRI is an essential aspect of PET studies. PET images are superimposed on to the MRI image for the visualization and analysis of anatomical properties of the brain structures underlying the PET signal. In this study we used a 1.5T MRI machine, as this is a rapid way to obtain optimal resolution of brain images which will also be used for the volumetric analysis used in the second study.

#### 2.4.3 Cognitive measures

In order to have an objective level of the general cognitive functioning of the recruited participants, we administered two well-known and commonly used measures in clinical settings, the Mini-Mental State Examination (MMSE) and the Montreal Cognitive Assessment (MoCA) (Folstein et al., 1975; Lonie et al., 2009; Nasreddine et al., 2005; Freitas et al., 2013, Costa et al., 2014). We did not focus on any specific cognitive domains, as this was not the aim of the study. Instead, we wanted to have a general cognitive index to correlate with the cortical FEOBV uptake. Moreover, as clinical depression is an exclusion criterion for AD, we used the commonly used screening questionnaire, Geriatric Depression scale- short version (GDS-15), to exclude participants with any clinical depressive symptoms (Yesavage et al., 1982). See table 2.1.

Table 2.1 Description of the different cognitive scales used in this thesis.

MMSE	MOCA	GDS-15
Clinically standardized questionnaire to measure cognitive impairment and follow up of AD progression. The total score is out of 30. Normal cognitive functioning score is between 28-30. Mild to moderate AD scores are between 10-26. Administration time: 8-10 minutes.	Clinically standardized and sensitive tool for diagnosis and follow of AD. The total score is out of 30. Normal cognitive functioning Scores $\geq 26$ Scores below 26 indicate cognitive impairment. Administration time: 10-15 minutes	Standardized screening tool for depressive symptoms in the elderly. Short form of the original 30-item GDS. Scores between (0-4 inclusive) signify no depressive, or minimal depressive symptoms. Administration time: 5-7 minutes.

### CHAPITRE 3

#### STUDY 1 - QUANTIFICATION OF BRAIN CHOLINERGIC DENERVATION IN ALZHEIMER'S DISEASE USING PET IMAGING WITH [<sup>18</sup>F]-FEOBV

M Aghourian<sup>1,2,3</sup>, C Legault-denis<sup>1,2,3</sup>, J-P Soucy<sup>2,4,5</sup>, P Rosa-Neto<sup>2,3,4</sup>, S Gauthier<sup>3,4</sup>, A  
Kostikov<sup>2,4</sup>, P Gravel<sup>2</sup> and M-A Bedard<sup>1,2,3</sup>

<sup>1</sup>Université du Québec à Montréal (UQAM), Cognitive Pharmacology Research Unit, Montreal, QC, Canada; <sup>2</sup>McConnell Brain Imaging Centre, Montreal Neurological Institute, Montreal, QC, Canada; <sup>3</sup>McGill Centre for Studies in Aging, Douglas Mental Health University Institute, Verdun, QC, Canada; <sup>4</sup>Department of Neurology and Neurosurgery, McGill University, Montreal, QC, Canada and <sup>5</sup>PERFORM Centre, Concordia University, Montreal, QC, Canada.

(Article published in *Molecular Psychiatry*, 2017, 22 :1531-1538)



## RÉSUMÉ

Le [18F]-fluoroéthoxybenzovesamicol (FEOBV) est un nouveau radiotracer TEP qui se lie au transporteur vésiculaire de l'acétylcholine. Chez l'animal et l'humain, le FEOBV s'est révélé sensible et fiable pour caractériser les terminaisons nerveuses cholinergiques présynaptiques dans le cerveau. Il a été utilisé ici pour la première fois chez des patients atteints de la maladie d'Alzheimer (MA) pour quantifier les pertes cholinergiques cérébrales. L'échantillon comprenait 12 participants répartis équitablement entre un groupe de sujets contrôle et de patients atteints de la maladie d'Alzheimer. Chaque participant a été évalué à l'aide des échelles cognitives Mini-Mental State Examination (MMSE) et Montréal Cognitive Assessment (MoCA). Chaque participant a effectué trois séances d'imagerie TEP avec (1) le FEOBV comme traceur des terminaisons cholinergiques, (2) le [18F]-NAV4694 (NAV) comme traceur de la protéine bêta-amyloïde et (3) le [18F]-Fluorodéoxyglucose (FDG) comme agent du métabolisme cérébral. Le ratio de la valeur de fixation standard normalisée (SUVR) a ensuite été calculé pour chaque traceur et comparé entre les deux groupes à l'aide de tests-t voxel-à-voxel. Des corrélations ont également été calculées entre chaque traceur et les échelles cognitives, ainsi qu'entre le FEOBV et les deux autres radiotraceurs. Les résultats ont montré des réductions importantes de l'activité du FEOBV dans de multiples zones corticales, évidentes chez chacun des sujets atteints de la MA et dans l'ensemble du groupe atteint de la maladie, par rapport au groupe contrôle. Les traceurs FDG et NAV ont également permis de distinguer les deux groupes, mais avec une plus faible sensibilité que le FEOBV. De plus, l'activité du FEOBV était positivement corrélée à l'activité du FDG dans de nombreuses régions corticales, et négativement corrélées à l'activité du NAV dans certaines zones restreintes. Les échelles cognitives MMSE et MoCA présentaient aussi de significatives corrélations avec l'activité du FEOBV et du FDG. Ainsi, nos résultats suggèrent que le traceur FEOBV est plus sensible que les traceurs FDG ou NAV pour distinguer les patients atteints de la MA des sujets sains et qu'il pourrait s'avérer utile pour quantifier la sévérité de la maladie. Le FEOBV pourrait ainsi être utilisé pour évaluer la dégénérescence cholinergique chez l'humain, et représenter un excellent biomarqueur de la MA.

Mots clés: Acétylcholine; Alzheimer; Biomarqueur; Démence; FEOBV; FDG; Vesamicol.

## ABSTRACT

[<sup>18</sup>F]-fluoroethoxybenzovesamicol (FEOBV) is a new PET radiotracer that binds to the vesicular acetylcholine transporter. In both animals and healthy humans, FEOBV was found sensitive and reliable to characterize presynaptic cholinergic nerve terminals in the brain. It has been used here for the first time in patients with Alzheimer's disease (AD) to quantify brain cholinergic losses. The sample included 12 participants evenly divided in healthy subjects and patients with AD, all assessed with the Mini-Mental State Examination (MMSE) and Montreal Cognitive Assessment (MoCA) cognitive scales. Every participant underwent three consecutive PET imaging sessions with (1) the FEOBV as a tracer of the cholinergic terminals, (2) the 18F-NAV4694 (NAV) as an amyloid-beta tracer, and (3) the 18F-Fluorodeoxyglucose (FDG) as a brain metabolism agent. Standardized uptake value ratios (SUVRs) were computed for each tracer and compared between the two groups using voxel wise t-tests. Correlations were also computed between each tracer and the cognitive scales, as well as between FEOBV and the two other radiotracers. Results showed major reductions of FEOBV uptake in multiple cortical areas that were evident in each AD subject, and in the AD group as a whole when compared to the control group. FDG and NAV were also able to distinguish the two groups, but with lower sensitivity than FEOBV. FEOBV uptake values were positively correlated with FDG in numerous cortical areas, and negatively correlated with NAV in some restricted areas. The MMSE and MoCA cognitive scales were found to correlate significantly with FEOBV and with FDG, but not with NAV. We concluded that PET imaging with FEOBV is more sensitive than either FDG or NAV to distinguish AD patients from control subjects and may be useful to quantify disease severity. FEOBV can be used to assess cholinergic degeneration in human, and may represent an excellent biomarker for AD.

Key words: Acetylcholine; Alzheimer; Biomarker; Dementia; FEOBV; FDG; Vesamicol.

### 3.1 Introduction

Postmortem studies have shown that cholinergic cell death occurs early in Alzheimer's disease (AD), and strongly correlates with symptom severity throughout the evolution of the disease (Dournaud et al., 1995; Grothe et al., 2014; Mufson et al., 2016). Recent neuroimaging evidence revealed that the Ch4 cell group of the basal forebrain known to contain the cholinergic cells innervating the cortex may degenerate many years prior to the cortical spread of amyloid plaques and the appearance of cognitive symptoms (Schmitz & Spreng, 2016). However, there is currently a lack of *in vivo* measurements sensitive enough to measure such cholinergic cell death in human.

Over the last decade, our team has conducted studies allowing us to better characterize the radiochemical properties (Landry et al., 2008a, 2008b; Mzengeza et al., 2007) and the PET imaging suitability (Cyr et al., 2014; Parent et al., 2012; Parent et al., 2013; Rosa-Neto et al., 2007; Soucy et al., 2010) of [<sup>18</sup>F]fluoroethoxybenzovesamicol (FEOBV). This radiotracer exhibits a very high binding affinity and an excellent specificity for the vesicular acetylcholine (ACh) transporter (VAChT), a glycoprotein found on the membrane of synaptic vesicles of cholinergic neurons, which ensures the translocation of cytoplasmic ACh into synaptic vesicles.

The use of FEOBV as an *in vivo* marker of cholinergic nerve terminals in the brain was first suggested by Mulholland et al., (1998) who identified the sub-nanomolar affinity of the (–)-FEOBV enantiomer toward the vesicular ACh transporter and described the dosimetry and biodistribution of its Fluor-18 equivalent in rodents. More recently, our studies in rats have demonstrated the ability of FEOBV PET imaging to detect and quantify experimentally induced brain cholinergic denervation. Excellent correlations were observed between the *in vivo* binding of FEOBV and the extent of cholinergic losses measured *ex vivo* by cholineacetyltransferase immunocytochemistry (Cyr et al., 2014 ; Parent et al., 2012 ; Parent et al., 2013). Moreover, this sensitivity was not only quantitative, as brain mapping revealed a different distribution of the tracer, depending on whether the lesions involved the nucleus basalis of Meynert (NBM) (Parent et al., 2012), whose cholinergic projections are essentially cortical, or the pedunculopontinenucleus (PPN) (Cyr et al., 2014), whose cholinergic projections are mainly thalamic. This feature suggests that FEOBV could be used clinically to differentiate neurodegenerative diseases. For instance, cholinergic lesions in AD affect the NBM but not the PPN, while the opposite is observed in other degenerative diseases, such as progressive supranuclear palsy (Mazère et al., 2012; Warren et al., 2005) or multiple system atrophy (Schmeichel et al., 2008).

FEOBV has recently been studied in healthy human volunteers (Petrou et al., 2014), and showed a very good safety profile for injected mass doses between 0.3 and 1.3 µg. Its brain distribution in human was similar to that observed in rats (Parent et al., 2012; Rosa-Neto et al., 2007) and primates (Soucy et al., 2010), with the greatest specific binding found in the neostriatum, followed by the thalamus, the cortex and the hippocampus. Thus far, FEOBV has never been used with PET imaging in humans presenting brain cholinergic degeneration. The aim of the present study was therefore to evaluate whether FEOBV PET can detect regionally specific cholinergic denervation in AD, and to compare its sensitivity to those of [18F]fluorodeoxyglucose (FDG), and [18F]NAV4694 (NAV) PET imaging in distinguishing AD patients from normal subjects. FDG uptake abnormalities in AD are thought to reflect regional cerebral hypometabolism associated with decreased neurotransmission, with potential applications in monitoring AD severity and progression, as well as assessing the efficacy of disease-modifying interventions (Jagust et al., 2007). NAV (formerly known as AZ4694) is an amyloid-beta PET imaging agent with characteristics similar to those of the more frequently used <sup>11</sup>CPIB, but with the convenience of <sup>18</sup>F labeling, and a higher specific cortical binding coupled to lower nonspecific white matter binding than those of the other available <sup>18</sup>F labeled agent (Rowe et al., 2013; Cselényi et al., 2012). We hypothesized that FEOBV imaging would distinguish patients with AD from healthy participants with greater accuracy than either FDG or NAV imaging.

## 3.2 Method

### 3.2.1 Subjects

The study sample consisted of 12 participants, including six patients diagnosed with probable AD, and six age-matched healthy volunteers enrolled mostly among the spouses of the patients. This sample size is similar to those of previous studies conducted with FEOBV in rodents, showing significant differences between the experimental group with induced mild cholinergic lesions and controls (Cyr et al., 2014; Parent et al., 2012). AD patients in the present study were diagnosed using the standard criteria of the 'Alzheimer's Association Workgroup on Diagnostic Guidelines for Alzheimer's Disease' (Dubois et al., 2007). Abnormal levels of brain amyloid-beta (Aβ) plaques were confirmed in patients with AD by using PET imaging with NAV, with a SUVR cut off value of 1.5 or greater. At the time of their enrolment, all AD patients had undergone treatment with a cholinesterase inhibitor for at least two months.

To be included in this study, all participants were assessed with the Mini-Mental State Examination (MMSE), and the Montreal Cognitive Assessment (MoCA). The main inclusion criteria for AD patients were MMSE and MoCa scores of 26 or lower. In control subjects, only participants with MMSE and MoCA scores

higher than 26 were included. The Geriatric Depression Scale (GDS) was also administered to all participants, in order to rule out the presence of mood disorders. Participants with a GDS score over five were excluded. Participants with other active medical or psychiatric issues that could affect cognitive function were also excluded from the study. In addition, any clinical or brain imaging evidence of vascular disease, Lewy body disease, any form of Primary Progressive Aphasia, or frontotemporal dementia/frontal temporal lobar were considered as exclusion criteria.

All participants were recruited at the McGill Center for Studies in Aging (MCSA) and assessed at the McConnell Brain Imaging Unit (BIC) of the Montreal Neurological Institute (MNI). The study protocol was approved by 'Université du Québec à Montréal' (UQAM) and McGill University Research Ethics Boards, covering all the authors and their affiliated hospitals and research centers (including the MCSA and MNI). Informed consent was obtained from all subjects prior to participation in the study.

### 3.2.2 Imaging data acquisition

All participants first underwent a structural T1 MRI (1.5T Siemens Sonata), followed by a PET scan (Siemens HRRT) done on the same day with one of the three radiotracers FEOBV, FDG, or NAV. PET scans using the two remaining tracers were completed within a 2-week interval. For FDG scans the participants had to fast for 3h prior to the injection of the tracer. FDG was purchased from a local vendor (Isologic Innovative Radiopharmaceuticals, Montreal, QC, Canada). FEOBV and NAV were synthesized at the BIC Cyclotron Facility. The precursor for both FEOBV and NAV were purchased from commercial vendors (ABX Advanced Biochemical Compounds, Radeberg, Germany and NAVIDEA Biopharmaceutical, Dublin, OH, USA). Radiolabeling methods for the compounds are similar and have been described elsewhere (Mzengeza et al., 2007). A total of 36 PET scans were performed for the purpose of this study, corresponding to one scan for each radiotracer (FEOBV, FDG and NAV) for each of the 12 participants. Each radiotracer was administered by slow IV bolus injection with radioactive doses varying between 160 and 340 MBq. Before data acquisition, the PET scanner was calibrated by performing a standard quality control protocol. A 5 min transmission scan for attenuation correction, using a source of [<sup>137</sup>Cs], was performed before injection of the tracer. PET data acquisition was done in 3D list mode. For FEOBV, data was acquired three hours following injection, over 30 min in six frames of 5 min. For FDG, data were obtained 30 min following injection, and acquired over 30 min in one frame of 1200s. For NAV, data were obtained 30 min following injection and acquired over 30 min in 6 frames of 5 min. A head holder was used to minimize head motion during the scan.

### 3.2.3 Image processing and analyses

PET images were reconstructed using an OP-OSEM (OrdinaryPoisson-Ordered Subset Expectation Maximization) algorithm correcting for scattering, random coincidences, attenuation, decay and dead time; frame-based motion corrections were also performed if needed. The MINC software toolbox was used to perform all image analyses (<http://www.bic.mni.mcgill.ca/ServicesSoftware/MINC>) according to the following steps: (1) MR images of all participants were first co-registered to the MNI-152 standard reference template by the CIVET image-processing pipeline, using a 6-parameter affine transformation and non-linear spatial normalization; (2) time-averaged PET images were normalized as a function of the injected dose of tracer and the subject's weight to obtain standard uptake values (SUVs); (3) The PET SUVs image was then co-registered to the subject's own MRI, and from there to the MNI-152 template using the linear and non-linear transformations obtained in the first step; (4) Standardized uptake value ratio (SUVR) maps were generated for FEOBV, FDG and NAV, by using respectively the global cerebral white matter, the pons, and the cerebellar cortex as reference regions. While previous studies (Cyr et al., 2015; Parent et al., 2012; Petrou et al., 2007) have used the cerebellar cortex as reference tissue for FEOBV, we chose the global cerebral white matter based on the non-specific binding observed on the time activity curves of each subject. In addition, it is known also that cerebellar cortex receives cholinergic projections from various brainstem nuclei, while the global cerebral white matter is devoid of such neurochemical projections; (5) Finally, smoothing of the PET images was performed using a Gaussian kernel of 8 mm. No correction for partial volume effect was applied to the PET imaging data.

The two groups were compared on demographic variables and on total score of each cognitive scale using independent Student t-tests. SUVR differences between AD and control subjects were explored separately for FEOBV, FDG and NAV, using voxel-wise analysis of covariance, with age as a covariate. Statistical t-maps were then generated for each radiotracer. In comparison to control subjects, AD subjects were expected to show lower SUVRs for both FEOBV and FDG, and higher SUVRs for NAV. Significance thresholds were therefore based on one-tailed t-tests with a minimal statistical significance of 2.2 ( $p = 0.03$ ).

Correlational analyses between FEOBV and each of the two other radiotracers (FDG and NAV) were performed in AD patients by using VOXELSTATS, a MATLAB package for multimodal voxel-wise brain image analyses (Mathotaarachchi et al., 2016). On the basis of the generated correlational statistical t-maps, significant voxel clusters were identified. MNI predefined brain topographical masks were applied over these voxel clusters for each subject, in order to extract the regional SUVRs. The SUVRs were then

corrected for age by using a linear model to obtain the standardized residual values. Pearson’s r-values were computed from these residuals.

In order to perform correlational analysis in AD between the cognitive scales (MMSE and MoCA) and the cortical SUVR values of each radiotracer, a mask covering the whole cortex was used. Standardized residuals for the cortical SUVR values and cognitive scales were obtained by using a general linear model adjusting for age and education, using Rstudio. Pearson’s r-values were the computed from these standardized residual values.

### 3.3 Results

Normal data distributions were confirmed by the non-significance of the Shapiro–Wilk tests for small groups. Demographic features of the sample are summarized in Table 3.1. The Male/Female ratio was the same in each group, and there was no significant difference for age, education or GDS scores. However, AD patients differed significantly from control subjects on the two cognitive scales (MMSE:  $t = -3.391$ ,  $P = 0.007$ ; MoCA:  $t = -5.198$ ,  $P = 0.005$ ). In the control group, MMSE and MoCA scores varied respectively from 29 to 30, and from 27 to 29. In patients with AD, scores on these scales ranged from 7 to 26 for the MMSE, and from 4 to 23 for the MoCA.

Table 3.1 Sample characteristics

	AD (n=6)	Control (n=6)
Gender ratio, F:M	3:3	3:3
Age, years	67.2 (10.24)	67.0 (11.12)
Education, years	16.8 (5.03)	14.7 (3.88)
MMSE, total score	18.3 (7.31)	29.2 (0.41)
MoCA, total score	12.8 (6.49)	27.0 (1.55)
GDS, total score	2.5 (2.16)	1.0 (0.89)

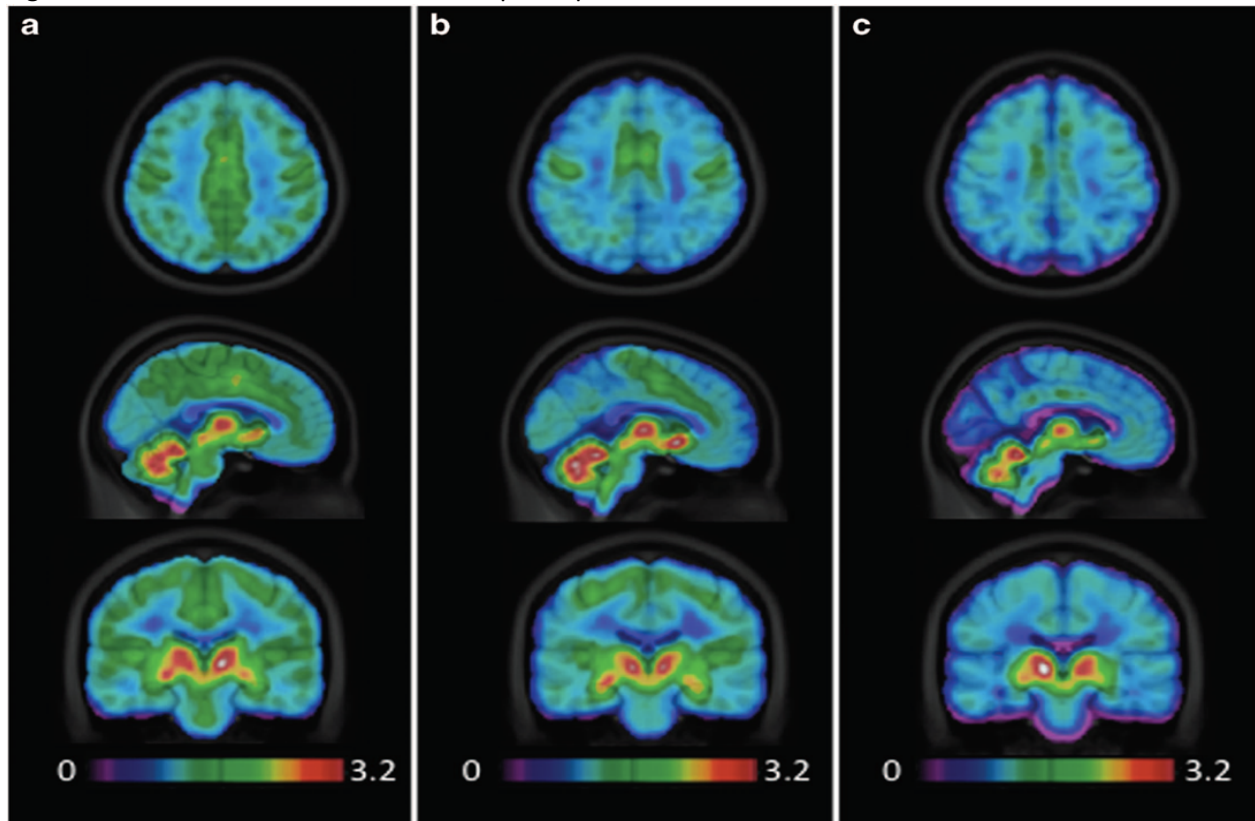
Abbreviations: AD, Alzheimer’s disease; F, female; GDS, Geriatric Depression Scale; M, male; MMSE, Mini-Mental State Examination; MoCA, Montreal Cognitive Assessment.

#### 3.3.1 PET imaging in AD and control subjects

PET images in control subjects, taken from each participant (Figure 3.1a) or from the group average (Figure 3.2a), revealed the greatest FEOBV uptake in brain areas known to be the most innervated by the cholinergic systems, including the striatum, thalamus, cerebral cortex as a whole, hippocampal area and

cerebellum. In AD patients, PET imaging revealed a significant reduction of FEOBV uptake in comparison with control subjects. This can be observed in both, images from each participant (Figure 3.1b), as well as from the group average (Figure 3.2b).

Figure 3.1 FEOBV SUVR in three different participants with AD.



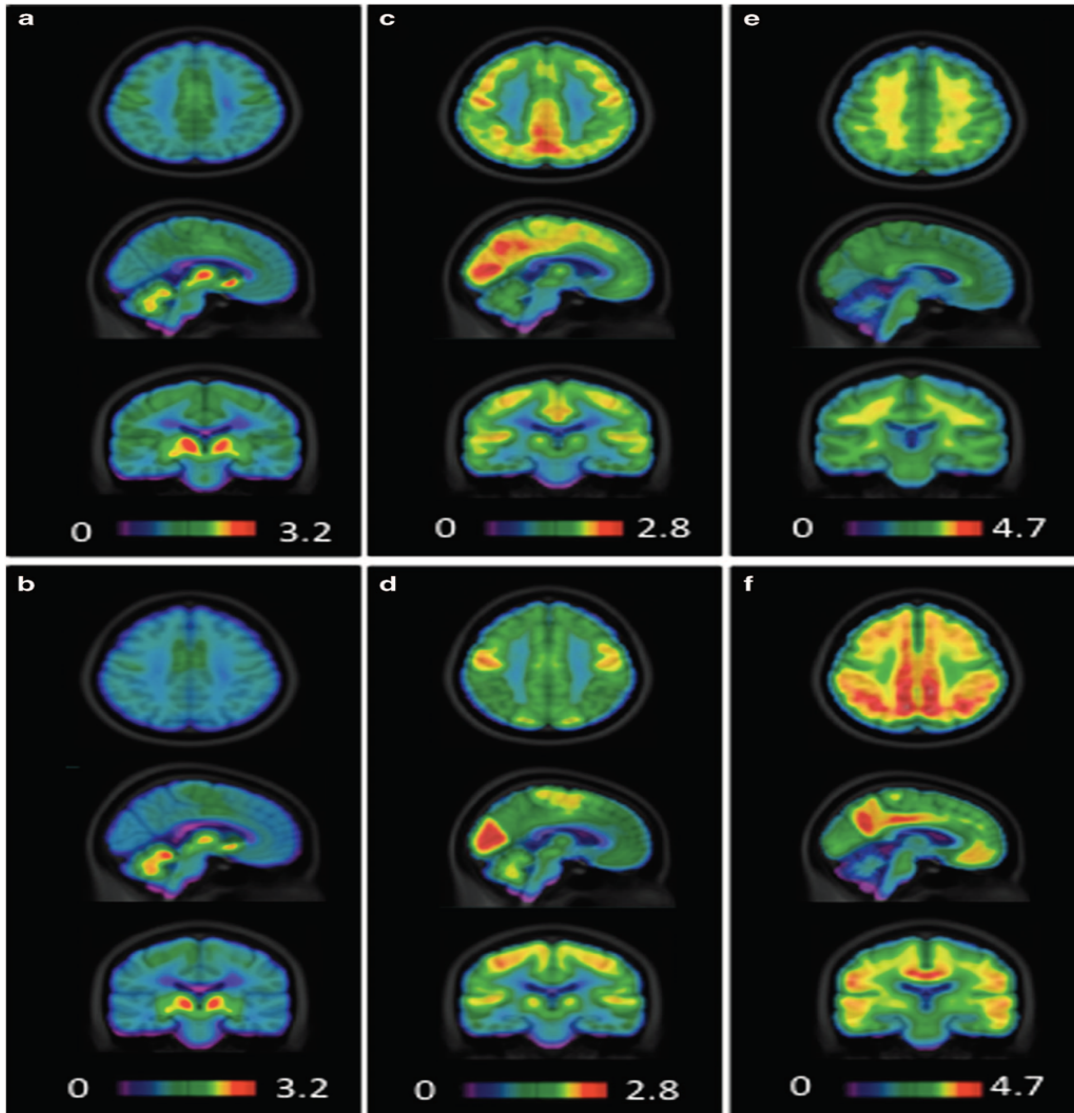
FEOBV SUVRs in three different participants showing a gradient of severity of the cortical cholinergic denervation. One healthy control subject (a), one patient with mild AD (b) and one patient with severe AD (c). AD, Alzheimer's disease; FEOBV, 18F-fluoroethoxybenzovesamicol; SUVR, standardized uptake value ratio.

Statistical analyses confirmed these observations, showing reduced FEOBV SUVR values compared to controls over the whole cortex, bilaterally, with t-values ranging between 5.6 and 12.5, all statistically significant at  $P < 0.0001$  (Figure 3a). The greatest FEOBV reductions in AD were observed in the superior and middle temporal cortex (right:  $t = 12.55$ ,  $P < 0.00001$ , left:  $t = 13.84$ ,  $P < 0.00001$ ), with an extension to the inferior parietal lobule (right:  $t = 6.70$ ,  $P = 0.00002$ , left:  $t = 9.10$ ,  $P < 0.00001$ ). Severe reductions were observed also in the posterior medial cortical territory that encompasses the cingulate cortex (right:  $t = 9.22$ ,  $P < 0.00001$ , left:  $t = 7.32$ ,  $P = 0.000013$ ), and the precuneus (right:  $t = 8.308$ ,  $P < 0.00001$ , left:  $t = 7.103$ ,  $P = 0.00001$ ). More anteriorly, there was also some reduction in the medial frontal cortex (right:  $t = 5.58$ ,  $P = 0.00011$ , left:  $t = 8.45$ ,  $P < 0.00001$ ) and lateral frontal cortex (right:  $t = 5.58$ ,  $P = 0.00011$ , left:  $t = 6.21$ ,



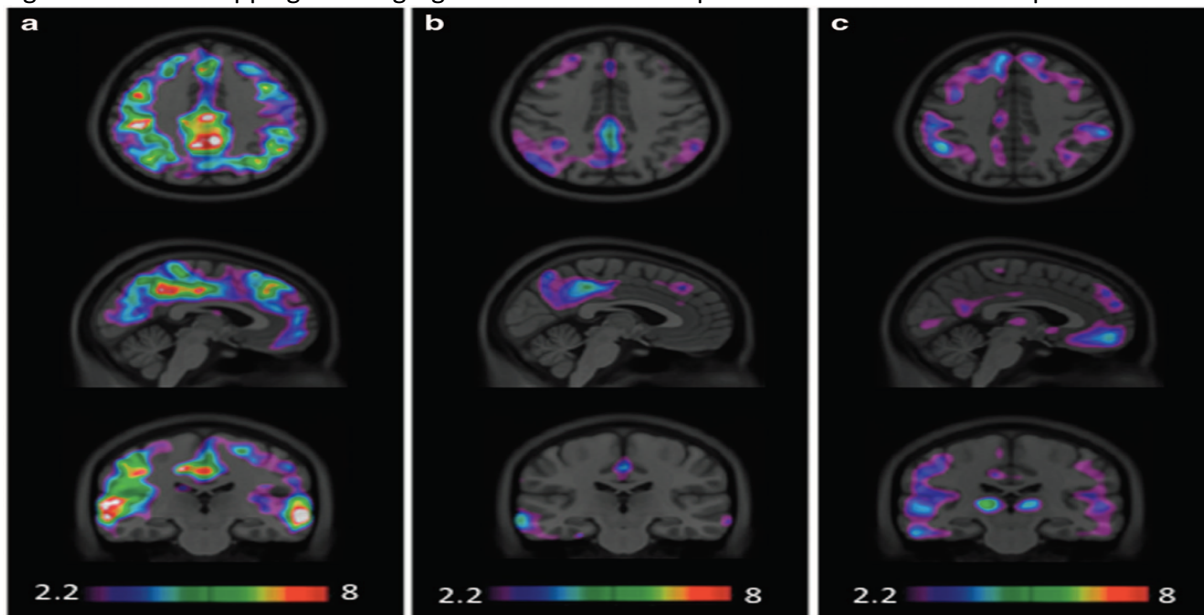
P0.00005). No significant differences were found in the hippocampus, thalamus, striatum or cerebellum. Regional FEOBV uptake reductions in patients with AD were highly variable among the different areas, ranging from 8.9% in the anterior cingulate, to 51% in the superior temporal gyrus.

Figure 3.2 Average SUVRs for the three PET radiotracers (FEOBV, FDG and NAV).



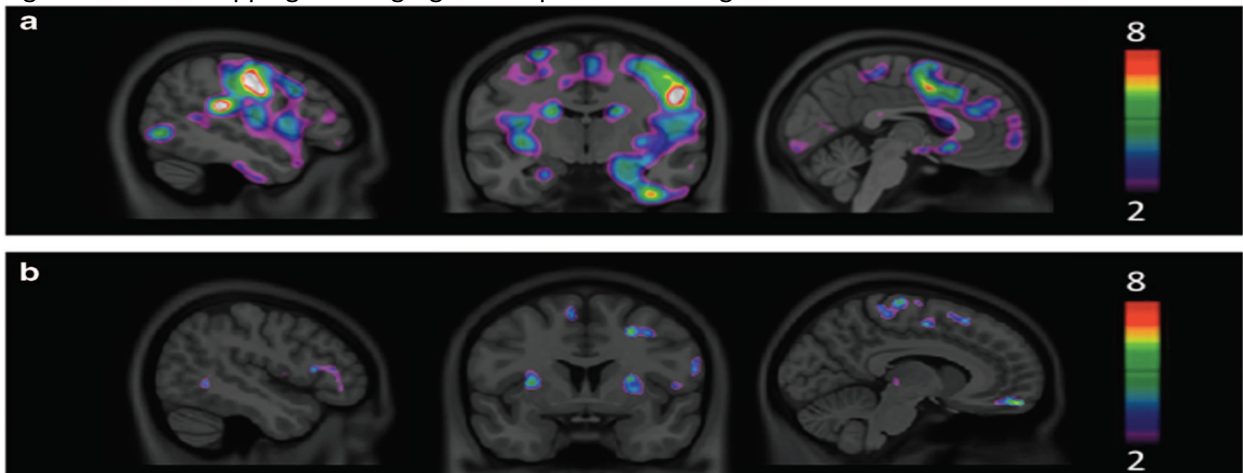
Average SUVR radiotracer uptake for the three radiotracers; FEOBV in healthy controls (a) and patients with AD (b). FDG in healthy controls (c) and patients with AD (d). NAV in healthy controls (e) and patients with AD (f). Scales differ for each tracer allowing optimal contrast for each image. AD, Alzheimer's disease; FDG, <sup>18</sup>F Fluorodeoxyglucose; FEOBV, <sup>18</sup>F-fluoroethoxybenzovesamicol; NAV, <sup>18</sup>F-NAV4694; SUVR, standardized uptake value ratio.

Figure 3.3 Brain mapping showing significant radiotracer uptake differences in AD compared to control.



Brain mapping showing the voxel based significant differences (t values) between healthy controls, and patients with AD for FEOBV (a), FDG (b) and NAV (c). Although all radiotracers revealed abnormalities in similar cortical areas, more extended territories and greater intergroup differences were detected with FEOBV than with the two other radiotracers. Scales are the same for the three tracers allowing comparisons. AD, Alzheimer's disease; FDG, 18F-Fluorodeoxyglucose; FEOBV, 18F-fluoroethoxybenzovesamicol; NAV, 18F-NAV4694.

Figure 3.4 Brain mapping showing significant positive and negative correlations between the radiotracers.



Brain mapping showing significant positive correlations (t-values) between FEOBV and FDG (a), and significant negative correlations between FEOBV and NAV (b), in patients with AD. Coefficient of correlation (r-values) are presented in the text. AD, Alzheimer's disease; FDG, 18F-Fluorodeoxyglucose; FEOBV, 18F-fluoroethoxybenzovesamicol; NAV, 18F-NAV4694.

Results of FDG PET imaging showed significant differences between the two groups in areas similar to those described above with FEOBV. However, FDG SUVR reductions in AD were of lower magnitude and included topographically smaller areas than those observed with FEOBV, as revealed by lower t-values ranging from 2.7 to 4.0 (Figure 3b). The differences in FDG uptake between the two groups were observed in areas that include the posterior cingulate cortex (right:  $t = 4.35$ ,  $P = 0.00072$ , left:  $t = 4.27$ ,  $P = 0.00081$ ), precuneus (right:  $t = 3.99$ ,  $P = 0.0012$ , left:  $t = 3.72$ ,  $P = 0.0019$ ), parietal cortex (right:  $t = 2.73$ ,  $P = 0.01$ , left:  $t = 3.6$ ,  $P = 0.0024$ ), middle temporal cortex (right:  $t = 2.99$ ,  $P = 0.007$ , left:  $t = 3.91$ ,  $P = 0.001$ ), and lateral frontal cortex (right:  $t = 2.67$ ,  $P = 0.011$ , left:  $t = 4.34$ ,  $P < 0.00073$ ).

PET imaging with NAV also revealed significant differences between the two groups in cortical areas similar to some of those described with FEOBV. These include the medial frontal (right:  $t = 3.14$ ,  $P = 0.0052$ , left:  $t = 4.21$ ,  $P = 0.0009$ ) and prefrontal cortex (right:  $t = 4.15$ ,  $P = 0.0009$ , left:  $t = 4.57$ ,  $P = 0.0005$ ), as well as the lateral frontal cortex (right:  $t = 5.19$ ,  $P = 0.0002$ , left:  $t = 4.35$ ,  $P = 0.0007$ ), the temporal cortex (right:  $t = 3.49$ ,  $P = 0.0029$ , left:  $t = 4.34$ ,  $P = 0.0007$ ), and the parietal cortex (right:  $t = 3.78$ ,  $P = 0.0018$ , left:  $t = 4.43$ ,  $P = 0.0006$ ). Contrary to what was observed with FEOBV and FDG, no difference was seen in the posterior portions of the cingulate gyri or precuneus. Moreover, as shown previously, the greatest difference between the two groups was observed in the thalamus (right:  $t = 5.21$ ,  $P = 0.0002$ , left:  $t = 5.55$ ,  $P = 0.0001$ ).

### 3.3.2 FEOBV correlations with FDG and NAV

In subjects with AD, there were positive correlations between FEOBV and FDG uptakes in some cortical areas (Figure 3a), although these regions do not always correspond to territories with the reduced FEOBV uptake. Correlations between FEOBV and FDG were particularly high in the right hemisphere, and involved the supramarginal ( $r = 0.98$ ), precentral ( $r = 0.94$ ), and inferior temporal gyri ( $r = 0.83$ ), as well as the medial frontal ( $r = 0.87$ ), and prefrontal cortex ( $r = 0.87$ ). There were also bilateral significant correlations between the two tracers in the insular area ( $r = 0.97$ ) and the hippocampal/entorhinal region ( $r = 0.81$ ).

Negative correlations between FEOBV and NAV in the cortex were statistically significant only in limited areas of the medial ( $r = -0.90$ ) and lateral prefrontal ( $r = -0.88$ ) cortex, as well as in the precentral gyrus ( $r = -0.97$ ) of the right hemisphere. The striatum, in both hemispheres, was also a site of strong negative correlations ( $r = -0.90$ ) between the two tracers (Figure 3b).

### 3.3.3 Correlations between FEOBV and cognitive scales

Patients with AD showed significant positive correlations between their average cortical FEOBV uptake and scores obtained on the MMSE ( $r = 0.88$ ,  $P = 0.02$ ) and MoCA ( $r = 0.86$ ,  $P = 0.02$ ) scales. The same was observed with FDG, which correlated with both MMSE ( $r = 0.86$ ,  $P = 0.02$ ) and MoCA ( $r = 0.85$ ,  $P = 0.03$ ). However, there was no significant correlation between the average NAV uptake and any of the cognitive scales.

## 3.4 Discussion

In the present study, PET imaging with FEOBV was performed for we believe the first time in AD subjects and allowed us to quantify and map brain cholinergic denervation. We observed major reductions of FEOBV uptake in the cortical areas known to be affected in AD. These reductions were not only evident from statistical comparisons between AD patients and healthy participants, but also from qualitative visual inspection of PET images of each AD participant. Moreover, reduction in FEOBV activity in AD varied as a function of the clinical severity of dementia as assessed with standardized scales, adding to the clinical relevance of this radiotracer.

### 3.4.1 FEOBV and the cholinergic systems in AD

The most significant reductions of FEOBV uptake in our AD patients were observed in the temporal–parietal cortex and the posterior portions of the cingulate gyri. Reductions were also found to be statistically significant in the medial and lateral frontal cortex. This topographic pattern of FEOBV uptake anomalies seems to follow the known pattern of cholinergic terminal losses observed during progression of the disease. Indeed, the Ch4 group of neurons of the basal forebrain, which is known to be affected in AD (Whitehouse et al., 1982), can be subdivided into multiple clusters of neurons oriented in a caudal–rostral axis. These in turn are known to innervate the cerebral cortex in a caudal–rostral pattern from the superior temporal gyrus, with its angular and supramarginal parietal extensions, toward the anterior areas that include the cingulate, medial, and lateral frontal cortices (Mesulam & Geula, 1988). An extensive review of the literature suggests that there is a caudal–rostral pattern of degeneration of the basal forebrain in AD brain (Liu et al., 2015), which corresponds to the cortical topographic gradient of severity observed here.

In patients with AD, there was no evidence of FEOBV uptake reduction in brain areas, known to remain unaffected by the disease, including the striatum, thalamus and cerebellum. However, the hippocampus,

which is heavily involved in AD, does not show a reduction in FEOBV uptake, despite a rich cholinergic innervation from the basal forebrain (Whitehouse et al., 1982; Mesulam & Geula, 1988). The explanation may reside in the specific cholinergic fibers innervating the hippocampus, which come essentially from the septum (Ch2), and not from the nucleus basalis of Meynert (Ch4). Ch2 cell loss in AD has been reported to be minimal (Lehéricy et al., 1993; Mufson et al., 1993) or even insignificant (Fujishiro et al., 2006) compared to that found in age-matched controls. This may also explain why FEOBV autoradiography previously performed on AD postmortem tissues has revealed significant changes in the cortex, but not in the dentate gyrus of the hippocampus (Parent et al., 2013). Alternatively, it has also been suggested that a compensatory cholinergic fiber sprouting may occur in the dentate gyrus in AD, possibly in response to deafferentation of glutamatergic perforant pathway fibers originating from the entorhinal cortex (Hyman et al., 1987).

FDG results in our AD patients confirmed the findings of others (Kato et al., 2016; Minoshima et al., 1995) that hypometabolism occurs mostly in the posterior cingulate cortex, precuneus and parietotemporal cortex, with a lesser reduction in the frontal cortex, and no change in the hippocampus. These FDG features involve the same cortical areas as those showing reduced FEOBV uptake. Such a concordance might indicate that cholinergic denervation in AD could underlie, at least in part, the metabolic reduction measured with FDG. This view is reinforced by recent results (Iizuka & Kameyama, 2016) showing that cholinergic treatment in patients with AD was able to restore the reduced cerebral perfusion—a measure directly correlated with hypometabolism with the greatest effect observed in the posterior cingulate cortex and precuneus. It should be stressed, however, that differences between AD patients and normal controls in the present study were larger and easier to observe with FEOBV than with FDG, suggesting a better sensitivity of FEOBV over FDG for the purpose of identifying AD-affected regions.

Similarly, t-test analyses performed on both FEOBV, and NAV revealed better accuracy of FEOBV in distinguishing patients with AD from healthy controls. Such a result may appear surprising as amyloid PET imaging agents, including NAV, are known for their very high sensitivity to detect AD (Rowe et al., 2013; Cselényi et al., 2012). However, it should be stressed that significant amyloid loads have also been well described with these amyloid agents in cognitively normal subjects. In our sample, two control participants showed relatively high NAV SUVRs with normal cognitive performance, and without reduction of either FDG or FEOBV uptakes. This adds to the preexisting evidence in the literature (Jack et al., 2013) questioning the relevance of amyloid imaging agents as reliable biomarkers for evaluating AD. In addition, contrary to

NAV, FEOBV uptake in the whole cortex showed very good correlations with both the MMSE and MoCA cognitive scales, suggesting its potential usefulness in assessing the severity of AD. Therefore, FEOBV, more than FDG or NAV, might be an excellent tool for both the clinical identification and the follow up of patients with AD.

One limitation of PET studies is the partial volume effect (PVE), which refers to spreading of signal over the surrounding cerebral areas. PVE is of particular importance in AD as cortical atrophy may enhance its effect. Although not sufficient on its own to explain the current results, PVE might partly affect the results observed here. However, PVE was minimized in this study by the high-resolution images acquired with the brain dedicated HRRT PET scanner. Furthermore, multiple partial volume corrections have been developed to reduce PVE, all presenting pros and cons, and potentially leading to a wide range of results (Thomas et al., 2011). Given that our FEOBV data remained practically unchanged following such partial volume correction, we chose to report non-corrected data, as they directly reflect the actual distribution of FEOBV in AD.

Besides FEOBV, other PET radiotracers have been used in the past to assess cholinergic terminal losses in AD, but their sensitivity and reliability remain questionable. For example, N-[11C]methyl-piperidin-4-yl propionate (PMP), a selective radiotracer for the acetylcholinesterase (AChE) enzyme (Irie et al., 1994), has shown a 9% to 33% reduced binding (Kuhl et al., 1999) in AD patients depending on the severity of the disease. However, this reduction was found to be significantly influenced by AChE inhibitors, such as donepezil (Bohnen et al., 2005). In addition, no correlation could be observed between PMP measurements and FDG imaging parameters (Kuhl et al., 1999). Such a modest or low sensitivity has also been obtained with another AChE enzyme radiotracer, N-[11C]methyl-4-piperidyl acetate (MP4A), as patients with AD dementia were barely distinguishable from patients with mild cognitive impairment (MCI) or control subjects, and no correlation could be found with MMSE scores (Rinne et al., 2003). Given that FEOBV does not bind to the AChE enzyme but rather to the vesicular ACh transporter (Landry et al., 2008a ; Mulholland et al., 1998) it provides a better estimate of presynaptic neuronal integrity, and remains unaffected by the use of AChE inhibitors.

#### 3.4.2 FEOBV amongst AD biomarkers

Substantial developments have taken place in the field of AD biomarkers in a relatively short time period, and neuroimaging remains a very promising approach (Jack et al., 2013). MRI volumetric methods have

shown hippocampal atrophy in AD, with a specificity of 80 to 90% in differentiating AD from Mild Cognitive Impairment and from cognitively normal cases (Westman et al., 2011a). MRI volumetry has also showed excellent correlations with both MMSE scores and Braak neuropathological staging of disease severity (Jack et al., 2002). However, MRI volumetric methods are much less satisfactory in distinguishing AD from other etiologies of dementia such as Parkinson's disease, dementia with Lewy body, vascular dementia, or frontotemporal lobar degeneration (Laakso et al., 1996; Hashimoto et al., 1998; Harper et al., 2016).

Cerebral hypoperfusion has been demonstrated in AD by using single-photon emission computed tomography (SPECT), and the cortical areas affected are the same as those showing reduced metabolic activity with FDG-PET.<sup>44</sup> These two methods can be considered as good indicators of synaptic dysfunction (Rocher et al., 2003), resulting in a 90% correct classification of AD patients (Mosconi, 2005), although the accuracy of SPECT perfusion imaging remains significantly inferior to that of PET (O'Brien et al., 2014). They can also predict the conversion from MCI to AD (Chetelat et al., 2003) and facilitate the differential diagnosis of AD (Foster et al., 2007; Minoshima et al., 2001; Mosconi et al., 2008), and hence they are recommended as complementary diagnostic tools (Jagust et al., 2007; Dubois et al., 2007; Bohnen et al., 2012). However, blood flow quantification with SPECT and brain metabolism assessment with FDG-PET provide indirect measurements of neuronal integrity, and therefore cannot be considered as direct biomarkers for determining neuropathological changes in AD.

Over the last 10 years, PET radiotracers of amyloid plaques and Tau protein aggregates have been investigated either separately (Klunk et al., 2004 ; Kolb & Andrés, 2017) or in combination (Pascoal et al., 2017) in the assessment of neurodegenerative diseases. Amyloid tracers such as PIB, NAV, or Florbetapir are all sensitive enough to detect the presence of amyloidosis at the pre-clinical stage, that is, in asymptomatic subjects (Aizenstein et al., 2008), or at the stage of MCI (Kemppainen et al., 2007). However, the utility of such amyloid imaging agents is limited because early on during the clinical evolution of the disease, amyloid load seems to reach a maximum, which makes assessment of AD severity difficult (Aizenstein et al., 2008; Kemppainen et al., 2007; Jack and Holtzman, 2013). Tau protein imaging is of more interest, as there seems to be a more linear deposition of Tau in relation to disease progression. However, the current concern with specificity of binding for these agents has yet to be addressed (Kolb & Andrés, 2017).

As discussed above, current AD biomarkers have several shortcomings, and the search for a reliable single biomarker that could facilitate both early detection, assessment of disease progression and grading of its severity is ongoing. According to the AD biomarker modeling suggested by Jack and Holtzman (2013), those that are sensitive to neurodegeneration might be the best candidates. As such, FEOBV, with its high sensitivity to cholinergic cell death is very promising.

Interest toward the cholinergic hypothesis in AD has considerably decreased over the last two decades, mostly because of the poor efficacy of the current AChE inhibitor treatments. However, recent evidence (Schmitz & Spreng, 2016) shows that cholinergic cell death in the basal forebrain could precede the formation and spreading of A $\beta$  aggregates in the cortex, adding to the importance of compounds such as FEOBV in studying AD. Caution is warranted, however, as results of the present study were obtained from a small sample of patients with AD. Further studies are required to better characterize FEOBV not only in AD, but also in other diseases associated with cholinergic depletion and clinical dementia such as in Lewy Body Disease, Progressive Supranuclear Palsy, Multiple System Atrophy or Parkinson's disease.



### 3.5 Author contributions

M.A.B and J.P.S were responsible for conception and design of the study. M.A., C.L.D., A.K., S.G., P.R.N., P.G. were responsible for acquisition and analysis of neuroimaging data. M.A., M.A.B. and J.P.S. were responsible for drafting the manuscript text, tables and figures.

### 3.6 References

- Aizenstein, H. J., Nebes, R. D., Saxton, J. A., Price, J. C., Mathis, C. A., Tsopelas, N. D., ... & Klunk, W. E. (2008). Frequent amyloid deposition without significant cognitive impairment among the elderly. *Archives of neurology*, *65*(11), 1509-1517.
- Bohnen, N. I., Djang, D. S., Herholz, K., Anzai, Y., & Minoshima, S. (2012). Effectiveness and safety of 18F-FDG PET in the evaluation of dementia: a review of the recent literature. *Journal of Nuclear Medicine*, *53*(1), 59-71.
- Bohnen, N. I., Kaufer, D. I., Hendrickson, R., Ivanco, L. S., Lopresti, B. J., Koeppe, R. A., ... & Moore, R. Y. (2005). Degree of inhibition of cortical acetylcholinesterase activity and cognitive effects by donepezil treatment in Alzheimer's disease. *Journal of Neurology, Neurosurgery & Psychiatry*, *76*(3), 315-319.
- Chetelat, G., Desgranges, B., De La Sayette, V., Viader, F., Eustache, F., & Baron, J. C. (2003). Mild cognitive impairment: can FDG-PET predict who is to rapidly convert to Alzheimer's disease?. *Neurology*, *60*(8), 1374-1377.
- Cselényi, Z., Jönhagen, M. E., Forsberg, A., Halldin, C., Julin, P., Schou, M., ... & Farde, L. (2012). Clinical validation of 18F-AZD4694, an amyloid- $\beta$ -specific PET radioligand. *Journal of Nuclear Medicine*, *53*(3), 415-424.
- Cyr, M., Parent, M. J., Mechawar, N., Rosa-Neto, P., Soucy, J. P., Aliaga, A., ... & Bedard, M. A. (2014). PET imaging with [18F] fluoroethoxybenzovesamicol ([18F] FEOBV) following selective lesion of cholinergic pedunclopontine tegmental neurons in rat. *Nuclear medicine and biology*, *41*(1), 96-101.
- Dournaud, P., Delaere, P., Hauw, J. J., & Epelbaum, J. (1995). Differential correlation between neurochemical deficits, neuropathology, and cognitive status in Alzheimer's disease. *Neurobiology of aging*, *16*(5), 817-823.
- Dubois, B., Feldman, H. H., Jacova, C., DeKosky, S. T., Barberger-Gateau, P., Cummings, J., ... & Scheltens, P. (2007). Research criteria for the diagnosis of Alzheimer's disease: revising the NINCDS-ADRDA criteria. *The Lancet Neurology*, *6*(8), 734-746.
- Foster, N. L., Heidebrink, J. L., Clark, C. M., Jagust, W. J., Arnold, S. E., Barbas, N. R., ... & Minoshima, S. (2007). FDG-PET improves accuracy in distinguishing frontotemporal dementia and Alzheimer's disease. *Brain*, *130*(10), 2616-2635.
- Fujishiro, H., Umegaki, H., Isojima, D., Akatsu, H., Iguchi, A., & Kosaka, K. (2006). Depletion of cholinergic neurons in the nucleus of the medial septum and the vertical limb of the diagonal band in dementia with Lewy bodies. *Acta neuropathologica*, *111*(2), 109-114.
- Grothe, M. J., Schuster, C., Bauer, F., Heinsen, H., Prudlo, J., & Teipel, S. J. (2014). Atrophy of the cholinergic basal forebrain in dementia with Lewy bodies and Alzheimer's disease dementia. *Journal of neurology*, *261*(10), 1939-1948.

- Harper, L., Fumagalli, G. G., Barkhof, F., Scheltens, P., O'Brien, J. T., Bouwman, F., ... & Schott, J. M. (2016). MRI visual rating scales in the diagnosis of dementia: evaluation in 184 post-mortem confirmed cases. *Brain*, *139*(4), 1211-1225.
- Hashimoto, M., Kitagaki, H., Imamura, T., Hirono, N., Shimomura, T., Kazui, H., ... & Mori, E. (1998). Medial temporal and whole-brain atrophy in dementia with Lewy bodies: a volumetric MRI study. *Neurology*, *51*(2), 357-362.
- Hyman, B. T., Van Hoesen, G. W., & Damasio, A. R. (1987). Alzheimer's disease: glutamate depletion in the hippocampal perforant pathway zone. *Annals of neurology*, *22*(1), 37-40.
- Iizuka, T., & Kameyama, M. (2017). Cholinergic enhancement increases regional cerebral blood flow to the posterior cingulate cortex in mild Alzheimer's disease. *Geriatrics & gerontology international*, *17*(6), 951-95.
- Irie, T., Fukushi, K., Akimoto, Y., Tamagami, H., & Nozaki, T. (1994). Design and evaluation of radioactive acetylcholine analogs for mapping brain acetylcholinesterase (AChE) in vivo. *Nuclear medicine and biology*, *21*(6), 801-808.
- Jack, C. R., Dickson, D. W., Parisi, J. E., Xu, Y. C., Cha, R. H., O'Brien, P. C., ... & Petersen, R. C. (2002). Antemortem MRI findings correlate with hippocampal neuropathology in typical aging and dementia. *Neurology*, *58*(5), 750-757.
- Jack Jr, C. R., Knopman, D. S., Jagust, W. J., Shaw, L. M., Aisen, P. S., Weiner, M. W., ... & Trojanowski, J. Q. (2010). Hypothetical model of dynamic biomarkers of the Alzheimer's pathological cascade. *The Lancet Neurology*, *9*(1), 119-128.
- Jack Jr, C. R., & Holtzman, D. M. (2013). Biomarker modeling of Alzheimer's disease. *Neuron*, *80*(6), 1347-1358.
- Jack Jr, C. R., Knopman, D. S., Jagust, W. J., Petersen, R. C., Weiner, M. W., Aisen, P. S., ... & Trojanowski, J. Q. (2013). Tracking pathophysiological processes in Alzheimer's disease: an updated hypothetical model of dynamic biomarkers. *The Lancet Neurology*, *12*(2), 207-216.
- Jagust, W. M. R. B., Reed, B., Mungas, D., Ellis, W., & DeCarli, C. (2007). What does fluorodeoxyglucose PET imaging add to a clinical diagnosis of dementia?. *Neurology*, *69*(9), 871-877.
- Jagust, W., Thisted, R., Devous, M. D., Van Heertum, R., Mayberg, H., Jobst, K., ... & Borys, N. (2001). SPECT perfusion imaging in the diagnosis of Alzheimer's disease: a clinical-pathologic study. *Neurology*, *56*(7), 950-956.
- Kato, T., Inui, Y., Nakamura, A., & Ito, K. (2016). Brain fluorodeoxyglucose (FDG) PET in dementia. *Ageing research reviews*, *30*, 73-84.
- Kemppainen, N. M., Aalto, S., Wilson, I. A., Någren, K., Helin, S., Brück, A., ... & Rinne, J. O. (2007). PET amyloid ligand [11C] PIB uptake is increased in mild cognitive impairment. *Neurology*, *68*(19), 1603-1606.

- Klunk, W. E., Engler, H., Nordberg, A., Wang, Y., Blomqvist, G., Holt, D. P., ... & Långström, B. (2004). Imaging brain amyloid in Alzheimer's disease with Pittsburgh Compound-B. *Annals of Neurology: Official Journal of the American Neurological Association and the Child Neurology Society*, 55(3), 306-319.
- Kolb, H. C., & Andrés, J. I. (2017). Tau positron emission tomography imaging. *Cold Spring Harbor perspectives in biology*, 9(5), a023721.
- Kuhl, D. E., Koeppe, R. A., Minoshima, S., Snyder, S. E., Ficaró, E. P., Foster, N. L., ... & Kilbourn, M. R. (1999). In vivo mapping of cerebral acetylcholinesterase activity in aging and Alzheimer's disease. *Neurology*, 52(4), 691-691.
- Laakso, M. P., Partanen, K., Riekkinen, P., Lehtovirta, M., Helkala, E. L., Hallikainen, M., ... & Soininen, H. (1996). Hippocampal volumes in Alzheimer's disease, Parkinson's disease with and without dementia, and in vascular dementia: An MRI study. *Neurology*, 46(3), 678-681.
- Landry, E., Rosa-Neto, P., Massarweh, G., Aliaga, A., Mzengeza, F., Bedard, M. A., & Soucy, J. P. (2008). Plasma chromatographic profile of [18F]-FEOBV in rat: results and implications for clinical applications. *Can J Neurol Sci*, 35, S46.
- Landry, E., Rosa-Neto, P., Massarweh, G., Aliaga, A., Mzengeza, S., Bedard, M. A., & Soucy, J. P. (2008). Distribution of [18F]-FEOBV in rat: a promising tracer for imaging cholinergic innervation densities. *Can J Neurol Sci*, 35, S46.
- Lehéricy, S., Hirsch, É. C., Cervera-Piérot, P., Hersh, L. B., Bakchine, S., Piette, F., ... & Agid, Y. (1993). Heterogeneity and selectivity of the degeneration of cholinergic neurons in the basal forebrain of patients with Alzheimer's disease. *Journal of Comparative Neurology*, 330(1), 15-31.
- Liu, A. K. L., Chang, R. C. C., Pearce, R. K., & Gentleman, S. M. (2015). Nucleus basalis of Meynert revisited: anatomy, history and differential involvement in Alzheimer's and Parkinson's disease. *Acta neuropathologica*, 129(4), 527-540.
- Mathotaarachchi, S., Wang, S., Shin, M., Pascoal, T. A., Benedet, A. L., Kang, M. S., ... & Rosa-Neto, P. (2016). VoxelStats: a MATLAB package for multi-modal voxel-wise brain image analysis. *Frontiers in neuroinformatics*, 10, 20.
- Mazère, J., Meissner, W. G., Mayo, W., Sibon, I., Lamare, F., Guilloteau, D., ... & Allard, M. (2012). Progressive supranuclear palsy: in vivo SPECT imaging of presynaptic vesicular acetylcholine transporter with [123I] iodobenzovesamicol. *Radiology*, 265(2), 537-543.
- Mesulam, M. M., & Geula, C. (1988). Nucleus basalis (Ch4) and cortical cholinergic innervation in the human brain: observations based on the distribution of acetylcholinesterase and choline acetyltransferase. *Journal of Comparative Neurology*, 275(2), 216-240.
- Minoshima, S., Foster, N. L., Sima, A. A., Frey, K. A., Albin, R. L., & Kuhl, D. E. (2001). Alzheimer's disease versus dementia with Lewy bodies: cerebral metabolic distinction with autopsy confirmation. *Annals of Neurology: Official Journal of the American Neurological Association and the Child Neurology Society*, 50(3), 358-365.

- Minoshima, S., Frey, K. A., Koeppe, R. A., Foster, N. L., & Kuhl, D. E. (1995). A diagnostic approach in Alzheimer's disease using three-dimensional stereotactic surface projections of fluorine-18-FDG PET. *Journal of Nuclear Medicine*, *36*(7), 1238-1248.
- Mosconi, L. (2005). Brain glucose metabolism in the early and specific diagnosis of Alzheimer's disease. *European journal of nuclear medicine and molecular imaging*, *32*(4), 486-510.
- Mosconi, L., Tsui, W. H., Herholz, K., Pupi, A., Drzezga, A., Lucignani, G., ... & De Leon, M. J. (2008). Multicenter standardized 18F-FDG PET diagnosis of mild cognitive impairment, Alzheimer's disease, and other dementias. *Journal of nuclear medicine*, *49*(3), 390-398.
- Mufson, E. J., Cochran, E., Benzing, W., & Kordower, J. H. (1993). Galaninergic innervation of the cholinergic vertical limb of the diagonal band (Ch2) and bed nucleus of the Stria terminalis in aging, Alzheimer's disease and down's syndrome (Part 1 of 2). *Dementia and Geriatric Cognitive Disorders*, *4*(5), 237-243.
- Mufson, E. J., Ikonovic, M. D., Counts, S. E., Perez, S. E., Malek-Ahmadi, M., Scheff, S. W., & Ginsberg, S. D. (2016). Molecular and cellular pathophysiology of preclinical Alzheimer's disease. *Behavioural brain research*, *311*, 54-69.
- Mulholland, G. K., Wieland, D. M., Kilbourn, M. R., Frey, K. A., Sherman, P. S., Carey, J. E., & Kuhl, D. E. (1998). [18F] fluoroethoxy-benzovesamicol, a PET radiotracer for the vesicular acetylcholine transporter and cholinergic synapses. *Synapse*, *30*(3), 263-274.
- Mzengeza, S., Massarweh, G., Rosa Neto, P., Soucy, J. P., & Bedard, M. A. (2007). Radiosynthesis of [18F] FEOV and in vivo PET imaging of acetylcholine vesicular transporter in the rat. *J Cereb Blood Flow Metab*, *27*(1S), 10-17U.
- O'Brien, J. T., Firbank, M. J., Davison, C., Barnett, N., Bamford, C., Donaldson, C., ... & Lloyd, J. (2014). 18F-FDG PET and perfusion SPECT in the diagnosis of Alzheimer and Lewy body dementias. *Journal of Nuclear Medicine*, *55*(12), 1959-1965.
- Parent, M. J., Bedard, M. A., Aliaga, A., Minuzzi, L., Mechawar, N., Soucy, J. P., ... & Rosa-Neto, P. (2013). Cholinergic depletion in Alzheimer's disease shown by [18F] FEOBV autoradiography. *International journal of molecular imaging*, *2013*.
- Parent, M., Bedard, M. A., Aliaga, A., Soucy, J. P., St-Pierre, E. L., Cyr, M., ... & Rosa-Neto, P. (2012). PET imaging of cholinergic deficits in rats using [18F] fluoroethoxybenzovesamicol ([18F] FEOBV). *Neuroimage*, *62*(1), 555-561.
- Pascoal, T. A., Mathotaarachchi, S., Mohades, S., Benedet, A. L., Chung, C. O., Shin, M., ... & Rosa-Neto, P. (2017). Amyloid- $\beta$  and hyperphosphorylated tau synergy drives metabolic decline in preclinical Alzheimer's disease. *Molecular psychiatry*, *22*(2), 306-311.
- Petrou, M., Frey, K. A., Kilbourn, M. R., Scott, P. J., Raffel, D. M., Bohnen, N. I., ... & Koeppe, R. A. (2014). In vivo imaging of human cholinergic nerve terminals with (-)-5-18F-Fluoroethoxybenzovesamicol: Biodistribution, dosimetry, and tracer kinetic analyses. *Journal of Nuclear Medicine*, *55*(3), 396-404.

- Rinne, J. O., Kaasinen, V., Järvenpää, T., Någren, K., Roivainen, A., Yu, M., ... & Kurki, T. (2003). Brain acetylcholinesterase activity in mild cognitive impairment and early Alzheimer's disease. *Journal of Neurology, Neurosurgery & Psychiatry*, *74*(1), 113-115.
- Rocher, A. B., Chapon, F., Blaizot, X., Baron, J. C., & Chavoix, C. (2003). Resting-state brain glucose utilization as measured by PET is directly related to regional synaptophysin levels: a study in baboons. *Neuroimage*, *20*(3), 1894-1898.
- Rosa-Neto, P., Alliaga, A., Mzengeza, S., Massarweh, G., Landry, E., Bédard, M. A., & Soucy, J. P. (2007). Imaging vesicular acetylcholine transporter in rodents using [18F] Fluoroethoxybenzovesamicol and micro-PET. *J Cer Blood Flow Metab*, *27*(Suppl 1), PP03-07M.
- Rowe, C. C., Pejoska, S., Mulligan, R. S., Jones, G., Chan, J. G., Svensson, S., ... & Villemagne, V. L. (2013). Head-to-head comparison of 11C-PiB and 18F-AZD4694 (NAV4694) for  $\beta$ -amyloid imaging in aging and dementia. *Journal of Nuclear Medicine*, *54*(6), 880-886.
- Schmeichel, A. M., Buchhalter, L. C., Low, P. A., Parisi, J. E., Boeve, B. W., Sandroni, P., & Benarroch, E. E. (2008). Mesopontine cholinergic neuron involvement in Lewy body dementia and multiple system atrophy. *Neurology*, *70*(5), 368-373.
- Schmitz, T. W., & Spreng, R. N. (2016). Basal forebrain degeneration precedes and predicts the cortical spread of Alzheimer's pathology. *Nature communications*, *7*(1), 1-13.
- Soucy, J. P., Rosa, P., Massarweh, G., Aliaga, A., Schirmacher, E., Bédard, M. A., ... & Reader, A. (2010). P1-388: Imaging of cholinergic terminals in the non-human primate brain using 18F-FEOBV PET: Development of a tool to assess cholinergic losses in Alzheimer's disease. *Alzheimer's & Dementia*, *6*, S286-S286.
- Thomas, B. A., Erlandsson, K., Modat, M., Thurfjell, L., Vandenberghe, R., Ourselin, S., & Hutton, B. F. (2011). The importance of appropriate partial volume correction for PET quantification in Alzheimer's disease. *European journal of nuclear medicine and molecular imaging*, *38*(6), 1104-1119.
- Warren, N. M., Piggott, M. A., Perry, E. K., & Burn, D. J. (2005). Cholinergic systems in progressive supranuclear palsy. *Brain*, *128*(2), 239-249.
- Westman, E., Simmons, A., Zhang, Y., Muehlboeck, J. S., Tunnard, C., Liu, Y., ... & AddNeuroMed Consortium. (2011). Multivariate analysis of MRI data for Alzheimer's disease, mild cognitive impairment and healthy controls. *Neuroimage*, *54*(2), 1178-1187.
- Whitehouse, P. J., Price, D. L., Struble, R. G., Clark, A. W., Coyle, J. T., & Delon, M. R. (1982). Alzheimer's disease and senile dementia: loss of neurons in the basal forebrain. *Science*, *215*(4537), 1237-1239.

### 3.7 Conclusion of the first study and the conception of the subsequent study

With the first study, we were able to conclude that quantification of cortical cholinergic depletion in AD with FEOBV-PET is a more sensitive tool than other surrogate markers of AD such as amyloid or metabolic PET, to identify AD and quantify its severity. Interestingly, the results also confirmed that the topography of cortical FEOBV depletion was concordant with the known pattern of basal forebrain cholinergic degeneration. In order to verify the concordance between cortical cholinergic denervation, measured with FEOBV-PET, with the basal forebrain cholinergic cell death, a second study is conducted with the data obtained from the first study. This second study would enable us to determine with certainty that the cortical decrease in FEOBV in AD is in fact due to the degeneration of the cortical projection of the NBM cholinergic neurons.

## CHAPITRE 4

### STUDY 2 – FEOBV-PET TO QUANTIFY CORTICAL CHOLINERGIC DENERVATION IN AD : RELATIONSHIP TO BASAL FOREBRAIN VOLUMETRY

Meghmik Aghourian<sup>1,2</sup>, Étienne Aumont<sup>1,2</sup>, Michel J. Grothe<sup>3,4</sup>, Jean-Paul Soucy<sup>2</sup>,  
Pedro Rosa-Neto<sup>2,5</sup>, and Marc-André Bedard<sup>1,2</sup>

<sup>1</sup>Cognitive Pharmacology Research Unit, Université du Québec à Montréal (UQAM), Canada; <sup>2</sup>McConnell Brain Imaging Centre, Montreal Neurological Institute, Canada; <sup>3</sup>Instituto de Biomedicina de Sevilla, Hospital Universitario Virgen del Rocío/CSIC/Universidad de Sevilla, Seville, Spain; <sup>4</sup>DZNE, German Center for Neurodegenerative Diseases, Rostock, Germany; <sup>5</sup>Translational Neuroimaging Laboratory, McGill University Research Centre for Studies in Aging, Douglas Mental Health University Institute, Canada.

(Article published in *Journal of Neuroimaging*, August 2021, 31(6), 1077-1081)



## Résumé

Dans la première étude nous avons montré que le 18F-fluoroéthoxybenzovesamicol ( $[^{18}\text{F}]$ -FEOBV) utilisé avec TEP était très sensible pour quantifier la dénervation cholinergique cérébrale dans la maladie d'Alzheimer (MA). La présente étude exploratoire vise ainsi à vérifier la fiabilité du FEOBV dans cette maladie en démontrant la concordance entre le volume des noyaux cholinergiques du prosencéphale basal (ChBF) et l'activité du FEOBV. L'échantillon comprend 12 participants répartis équitablement entre un groupe de sujets contrôle et de patients atteints de la MA. Tous les participants ont effectué une imagerie par résonance magnétique (IRM) et une imagerie TEP avec le  $[^{18}\text{F}]$ -FEOBV, et une segmentation du ChBF a été effectuée chez chaque participant. Des comparaisons ont ensuite été réalisées entre les deux groupes, ainsi que des corrélations chez les patients atteints de la MA entre l'activité du  $[^{18}\text{F}]$ -FEOBV dans des régions d'intérêt (ROI) corticales et le volume des noyaux du ChBF, comprenant le noyau basal de Meynert (Ch4) et le septum médial/membrane verticale de la bande diagonale de Broca (Ch1/2). Les patients atteints de la MA ont montré à la fois des volumes du ChBF-Ch4 et une activité du  $[^{18}\text{F}]$ -FEOBV plus faible que les sujets sains. De plus, les volumes de la subdivision du noyau Ch4 étaient significativement corrélés à l'activité du  $[^{18}\text{F}]$ -FEOBV observée dans les ROIs. Par ailleurs, les volumes de la subdivision du noyau Ch1/2, qui reste relativement intacte dans la MA, n'étaient pas corrélés à l'activité du  $[^{18}\text{F}]$ -FEOBV dans l'hippocampe, ni dans aucune zone corticale. Ces résultats suggèrent que la dénervation cholinergique corticale mesurée par le  $[^{18}\text{F}]$ -FEOBV est proportionnelle à l'atrophie du ChBF mesurée par IRM, ce qui confirme la fiabilité et la validité du traceur  $[^{18}\text{F}]$ -FEOBV pour quantifier la dégénérescence cholinergique dans la MA.

Mots clés: FEOBV, imagerie TEP, volume des noyaux cholinergiques du prosencéphale basal, le système cholinergique, maladie d'Alzheimer.

## ABSTRACT

**Background and Purpose:** Fluorine-18-fluoroethoxybenzovesamicol ( $[^{18}\text{F}]$ -FEOBV) is a PET radiotracer previously used in neurodegenerative diseases to quantify brain cholinergic denervation. The current exploratory study aimed at verifying the reliability of such an approach in Alzheimer Disease (AD) by demonstrating its concordance with MRI volumetry of the cholinergic basal forebrain (ChBF). **Methods:** The sample included 12 participants evenly divided between healthy volunteers and patients with AD. All participants underwent MRI ChBF volumetry and PET imaging with  $[^{18}\text{F}]$ -FEOBV. Comparisons were made between the two groups, and partial correlations were performed in the AD patients between  $[^{18}\text{F}]$ -FEOBV uptake in specific cortical regions of interest (ROIs) and volumetry of the corresponding ChBF subareas, which include the nucleus basalis of Meynert (Ch4), and the medial septum/vertical limb of the diagonal band of Broca (Ch1/2). **Results:** Patients with AD showed both lower ChBF-Ch4 volumetric values and lower  $[^{18}\text{F}]$ -FEOBV cortical uptake than healthy volunteers. Volumes of the Ch4 subdivision were significantly correlated with the  $[^{18}\text{F}]$ -FEOBV uptake values observed in the relevant ROIs. Volumes of the Ch1/2, which remains relatively unaffected in AD, did not correlate with  $[^{18}\text{F}]$ -FEOBV uptake in the hippocampus, nor in any cortical area. **Conclusion:** These results suggest that cortical cholinergic denervation as measured with  $[^{18}\text{F}]$ -FEOBV PET is proportional to ChBF atrophy measured by MRI-based volumetry, further supporting the reliability and validity of  $[^{18}\text{F}]$ -FEOBV PET to quantify cholinergic degeneration in AD.

**Keywords:** FEOBV, PET imaging, volumetry, basal forebrain, cholinergic system, Alzheimer disease.

## 4.1 Introduction

Alzheimer's Disease (AD) is characterized by a progressive degeneration of the basal forebrain cholinergic neurons, resulting in a severe cholinergic denervation of the whole cortical mantle. Several PET-radiotracers have been developed to quantify in vivo this cortical cholinergic denervation; so far,  $^{18}\text{F}$ -fluroethoxybenzovesamicol ( $^{18}\text{F}$ -FEOBV) is believed to be the most sensitive and reliable one to assess that parameter (Wenzel et al., 2021) This radiotracer exhibits a very high binding affinity and selectivity for the vesicular acetylcholine transporter (VACHT) (Mulholland et al., 1998), a glycoprotein found essentially in cholinergic synapses. PET imaging with  $^{18}\text{F}$ -FEOBV was found sensitive to even very subtle cholinergic denervation resulting from selective basal forebrain or mesopontine lesions (Cyr et al., 2015; Parent et al., 2012).

Measuring brain cholinergic denervation with  $^{18}\text{F}$ -FEOBV was recently found to be more sensitive than AD surrogate biomarkers of amyloid and metabolic PET (Aghourian et al., 2017). Indeed, the cholinergic denervation measured by  $^{18}\text{F}$ -FEOBV in AD followed a cortical topography and a temporal-cingulate severity pattern that seemed concordant with the posterior-anterior pattern of basal forebrain degeneration described in post-mortem (Liu et al., 2015) and MRI volumetric studies (Grothe et al., 2012; Fernández-Cabello et al., 2020; Schmitz et al., 2018). However, this has never been directly demonstrated within a given sample of patients. In the current study we explored, in AD subjects, the possibility of a concordance between the topography of  $^{18}\text{F}$ -FEOBV uptake reduction in the cerebral cortex, and the topography of the cholinergic basal forebrain (ChBF) neurodegeneration as estimated with MRI volumetry.

## 4.2 Method

### 4.2.1 Participants

The study sample consisted of 12 participants, including six patients diagnosed with probable AD, and six age-matched healthy volunteers. AD patients were diagnosed using the standard criteria of the "Alzheimer's Association Workgroup on Diagnostic Guidelines for Alzheimer's Disease" (Dubois et al., 2007). All participants underwent an extensive neuropsychological assessment, in addition to a T1-weighted 1.5T structural MRI, and a PET scan with  $^{18}\text{F}$ -FEOBV, all performed at the Brain Imaging Center of the Montreal Neurological Institute. At the time of their enrollment, all AD patients had undergone treatment with a cholinesterase inhibitor for more than six months. All sample features and brain imaging data acquisition methods have been described in detail in Aghourian et al., (2017). The study protocol was

approved by “Université du Québec à Montréal” (UQAM) and McGill University Research Ethics Boards. Informed consent was obtained from all participants prior to their inclusion in the study.

#### 4.2.2 PET and MRI data processing

Based on the voxel wise analyses of [<sup>18</sup>F]-FEOBV uptake reduction described previously in AD (Aghourian et al., 2017), several cortical regions were identified. The MNI-152 atlas was used to delineate these regions of interest (ROI) on each subject’s PET images. Seven PET ROIs were used including: 1) superior temporal gyrus; 2) inferior parietal lobule (IPL); 3) cingulate cortex; 4) precuneus; 5) medial frontal cortex; 6) occipital cortex; 7) hippocampus. Occipital lobe and hippocampus were used here as control ROIs, as they were previously shown to not suffer significant cholinergic denervation in AD. For each subject the mean standard uptake value ratios (SUVR) were computed in these ROIs using a supraventricular white matter (WM) mask as reference region. This WM mask encompassed both hemispheres and excluded voxels close to the cortex and ventricles to avoid partial volume effects.

The MRI volumetry of ChBF was performed in each participant using an automated volumetry pipeline previously described in detail in Grothe and colleagues (2018). Preprocessing included automated tissue type segmentation and spatial normalization of each participant’s MR image to the MNI standard space using the high-dimensional registration algorithm DARTEL to obtain a modulated grey matter (GM) map. GM volumes of the individual cholinergic nuclei were extracted using ChBF cytoarchitectonic maps defined by Kilimann and colleagues (2014). The latter were obtained from histologically delineated ChBF subareas of a post-mortem brain and its corresponding MRI coordinates, allowing projection into MNI standard space. From these subareas the following were kept because of their relevance in AD: 1) The cholinergic nuclei of the medial septum (Ch1) and vertical limb of the diagonal band of Broca (Ch2), taken together (Ch1/2), as they both provide the cholinergic innervation for the whole hippocampal complex; 2) the nucleus basalis of Meynert (Ch4), which projects to the entire cerebral cortex (Mesulam, 2004; Mesulam & Geula, 1988). The latter Ch4 nucleus was further subdivided into three components. A posterior (Ch4p) part was delineated given the importance of this area in AD-related ChBF atrophy (Kiliman et al., 2014; Grothe et al., 2012). Anterior and intermediate parts were also delineated but had to be grouped together (Ch4a-i) because of their very small extent. We did not differentiate between left and right hemispheres, as evidence suggests bilateral projections for these nuclei (Parent et al., 2012). ChBF volumes (mm<sup>3</sup>) were normalized for the total intracranial volume (TIV), corresponding to the sum of GM, WM and cerebrospinal

fluid volumes. An overview on the spatial location and the extent of the ChBF nuclei in MNI-space is given in Fig. 4.1.

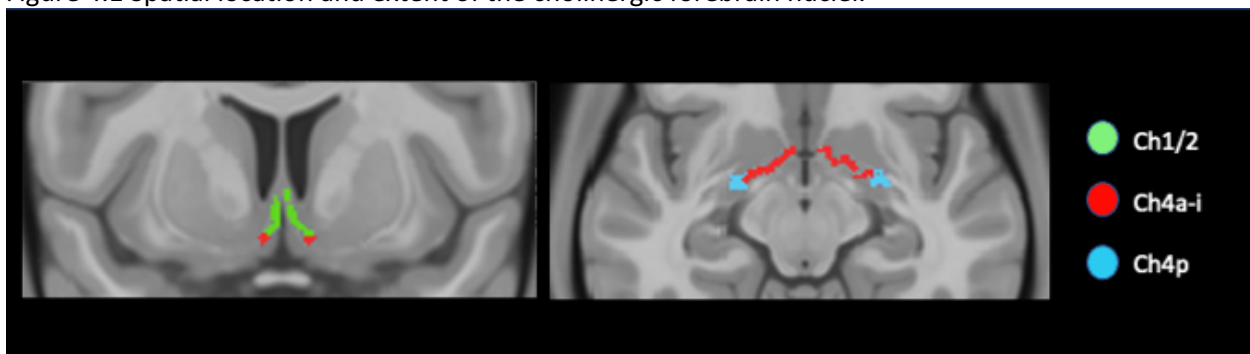
#### 4.2.3 Statistical analyses

The group differences in [<sup>18</sup>F]-FEOBV SUVRs and normalized ChBF volumes were analyzed using one-way analysis of covariance (ANCOVA) controlling for age. Concordances between ChBF volumes and [<sup>18</sup>F]-FEOBV SUVRs were assessed using partial correlation analyses in the AD group, controlling for age. In comparison to controls, AD subjects were expected to have lower cortical SUVRs and smaller ChBF volumes, while positive correlations were expected between these both parameters in AD. Adjustment for multiple testing was not performed as this is an exploratory study. For all analyses significance threshold was based on one-tailed tests with minimal statistical significance of  $p < 0.05$ .

### 4.3 Results

Demographic features and performances in the dementia scales (Mini-Mental State Examination, Montreal Cognitive Assessment; MMSE & MoCA) are presented in Table 4.1. Gender is equally presented and there was no significant group difference for age and education. Expectedly, scores on the cognitive measures were significantly lower in the AD group.

Figure 4.1 Spatial location and extent of the cholinergic forebrain nuclei.



Superimposition of the cholinergic basal forebrain nuclei (ChBF) maps onto the T1-weighted MNI-template, as described in detail by Kilimann et al., 2014. The different colors refer to the different cholinergic nuclei. Green represents the Ch1/2 which correspond to the cholinergic nuclei of the medial septum and vertical limb of the diagonal band, red is the anterior-intermediate (Ch4a-i) and blue represents the posterior part (Ch4p) of the of nucleus basalis of Meynert.

Table 4.1 Sociodemographic and clinical features

	AD (n=6)	HV (n=6)
Gender ratio, F:M	3:3	3:3
Age (y)	67.2 ± 10.24	67.0 ± 11.12
Education (y)	16.8 ± 5.03	14.7 ± 3.88
MMSE	18.3 ± 7.31	29.2 ± 0.41
MoCA	12.8 ± 6.49	27.0 ± 1.55

All the data are represented as mean ± standard deviation unless otherwise indicated. Abbreviations: AD= Alzheimer disease, HV= Healthy volunteers, n= number of subjects, y= years, F= female, M= male, MMSE= Mini Mental Status Examination Scale; MoCA= Montreal Cognitive Assessment scale.

#### 4.3.1 Between groups differences of [<sup>18</sup>F]-FEOBV uptake and ChBF volumes

The ROIs between-group comparisons confirmed previous findings obtained from voxel wise analyses in these patients and showed lower [<sup>18</sup>F]-FEOBV uptakes in AD subjects than in healthy volunteer (see Table 4.2). Affected ROIs in AD included the superior temporal gyri (left p=0.00001, right p=0.001), precuneus (left p=0.001, right p=0.0001), medial frontal gyri (left: p=0.003, right: p=0.014), cingulate cortex (left and right p=0.001), and IPL (left p=0.002, right p=0.0001). There was no significant difference in the occipital cortex, nor the hippocampus. The ChBF volumetric values were all lower in AD than in healthy volunteers (see Table 4.3), with the Ch4p (p=0.003) and the Ch4a-i (p=0.016) showing the largest difference, followed by the Ch1/2 volume (p=0.045).

Table 4.2 Between group comparisons of [<sup>18</sup>F]-FEOBV SUVRs for each hemisphere.

	Left hemisphere			Right hemisphere		
	AD (n=6)	HV (n=6)	p-value	AD (n=6)	HV (n=6)	p-value
Superior temporal gyrus	0.91 ± 0.09	1.18 ± 0.07	0.00001	0.90 ± 0.14	1.17 ± 0.09	0.001
Precuneus	0.94 ± 0.11	1.34 ± 0.12	0.001	0.90 ± 0.80	1.33 ± 0.12	0.0001
Medial frontal gyrus	1.06 ± 0.10	1.2 ± 0.13	0.003	0.96 ± 0.10	1.19 ± 0.13	0.014
Cingulate gyrus	1.15 ± 0.12	1.53 ± 0.13	0.001	1.09 ± 0.09	1.49 ± 0.13	0.001
Inferior parietal lobule	1.01 ± 0.08	1.25 ± 0.07	0.002	0.94 ± 0.06	1.21 ± 0.07	0.0001
Occipital cortex	0.85 ± 0.14	0.93 ± 0.8	NS	0.83 ± 0.15	0.96 ± 0.10	NS
Hippocampus	1.22 ± 0.28	1.34 ± 0.18	NS	1.30 ± 0.28	1.41 ± 0.17	NS

All the data are represented as mean ± standard deviation. p value= statistical significance level. Abbreviations: AD= Alzheimer disease, HV= Healthy volunteers, n= number of subjects, NS= not significant, SUVRs= Standardized uptake value ratios.

Table 4.3 Between group comparisons of ChBFs volumetric values\*

	AD (n=6)	HV (n=6)	p-value
Ch4p	55.29 ± 11.12	76.96 ± 8.71	0.003
Ch4a-i	83.58 ± 13.13	116.75 ± 20.03	0.016
Ch1/2	74.52 ± 21.55	90.03 ± 11.18	0.045

\* TIV-normalized ChBF volumes (mm<sup>3</sup>). Values correspond to mean ± standard deviation. p value= statistical significance level. Abbreviations: AD= Alzheimer disease, HV= Healthy volunteers, n= number of subjects, TIV= total intracranial volume, ChBF= cholinergic basal forebrain, Ch4p and Ch4a-i= posterior and anterior-intermediate part of the cholinergic nuclei of nucleus basalis of Meynert, Ch1/2= cholinergic nuclei of medial septal and vertical limb of diagonal band of Broca.

#### 4.3.2 Correlations between [<sup>18</sup>F]-FEOBV uptake and ChBF volumes

There were highly significant correlations between the Ch4 volumes and the [<sup>18</sup>F]-FEOBV uptake in the cortical ROIs known to be affected in AD, while such correlations were not observed in other ROIs that remain unaffected in AD (See Table 4.4). More specifically, positive correlations were observed between Ch4a-i volume and its corresponding cortical ROIs in the right medial frontal cortex (r= 0.96, p<0.005), bilateral cingulate cortices (left r=0.84, p<0.05; right r= 0.87, p<0.05), and the left superior temporal cortex (r=0.8, p<0.05). The Ch4p showed positive correlations with the superior temporal cortex bilaterally (left r=0.82, p<0.05; right r=0.8, p<0.05). The only cortical ROIs known to be affected in AD that did not correlate with any of the Ch4 volumes were the IPL and precuneus. There were no significant correlations either between Ch1/2 volume and the hippocampus or any cortical ROIs.

Table 4.4 Partial correlations, controlling for age.

	Superior temporal cortex		Medial Frontal cortex		Cingulate cortex		Inferior parietal lobule		Precuneus		Occipital cortex		Hippocampus	
	L	R	L	R	L	R	L	R	L	R	L	R	L	R
Ch4p	0.82*	0.8*	0.64	0.5	0.59	0.65	0.55	0.54	-0.32	-0.42	0.4	0.51	0.68	0.7
Ch4a-i	0.8*	0.54	0.62	0.96**	0.84*	0.87*	0.45	0.46	-0.61	-0.64	0.22	0.31	0.49	0.65
Ch1/2	0.21	0.26	-0.7	-0.52	0.69	0.71	-0.26	0.32	-0.51	-0.54	-0.44	-0.62	-0.35	-0.2

Partial correlations (r), in AD subjects, controlled for age, between different cholinergic basal forebrain volumes normalized by total intracranial volume and hemispheric FEOBV standardized uptake ratio values in brain regions affected and unaffected in AD. Abbreviations: L= left hemisphere, R= right hemisphere, AD= Alzheimer disease, Ch4p and Ch4a-i= Posterior and anterior-intermediate part of the cholinergic

nuclei of nucleus basalis of Meynert Ch1/2= cholinergic nuclei of medial septal and vertical limb of diagonal band of Broca. \*p<0.05 \*\*p<0.005.

#### 4.4 Discussion

Results of this exploratory study have demonstrated an association between cortical [<sup>18</sup>F]-FEOBV uptake reduction and Ch4 volumetric changes in a small sample of patients with AD, suggesting a good concordance between cortical cholinergic denervation and basal forebrain cholinergic cell loss. Furthermore, this association was concordant with most of the cortical projection topography of the Ch4 divisions, including the anterior-intermediate subarea (Ch4a-i), projecting to the medial frontal/cingulate cortex, and the posterior subarea (Ch4-p), projecting mainly to the superior temporal cortex. These two projecting systems show the most severe cholinergic degeneration described in AD (Liu et al., 2015; Geula et Mesulam, 1996, Kilimann et al., 2014; Fritz et al., 2019), further supporting the role of [<sup>18</sup>F]-FEOBV as a direct, quantitative biomarker of the cholinergic degeneration in AD. Such an assumption is also in accordance with the lack of significant correlations between ChBF volumetry and [<sup>18</sup>F]-FEOBV uptake in the hippocampus and the occipital cortex, both known to remain relatively unaffected by cholinergic denervation in AD.

The only cortical areas known to be affected in AD which did not show a significant association between [<sup>18</sup>F]-FEOBV uptake and Ch4 volumes were the precuneus and the IPL, which could have raised concerns regarding their assumed connectivity with Ch4. However, retrograde labeling studies in primates and immunohistochemical studies in humans (Mesulam & Geula, 1988 ; Fritz et al., 2019), have confirmed the cholinergic innervation of these two cortical areas as originating from Ch4, although in specific regions that differ from the subareas used in the current study. Indeed, IPL is mainly innervated by the dorsal-intermediate and ventral-intermediate sectors of Ch4 (Ch4id and Ch4iv), and the precuneus by its anteromedial (Ch4am) subarea (Liu et al., 2015; Mesulam & Geula, 1988). Different ChBF subdivisions like those used in the current study might therefore undermine the capacity to detect a clear relationship with [<sup>18</sup>F]-FEOBV uptake in these specific cortical areas.

The difference of sensitivity to detect correlations in different cortical areas may also relate to the overlap of the cholinergic innervation in most cortical areas, as different sectors of Ch4 are known to project to similar cortical territories (Mesulam, 2013 ; Mesulam et al., 1983). Actually, each Ch4 subdivision sends a set of major projections to its main cortical targets along with minor projections to adjacent and non-



adjacent cortical regions (Gratwicke et al., 2013). The exception to this is the superior temporal area, which predominantly receives cholinergic efferent from Ch4p, and the medial frontal area receiving major inputs from Ch4a-i, which is concordant with the very good correlations obtained here in these two cortical areas. However, for other cortical areas like the inferior parietal lobule and precuneus, the connectivity overlap in the cortex could affect the relationship between Ch4 subareas volumetry and [<sup>18</sup>F]-FEOBV uptake in the cortex, especially in small samples like the one used here.

In conclusion, the current exploratory study showed for the first time that cortical cholinergic denervation as measured with [<sup>18</sup>F]-FEOBV PET was proportional to ChBF atrophy as estimated with MRI-based volumetry, further supporting the role of [<sup>18</sup>F]-FEOBV as a direct and quantitative biomarker of the cholinergic denervation in AD.

#### 4.5 Author contribution

M.A. and P.R.N. were responsible for conception and design of the study. M.A., M.J.G., E.A., P.R.N. were responsible for acquisition and analysis of neuroimaging data. M.A., and M.A.B. were responsible for drafting the manuscript text, tables and figures.

## 4.6 References

- Aghourian, M., Legault-Denis, C., Soucy, J. P., Rosa-Neto, P., Gauthier, S., Kostikov, A., ... & Bedard, M. A. (2017). Quantification of brain cholinergic denervation in Alzheimer's disease using PET imaging with [18 F]-FEOBV. *Molecular psychiatry*, 22(11), 1531-1538.
- Cyr, M., Parent, M. J., Mechawar, N., Rosa-Neto, P., Soucy, J. P., Clark, S. D., ... & Bedard, M. A. (2015). Deficit in sustained attention following selective cholinergic lesion of the pedunculopontine tegmental nucleus in rat, as measured with both post-mortem immunocytochemistry and in vivo PET imaging with [18F] fluoroethoxybenzovesamicol. *Behavioural brain research*, 278, 107-114.
- Grothe, M., Heinsen, H., & Teipel, S. J. (2012). Atrophy of the cholinergic basal forebrain over the adult age range and in early stages of Alzheimer's disease. *Biological psychiatry*, 71(9), 805-813.
- Fernández-Cabello, S., Kronbichler, M., Van Dijk, K. R., Goodman, J. A., Spreng, R. N., Schmitz, T. W., & Alzheimer's Disease Neuroimaging Initiative. (2020). Basal forebrain volume reliably predicts the cortical spread of Alzheimer's degeneration. *Brain*, 143(3), 993-1009.
- Dubois, B., Feldman, H. H., Jacova, C., DeKosky, S. T., Barberger-Gateau, P., Cummings, J., ... & Scheltens, P. (2007). Research criteria for the diagnosis of Alzheimer's disease: revising the NINCDS-ADRDA criteria. *The Lancet Neurology*, 6(8), 734-746.
- Fritz, H. J., Ray, N., Dyrba, M., Sorg, C., Teipel, S. et Grothe, M. J. (2019). The corticotopic organization of the human basal forebrain as revealed by regionally selective functional connectivity profiles. *Human Brain Mapping*, 40(3), 868-878. doi: 10.1002/hbm.24417
- Geula, C., & Mesulam, M. M. (1996). Systematic regional variations in the loss of cortical cholinergic fibers in Alzheimer's disease. *Cerebral Cortex*, 6(2), 165-177.
- Grothe, M., Heinsen, H., & Teipel, S. J. (2012). Atrophy of the cholinergic basal forebrain over the adult age range and in early stages of Alzheimer's disease. *Biological psychiatry*, 71(9), 805-813.
- Grothe, M. J., Kilimann, I., Grinberg, L., Heinsen, H., & Teipel, S. (2018). In vivo Volumetry of the cholinergic basal forebrain. In *Biomarkers for Preclinical Alzheimer's Disease* (pp. 213-232). Humana Press, New York, NY.
- Gratwicke, J., Kahan, J., Zrinzo, L., Hariz, M., Limousin, P., Foltynie, T. et Jahanshahi, M. (2013). The nucleus basalis of Meynert: A new target for deep brain stimulation in dementia? *Neuroscience & Biobehavioral Reviews*, 37(10), 2676-2688. doi: 10.1016/j.neubiorev.2013.09.003
- Kilimann, I., Grothe, M., Heinsen, H., Alho, E. J. L., Grinberg, L., Amaro Jr, E., Teipel, S. J. (2014). Subregional basal forebrain atrophy in Alzheimer's disease: a multicenter study. *Journal of Alzheimer's Disease*, 40(3), 687-700.
- Liu, A. K. L., Chang, R. C. C., Pearce, R. K., & Gentleman, S. M. (2015). Nucleus basalis of Meynert revisited: anatomy, history and differential involvement in Alzheimer's and Parkinson's disease. *Acta neuropathologica*, 129(4), 527-540.

- Mesulam, M. M. (2004). The cholinergic innervation of the human cerebral cortex. *Progress in brain research, 145*, 67-78.
- Mesulam, M.-M. (2013). Cholinergic circuitry of the human nucleus basalis and its fate in Alzheimer's disease: Human Cholinergic Circuitry. *Journal of Comparative Neurology, 521*(18), 4124-4144. doi: 10.1002/cne.23415
- Mesulam, M.-M. et Geula, C. (1988). Nucleus basalis (Ch4) and cortical cholinergic innervation in the human brain: Observations based on the distribution of acetylcholinesterase and choline acetyltransferase. *The Journal of Comparative Neurology, 275*(2), 216-240. doi: 10.1002/cne.902750205
- Mesulam, M.-M., Mufson, E. J., Levey, A. I. et Wainer, B. H. (1983). Cholinergic innervation of cortex by the basal forebrain: Cytochemistry and cortical connections of the septal area, diagonal band nuclei, nucleus basalis (Substantia innominata), and hypothalamus in the rhesus monkey. *The Journal of Comparative Neurology, 214*(2), 170-197. doi: 10.1002/cne.902140206
- Mulholland, G. K., Wieland, D. M., Kilbourn, M. R., Frey, K. A., Sherman, P. S., Carey, J. E., & Kuhl, D. E. (1998). [18F] fluoroethoxy-benzovesamicol, a PET radiotracer for the vesicular acetylcholine transporter and cholinergic synapses. *Synapse, 30*(3), 263-274.
- Parent, M., Bedard, M. A., Aliaga, A., Soucy, J. P., St-Pierre, E. L., Cyr, M., ... & Rosa-Neto, P. (2012). PET imaging of cholinergic deficits in rats using [18F] fluoroethoxybenzovesamicol ([18F] FEOBV). *Neuroimage, 62*(1), 555-561.
- Schmitz, T. W., Mur, M., Aghourian, M., Bedard, M. A., Spreng, R. N., & Alzheimer's Disease Neuroimaging Initiative. (2018). Longitudinal Alzheimer's degeneration reflects the spatial topography of cholinergic basal forebrain projections. *Cell reports, 24*(1), 38-46.
- Wenzel, B., Deuther-Conrad, W., Scheunemann, M., & Brust, P. (2021). Radioligand development for PET imaging of the vesicular acetylcholine transporter (VACHT) in the brain. In *PET and SPECT of Neurobiological Systems* (pp. 1061-1090). Springer, Cham.

#### 4.7 Conclusion of the second study

With the results obtained in the second study, we concluded that cortical cholinergic denervation measured with FEOBV-PET is concordant and proportional to ChBF atrophy measured by MRI volumetry. These findings further support the reliability and validity of FEOBV-PET as a surrogate measure to quantify cholinergic degeneration in AD. Such a conclusion was also obtained by a team of Canadian researchers (Schmitz et al., 2018) who used our data with FEOBV in AD, to illustrate the strong overlap with the ChBF volumetry obtained in a large sample from the AD Neuroimaging Initiative (ADNI). Their results (see the reprint in appendix D) showed that the cholinergic denervation topography as measured by FEOBV in AD was consistent with the patterns of ChBF degeneration, reinforcing therefore the consistency of our own results.

## CHAPITRE 5

### GENERAL DISCUSSION AND CONCLUSION

FEOBV is a novel cholinergic PET radiotracer that has been extensively validated in animals and in healthy humans. The two studies conducted within the scope of this thesis aimed to validate PET imaging with FEOBV as a reliable *in vivo* tool for the quantification of cholinergic depletion in AD. This was done for the first time in AD. FEOBV showed greater sensitivity and reliability compared to AD biomarkers of amyloid and metabolism and was concordant with the atrophy of the cholinergic neurons of the basal forebrain. PET imaging with FEOBV can thus be considered as a promising surrogate biomarker of AD.

#### 5.1 Recapitulation of the two studies

PET imaging with FEOBV was performed for the first time in AD subjects to quantify and map brain cholinergic denervation *in vivo*. Using voxel-wise ANCOVAs, we showed that FEOBV was more sensitive than PET biomarkers of metabolism and amyloid deposition (FDG and NAV respectively) to distinguish AD from control. The group difference showed a heavy depletion of FEOBV in several cortical regions in AD; superior temporal-parietal areas, posterior cingulate and to a lesser extent in frontal cortex. No significant reductions were observed in brain regions that are known to remain unaffected in AD, such as the striatum, thalamus, and cerebellum. Furthermore, FEOBV uptake was positively correlated with FDG in multiple cortical areas showing cholinergic depletion, and negatively correlated with NAV in some restricted areas. Unlike NAV, FEOBV and FDG correlated positively with cognitive measure (MMSE and MoCA scores) in AD. As such, FEOBV-PET was found to be more sensitive than the other PET biomarkers to distinguish AD from control and to quantify disease severity. Therefore, we concluded that FEOBV is a reliable *in vivo* tool to quantify and map cholinergic deletion in AD and can be considered as an excellent biomarker for AD.

We then explored the *in vivo* concordance between cortical PET-FEOBV uptake and ChBF volumes within the same sample of AD patients, using imaging data obtained in the first study. We chose cortical areas showing severe FEOBV reductions in AD (temporal, parietal, cingulate and frontal areas) and other areas that did not show significant FEOBV reduction (hippocampus and occipital cortex). MRI volumetry was used to measure the volumes of the different ChBF nuclei; Ch4 (Chp and Ch4a-i) and Ch1/2, using a specific BF mask (Grothe et al., 2018). We compared these variables between groups using ANCOVAs and used partial correlations to explore association between FEOBV uptake and volumes of these nuclei in AD. Results showed that AD patients had both lower ChBF-Ch4 volumes and lower FEOBV uptakes in affected

cortical areas compared to control. As expected, specific pattern of correlations was obtained with FEOBV uptake and corresponding Ch4 subareas; FEOBV uptake in the superior temporal correlated with the Ch4p volume and uptake in cingulate and frontal areas correlated with the Ch4ai volume. There was no significant correlation with Ch1/2 volume and FEOBV uptake in the hippocampus nor any other cortical areas. We were able to confirm the selective cholinergic denervation in AD with FEOBV which was proportional to the AD associated ChBF atrophy, further supporting the reliability and specificity of PET-FEOBV as a direct and quantitative biomarker of the cholinergic integrity in AD.

## 5.2 Reliability of the current findings

In this thesis, we quantified and mapped region-specific cholinergic denervation in AD using PET imaging with FEOBV. The results obtained in the two studies are in accordance with the formulated hypotheses validating PET-FEOBV as a reliable *in vivo* tool for quantifying cholinergic integrity in AD. Some methodological limitations should however be addressed in order to support the reliability of our findings.

### 5.2.1 The representativeness of the current results

PET scan is a very costly neuroimaging method, which could be a limiting factor to conduct studies with large sample sizes. This was a primary consideration in the current studies, as all participants underwent three PET imaging scans with three different radiotracers. Although we acknowledge the limitation regarding our small sample size as a potential weakness of the current research design, we do not believe that it impedes the reliability and representativeness of our findings. One of the primary reason is the observation that *in vivo* reductions of FEOBV uptake in AD were not only seen as a group effect, evidenced by statistical analyses, but also as direct visual observations of each individual PET images. This, not only supports the finding that FEOBV can clearly characterize a group of patients with AD, but also raises the possibility of its utility in clinical diagnosis or follow-up of single individuals with AD. It is also important to mention that the findings of the current thesis regarding PET imaging with FDG and NAV radiotracers were concordant with the known AD-associated hypometabolism and amyloid deposition (Minoshima et al., 1995; Rowe et al., 2013; van Waarde et al., 2021), emphasizing that the statistical power could efficiently be reached by our sample size (n=12).

The reliability and representativeness of our results is also supported by the topography of FEOBV uptake in both healthy controls and AD subjects, which was concordant with those described in the literature regarding these two populations. The FEOBV uptake in the healthy controls showed the highest FEOBV

uptake in the striatum, thalamus, cerebral cortex, hippocampus and the cerebellum. These areas are known to be the most innervated by the different cholinergic systems and closely match the cortical distributions of other cholinergic markers such as ChAT or AChE in healthy subjects obtained in neuroimaging or histological studies (Mesulam & Geula, 1988; Geula & Mesulam, 1996; Kuhl et al., 1999, Mesulam, 2004; Liu et al., 2015). Furthermore, VAcHT distribution is also shown to be highly correlated with the cortical distribution of ChAT and AChE markers (Gilmor et al., 1996; Rinne et al., 2003; Richter et al., 2018), confirming that FEOBV binding is a reliable marker of VAcHT and cholinergic terminals. A recent study using PET-FEOBV in a large cohort of healthy human also showed brain topography of FEOBV-VAcHT binding that was the same as the one reported in our healthy controls (Albin et al., 2018).

The greatest FEOBV reductions in our patients with AD were seen in the temporal-parietal and posterior cingulate areas, followed by more medial and lateral frontal areas. These are regions known to be heavily affected by cholinergic lesions in AD while other cortical regions remained relatively preserved (Mesulam, 2004). These results are in support of AD postmortem studies using cholinergic markers such as ChAT, showing severely reduced cholinergic synapse in the temporal and parietal areas followed by more frontal cortices (Gil-Bea et al., 2005; Araujo et al., 1988; Geula & Mesulma 1996). In contrast, primary visual, somatosensory, and motor cortex display a relative preservation of cholinergic fibers, shown by lack of ChAT reduction (Geula & Mesulma 1996; Araujo et al., 1988). This is concordant with the relatively preserved FEOBV binding in these cortical regions in our AD group.

Interestingly, the topography of FEOBV reduction obtained in our AD subjects is in agreement with the known caudal-rostral pattern of NBM/Ch4 neuronal loss documented during the progression of AD with superior temporal areas showing severe cholinergic depletion compared to rostral/frontal parts (Liu et al., 2015; Mesulam, 2013). We were able to confirm this directly by showing significant concordance between FEOBV uptake in the affected cortical areas and their corresponding Ch4 volumes. The posterior Ch4 (Ch4p) volume was indeed severely atrophied and correlated significantly with cholinergic terminal density measured with FEOBV in the superior temporal cortex bilaterally. This was also true when looking at the volume of the more anterior-intermediate portion of the Ch4 (Ch4a-i) with its cortical targets, mainly the cingulate and frontal cortex. No correlation was seen with FEOBV uptake in the occipital cortex and volumes of Ch4 subareas, as this cortical area remains unaffected in AD (Fritz et al., 2019; Mesulam & Geula, 1988). The association between FEOBV uptake reduction and Ch4 volumetric loss, observed here,



is once again in line with the caudal-rostral pattern of basal forebrain cholinergic cell loss and cortical cholinergic denervation in AD, supporting the reliability and representativeness of our findings.

As expected, the group difference did not show a reduction of FEOBV in brain areas that are known to be unaffected in AD, such as the striatum, thalamus and cerebellum (Mesulam, 1990). Moreover, the hippocampus which is heavily involved in AD, did not show a reduction of FEOBV, despite receiving major innervation from BF. This finding is in line with previous postmortem FEOBV autoradiographic study, showing no uptake reduction in the hippocampus of AD brain tissue (Parent et al., 2013). This observation is not surprising, as cholinergic projections from Ch1/2 and not Ch4 innervate the hippocampus (Mesulam, 1990). Moreover, post-mortem studies show that Ch1/2 is relatively preserved from cholinergic lesion in mild-moderate AD with minimal or insignificant cell loss compared to aged-matched control (Mesulam et al., 1983; Mufson et al., 1993; Tiernan et al., 2018b), which could explain lack of reduction. Concordant to this, our AD group showed mild Ch1/2 volume loss, compared to the severe Ch4 atrophy. Additionally, there was no relationship between Ch1/2 volumetric measure and FEOBV uptake in hippocampus nor any other cortical areas, highlighting again the sensitivity of FEOBV to detect AD specific cholinergic loss.

### 5.2.2 Potential nonspecific FEOBV binding

To date, the development of PET radioligands for VACHT is mostly based on vesamicol, which is a compound known to display nanomolar affinity for the sigma receptors ( $\sigma_1$  and  $\sigma_2$ ). These are ubiquitous orphan receptors, situated primarily at the mitochondria-associated endoplasmic reticulum (Fontanilla et al., 2009). Such a non-specific binding of vesamicol could potentially undermine the reliability of the VACHT radiotracers. However, a multitude of structurally diverse vesamicol analogs have been chemically engineered to overcome this specific limitation, and FEOBV is currently considered as the most specific one in respect with its binding potential to the VACHT. As a benzo-vesamicol derivative, FEOBV has demonstrated a binding affinity to VACHT that is almost 20 folds higher than vesamicol per se (Rogers et al. 1994). Furthermore, as an (-)-enantiomer, FEOBV has shown a distinctly higher affinity to the VACHT binding site over sigma receptors, compared to the (+)-enantiomer or any other benzo-vesamicol derivatives (Mulholland, et al., 1993).

Many studies support the lack of significant interaction between FEOBV and sigma receptors in vivo and in vitro. It is shown that in vivo pharmacological pre-treatment with large doses of drugs with high affinity to sigma receptors (3-PPP or E-2020) did not significantly alter the brain uptake or regional localization of

FEOBV in rodents (Mulholand et al., 1998). Furthermore, *in vitro* ligand binding, showed that the very specific and saturable binding of FEOBV in striatal, cortical, hippocampal areas, was inhibited by subnanomolar concentrations of structurally related benzovesamicols (Mulholand et al., 1998). This was also confirmed by *in vivo* partial blocking studies, showing that administration of smaller doses of cold FEOBV (unlabeled) reduced the retention of radioactive FEOBV in regions of high VAcHT concentration (striatum and cortex) (Kilbourn et al., 2009).

Recently, the inhibition constant ( $K_i$ ) of FEOBV was found to be of 6.75 nM toward the VAcHT (on rVAcHT PC12 cells), while for  $\sigma_1$  and  $\sigma_2$  receptors, FEOBV  $K_i$  values were in the range of 2000 nM (Helbert et al. 2019).  $K_i$  is an indication of how potent an inhibitor (ligand) is to occupy the receptors, with lower concentrations of a ligand indicating greater binding affinity. These FEOBV data correspond to an excellent affinity to VAcHT compared to insignificant affinity to sigma receptors. We are therefore confident that the current results obtained with FEOBV in our study is representative of a VAcHT and not sigma receptors labeling.

### 5.3 Implications of the current findings

#### 5.3.1 Using PET-FEOBV as a tool for differential diagnosis of AD

The results presented in this thesis suggest that PET imaging with FEOBV is a reliable tool for quantifying and mapping the brain cholinergic denervation in AD, as well as distinguishing AD from control and quantifying cognitive decline in AD. This raises the possibility of using PET imaging with FEOBV for the purpose of identifying, quantifying and following-up of patients with AD. Indeed, given that cholinergic degeneration also occurs in many other forms of dementia but with distinct topographic patterns, PET imaging with FEOBV might become a useful tool for the differential diagnosis of these dementias.

In neurodegenerative diseases such as lewy body diseases (LBD and PDD), there is a significant overlap in clinical and neuropathological presentation which renders the differential diagnosis very challenging. For example, DLB and PDD are classified as synucleopathies, but 50% to 80% of these patients may present with an AD pathological feature such as Amyloid- $\beta$  or Tau protein aggregates (Irwin et al., 2018). Even though, significant effort has gone into identifying *in vivo* proteinopathy biomarkers for use in clinical practice, these type of biomarkers are less useful for the purpose of differential diagnosis given the inconsistency and overlap in neuropathological and clinical classifications in these dementias.

As with AD, the cholinergic dysfunction is an important feature of DLB and PDD, and it is also considered the best correlate of clinical symptoms (Dournaud et al., 1995; Tiepolt et al., 2022). Post-mortem studies have shown different patterns of cholinergic depletion in these disorders, which can be used as a distinguishable factor, making the use of FEOBV very much informative. For example, while cholinergic lesions in AD are restricted to the basal forebrain and its cortical projections, those observed in DLB and PDD are also known to affect the mesopontine nuclei and their projections to the subcortical structures (Hilker et al., 2005; Kotagal et al., 2012). This topographic distinction has been clearly observed recently in a PET imaging study with FEOBV in patients with DLB (Nejad-Davarani et al., 2019). Furthermore, lesion studies in animals have also shown that PET imaging with FEOBV can detect and quantify specific cholinergic denervation, depending on whether the lesions were restricted to the basal forebrain (Parent et al., 2012), with a reduced FEOBV binding in the cortex, or to the mesopontine nuclei (Cyr et al., 2014), with a reduced FEOBV binding in the thalamus and other subcortical areas. It is therefore promising to further assess the reliability of PET imaging with FEOBV to distinguish different types of degenerative diseases, based on their cholinergic cell death severity and topography.

In a recent preliminary study, Kanel and colleagues used FEOBV for the first time to compare AD with DLB and healthy subjects. Results confirmed a large number of subcortical structures which were characterized by a FEOBV binding loss in DLB than in AD. More specifically, binding loss in DLB was seen in the thalamus, basal ganglia, vermis, and dorsal pontomesencephalic region, in addition to the whole neocortex, hippocampus, and amygdala, (Kanel et al., 2021). These results support topographically distinct cortical and subcortical cholinergic lesions using FEOBV which can distinguish AD and LBD subjects, highlighting differential vulnerability of specific cholinergic projections in these two diseases.

In Frontotemporal lobar degeneration (FTLD), cholinergic studies are scarce, and the available data is less consistent than for AD or DLB. In the different subtypes of primary progressive aphasia (PPA), considered as a variant of FTD, cholinergic deficits have been somewhat more extensively studied, probably because of their frequent association with AD pathology. Loss of muscarinic receptors has been described in the temporal lobes of patients with semantic PPA (s-PPA) (Odawara et al., 2003). Molecular PET imaging with PMP also revealed decreased AChE activity levels in the left temporal cortex that was more evident in the logopenic PPA (l-PPA) than in the s-PPA or non-fluent PPA (nf-PPA) (Schaeffer et al., 2017). Disproportionate atrophy of the basal forebrain was also identified in a high-resolution MRI study, more marked in s-PPA and nf-PPA, than in l-PPA (Teipel et al., 2016). This atrophy of the basal forebrain was

lateralised to the left, and proportional to left temporal and frontal cortical atrophy, including Broca's area. Left lateralisation of these anomalies is of particular interest if we consider the asymmetry of the cholinergic innervation of language areas in human (Tanaka & Bachman, 2002). Although there is some evidence of cholinergic denervation in PPAs, the magnitude and topography of this degeneration remain to be clarified within and between s-PPA, l-PPA, and nf-PPA. Although this has not yet been done before, we speculate that compared with AD and DLB, PPAs might be more likely to present with a reduced FEOBV uptake lateralised to the left hemisphere, as some evidence converges toward a left hemisphere lateralisation of the cholinergic denervation (Mesulam et al., 2019). This remains to be verified experimentally, however.

### 5.3.2 Using PET-FEOBV as an AD biomarker

As a sensitive and reliable cholinergic biomarker, PET imaging with FEOBV would be an important tool not only for diagnosis per se but also for early detection, follow-up, and assessment of efficacy of therapeutic interventions in AD.

A reliable preclinical AD biomarker for early detection is sought after as early interventions have been shown to slow decline rate and delay clinically relevant impairment by several years (Insel et al., 2019). There is now new evidence suggesting the primacy of the cholinergic involvement in the pathology of AD as the NBM-Ch4 cholinergic lesions emerge as early as the asymptomatic stage of the disease. Indeed, recent longitudinal MRI studies have shown that annual rate of gray matter loss in the NBM-Ch4p subregion is already detectable in cognitively normal older adults with abnormal counts of CSF amyloid and tau, and that this event precedes cortical spread of tau/amyloid and entorhinal degeneration (Schmitz & Spreng, 2016; Schmitz et al., 2020; Fernandez-Cabello et al., 2020). Because degeneration of the cholinergic cell body in the NBM-Ch4p is likely preceded by a period of distal axonal degeneration (Yan et al., 2018), PET imaging with FEOBV can be used to map and quantify presynaptic cholinergic alternation at this stage. As a sensitive biomarker of the cholinergic terminal integrity, FEOBV will help facilitate the accurate identification of individuals at risk of AD progression towards clinical stage.

An important step in validating FEOBV as a reliable AD biomarker remains to be its sensitivity to distinguish AD from the earlier stages of the disease, such as the MCI stage, a transitional stage that precedes dementia per se. MCI has been associated with increased cholinergic degeneration compared with healthy controls, both in terms of neurochemical changes and volumetric changes (Mesulam, 2004; Mufson et al.

2007). Indeed, PET imaging studies show significant decline in cortical AChE activity in MCI patients compared to controls, most pronounced in the tempoparietal neocortex, and to a lesser extent in the limbic and frontal areas (Haense et al., 2012). Complementary to these findings, MRI studies in MCI have consistently shown reduced Ch4p volume and a higher Ch4 atrophy rate than control (Grothe et al. 2010, 2013; Muth et al. 2010). We believe that PET imaging with FEOBV would be even more sensitive than AChE markers to detect such cholinergic depletion in MCI. Interestingly, a very recent study conducted with a small cohort of MCI patients showed the promising usefulness of PET-FEOBV in detecting similar topography of cortical cholinergic reduction and with positive correlation with cognitive decline (Xia et al., 2022). The specificity and sensitivity of PET-FEOBV in MCI needs to be demonstrated, however with a bigger cohort and as a longitudinal design, as up to half of MCI cases do no progress to AD dementia. Furthermore, the cholinergic changes associated to normal aging should also be addressed with PET-FEOBV in order to improve the positive predictive value of such tool when identifying the prodromal/MCI stage of AD.

At the present time, neuroimaging techniques such as FDG-PET or structural MRI are used for the follow-up of MCI and AD patients (Frisoni et al., 2010; Bohnen et al., 2012; Mosconi et al., 2013). However, these imaging methods are indirect measurements of neuronal integrity, and they cannot be considered as direct biomarkers of AD. This puts forth the need to conduct longitudinal studies using FEOBV in AD continuum to quantify cholinergic depletion over the progression of AD. Given the sensitivity of PET-FEOBV as a direct biomarker of cholinergic integrity and its correlation with symptom severity, it can be more informative and reliable for the follow-up of AD patients, from the asymptomatic stage to the dementia stage.

An ultimate purpose for a reliable biomarker in the field of AD, however, remains to be the assessment of efficacy of pharmacological interventions. So far, the disease modifying drugs that directly impact one specific target in the AD neuropathology, such as those involved in amyloid/tau accumulation, still lack evidence (Long & Holtzman, 2019). Given the complex neuropathology of AD, and the interplay between the various pathways, the newest therapeutic avenue is considering a combination of treatments that have actions at multiple targets, namely anti-amyloid and anti-tau effects, in combination with neurotransmitter modification, anti-neuroinflammatory and neuroprotective effects (Huang et al., 2020; Long & Holtzman, 2019). Therefore, the use of diagnostic tools that are based on detection and quantification of tau, amyloid and neuroinflammatory proteins might not be ideal biomarkers. Perhaps,

the best approach to measure the efficacy of such treatment would be to measure neurodegeneration, irrespective of the pathophysiology, as neuronal loss is the ultimate result of these pathways and is the best indicator of symptom severity.

It would be important here to discuss the potential of the general synaptic ligands such as those targeting the synaptic vesicle 2A protein (SV2A) as compared to FEOBV. As discussed in the introduction, the SV2A protein is found ubiquitously in the synaptic vesicles of all neurons, regardless of their neurotransmitter or neuron type (Becker et al., 2020). This means that SV2A-based biomarkers are a direct measure of general synaptic density and would be most sensitive to general changes in synaptic terminals, rather than system-specific changes. Such that SV2A ligands can be used in any condition with neurodegeneration and eventually replace glucose metabolism biomarkers as synaptic density measures. Because SV2A ligands encompass general neuronal death, they can be a better predictor of cognitive impairment in any neurodegenerative condition. But in AD or any other condition in which cholinergic dysfunction is at the forefront of the disease, FEOBV has a more direct relationship with clinical symptoms. Furthermore, as compared to VAcHT which is exclusively found in cholinergic synapses, SV2A proteins are not exclusive to synaptic vesicles, as they are also expressed in mitochondria, which could impact sensitivity of PET ligands targeting this protein (Stockburger et al., 2016). Despite this, we believe that as markers of synaptic loss both SV2A ligands and FEOBV are more sensitive than other AD neuropathological biomarkers to monitor disease progression and cognitive decline. Future studies directly comparing FEOBV with general synaptic PET ligands in AD would indeed be needed to clarify this stance.

Nonetheless, measuring cholinergic cell death could become a gold standard in disorders with cholinergic deficits. As such, PET imaging with FEOBV would be a valuable tool to assess efficacy of novel pharmacological interventions in AD as a function of alterations in the BF cholinergic system.

### 5.3.3 FEOBV and cognition

Cholinergic dysfunction is the best correlate of cognitive functioning in AD when compared to other neurochemical systems, as it is severely impacted early on in AD (Mesulam, 2004). Results from the current thesis have confirmed such a view by showing that FEOBV uptake varied as a function of AD severity as measured with MMSE and MoCA tests. We used these general cognitive measures, as it was imperative to explore the association of FEOBV uptake with global cognition since this was the first time that FEOBV

was used in AD patients. We did not look at domain specific cognitive scores or regional FEOBV uptake, as this was not the aim of the study.

As already mentioned in the introduction of this thesis (see 1.4), the exact role of the cholinergic system in cognition is complex, as ACh acts as a neuromodulator on many downstream neurotransmitter systems and its role differs per brain regions and per cholinergic receptor. However, given that in AD, the Ch4-cortical cholinergic system is selectively affected compared to the Ch1/2-hippocampus, we assume that the observed cortical FEOBV depletion in AD would be non-specific, although better associated with higher order cognitive processes such as attention, perception and executive functions, rather than episodic memory. As such, we would expect correlations of FEOBV with various attention and working memory tasks, but not with those of memory/consolidation measures. However, such a simplistic view of an association between a specific cognitive function and a specific neurotransmitter remains very unlikely, especially with a non-specific neuromodulator like ACh.

New evidence suggests that cognitive deficits in AD may correspond to general processes that involve overlapping cortical areas which share overlapping projections arising from the Ch4 nuclei (Liu et al., 2015). Indeed, the PET-FEOBV results obtained in our AD group revealed severe cholinergic denervation in the three neurocortical networks known to support different networks of cognition, including the “salience network”, the “default mode network”, and the “central executive network” (Seeley et al., 2007). Because of cholinergic denervation in AD, and the consequences on the lack of cholinergic modulation, these networks may become dysfunctional and produce the characteristic AD cognitive features. In line with this, a very recent study using PET-FEOBV, investigated the topographic relationship between cognitive functioning and regional cholinergic denervation in PD. Results demonstrated partial overlapping cortical topography across different cognitive domains such as attention, memory and executive functions (Van der Zee et al., 2021). The authors suggested that the cortical topographic overlap of the different cholinergic systems may reflect a shared cholinergic network sub-serving overall cognitive functioning in PD.

Future studies using PET-FEOBV in AD, are necessary and should focus on regional FEOBV uptake and its impact on the three cognitive networks, instead of the more traditional specific cognitive sub-domains such as memory, attention, and executive functioning. The relationship between regional cholinergic denervation and clinical symptomatology in AD should be investigated, as an improved understanding of

the mechanisms and roles of cholinergic neurotransmission may lead to more effective symptomatic therapies in AD.

#### 5.4 Conclusion

This thesis showed for the first time that PET imaging with FEOBV is a very promising approach to identify and quantify AD on the basis of the cholinergic denervation. Indeed, PET-FEOBV is shown to be more sensitive than the currently used biomarkers of AD such as amyloid and hypometabolism PET imaging. Furthermore, cholinergic denervation as measured with FEOBV is proportional to the ChBF atrophy as measured with MRI volumetry, supporting the validity of this tool to quantify cholinergic degeneration in AD. FEOBV can therefore be considered as a very promising tool that would be interesting to further assess for its use in the early diagnosis, follow up and therapeutic assessments of AD and other forms of diseases.



**APPENDIX A**  
**ETHICS CERTIFICATE-UQÀM**

## CERTIFICAT D'ÉTHIQUE

Le protocole de recherche suivant a été examiné en mode délégué et jugé conforme aux pratiques habituelles et répond aux normes établies par le Cadre normatif pour l'éthique de la recherche avec des êtres humains de l'UQAM (juin 2012).

### Protocole de recherche

**Chercheur(e) principal(e) désigné:** Marc-André Bédard

**Unité de rattachement :** Département de psychologie

**Équipe de recherche:**

**Co-chercheur(s) :** Pedro Rosa-Neto (Université McGill); Jean-Paul Soucy (Université de Montréal);

**Collaborateur :** Serge Gauthier (Université McGill)

**Étudiant(s) réalisant leurs projets de mémoire ou de thèse (incluant les thèses de spécialisation) dans le cadre du présent protocole de recherche :**

**Titre du protocole de recherche :** *Validation du 18F-Fluoroethoxybenzovesamicol (FEOBV) comme biomarqueur de la maladie d'Alzheimer*

**Organisme de financement (le cas échéant):** FRQS (2013-2015)

*Ce projet a été approuvé initialement par le CÉR de la faculté de médecine de l'Université McGill (FWA 00004545).*

### Modalités d'application

Le présent certificat est valide pour le projet tel que soumis au CIEREH. Les modifications importantes pouvant être apportées au protocole de recherche en cours de réalisation doivent être communiquées au comité<sup>1</sup>.

Tout évènement ou renseignement pouvant affecter l'intégrité ou l'éthicité de la recherche doit être communiqué au comité.

Toute suspension ou cessation du protocole (temporaire ou définitive) doit être communiquée au comité dans les meilleurs délais.

Le présent certificat d'éthique est valide jusqu'au **31 mars 2015**. Selon les normes de l'Université en vigueur, un suivi annuel est minimalement exigé pour maintenir la validité de la présente approbation éthique. Le rapport d'avancement de projet (renouvellement annuel ou fin de projet) est requis pour le : **15 mars 2015** : <http://www.recherche.uqam.ca/ethique/humains/comites-reunions-formulaires-eth-humains/cier-comite-institutionnel-dethique-de-la-recherche-avec-des-etres-humains.html>



Maria Nengeh Mensah  
Professeure  
Présidente

29 mai 2014

Date d'émission initiale du certificat

<sup>1</sup> Modifications apportées aux objectifs du projet et à ses étapes de réalisation, au choix des groupes de participants et à la façon de les recruter et aux formulaires de consentement. Les modifications incluent les risques de préjudices non-prévus pour les participants, les précautions mises en place pour les minimiser, les changements au niveau de la protection accordée aux participants en termes d'anonymat et de confidentialité ainsi que les changements au niveau de l'équipe (ajout ou retrait de membres).

No. du certificat : S-702624

Date : 22 mars 2022

## AVIS FINAL DE CONFORMITÉ

Titre du projet : *Validation clinique du [18F]-fluoroethoxybenzovezamicol utilisé avec l'imagerie cérébrale par tomographie d'émission de positons, pour détecter et quantifier la maladie d'Alzheimer à partir de la dénervation cholinergique*

Nom de l'étudiante : Meghmik Aghourian Namagerdy (AGHM01588703)

Programme d'étude : Doctorat en psychologie

Direction de recherche : Marc-André Bédard

OBJET : fin de projet

Le Comité institutionnel d'éthique de la recherche avec des êtres humains (CIEREH) confirme que Meghmik Aghourian Namagerdy a réalisé sa thèse de doctorat sous la direction de Marc-André Bédard conformément aux normes et politiques éthiques en vigueur, en tant que membre de l'équipe de recherche pour le projet couvert par le certificat d'éthique no. S-702624.

Merci de bien vouloir inclure le présent document et du certificat d'éthique susmentionné en annexe de votre travail de recherche.

Les membres du CIEREH vous félicitent pour la réalisation de votre recherche et vous offrent leurs meilleurs vœux pour la suite de vos activités.

Le président,



---

Yanick Farmer, Ph. D.  
Professeur

**APPENDIX B**  
**ETHICS CERTIFICATE- MCGILL UNIVERSITY**



12 May 2014

Dr. Jean-Paul Soucy  
Marc-André Bédard, PhD  
PET Unit  
McConnell Brain Imaging Centre  
Montreal Neurological Institute  
3801 University

**RE: IRB Study Number A03-M22-14A**

*Clinical validation of the 18F-Fluoroethoxybenzovesamicol (FEOBV) as a reliable biomarker for Alzheimer's disease*

Dear Dr. Soucy,

Thank you for responding to the IRB's correspondence concerning the 10 March 2014 full Board review of the above-referenced study.

The submitted response and revisions are acceptable. Final ethics approval for this study is provided on 12 May 2014:

- Research Protocol, version 11 April 2014;
- Consent Form, version 6 May 2014.

The ethics approval for this study is valid until **March 2015**. The Certificate of Ethical Acceptability is enclosed.


All research is required to undergo an annual ethics review in compliance with both federal and provincial frameworks guiding research involving human subjects. This annual review is scheduled according to the date of the study's initial ethics approval, and it is the Investigator's responsibility to submit a completed application form for Continuing Ethics Review to the IRB prior to the cessation of the study's ethics approval. A copy of the Continuing Review form is available on the IRB website at: <http://www.mcgill.ca/medresearch/ethics/forms>.

Any modifications or unanticipated developments that may occur to the study prior to the annual review must be reported to the IRB promptly. Study modifications cannot be implemented prior to ethics review and approval of the change.

In addition to the continuing review requirements, it is the Investigator's responsibility for ensuring that all documents approved by this IRB are reported to and meet the standards in effect at the institution where subject recruitment occurs and/or where study data is collected. There is a risk that the study's data may be invalidated and research funds frozen for failing to comply. *This study cannot be initiated until the Research Ethics Board or Office provides administrative approval for the study.*

The IRB has assigned this study the following **IRB Study Number: A03-M22-14A**. Please reference this number for all correspondence with our office.

Regards,



Roberta Palmour, PhD  
Chair  
Institutional Review Board

Cc: Ms. E. Campeau – DH  
Ms. L. Zegarelli - MNI  
A03-M22-14A

## CERTIFICATION OF ETHICAL ACCEPTABILITY FOR RESEARCH INVOLVING HUMAN SUBJECTS

The Faculty of Medicine Institutional Review Board (IRB) is a registered University IRB working under the published guidelines of the Tri-Council Policy Statement, in compliance with the Plan d'action ministériel en éthique de la recherche et en intégrité scientifique (MSSS, 1998), and the Food and Drugs Act (17 June 2001); and acts in accordance with the U.S. Code of Federal Regulations that govern research on human subjects. The IRB working procedures are consistent with internationally accepted principles of Good Clinical Practices.

At a full Board meeting on March 10, 2014, the Faculty of Medicine Institutional Review Board, consisting of:

John Breitner, MD

Patricia Dobkin, PhD

Daniel Mastine, BN, LLB(c)

Robert L. Munro, BCL

Scott Owen, MD

Roberta Palmour, PhD

Blossom Shaffer, MBA

John Storrington, MD

Margaret Swaine, BA

Examined the research project **A03-M22-14A** titled: *Clinical validation of the 18F-Fluoroethoxybenzovesamicol (FEOBV) as a reliable biomarker for Alzheimer's disease (AD)*

As proposed by: J.-P. Soucy/M.-A. Bedard to \_\_\_\_\_  
Applicant Granting Agency, if any

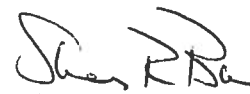
And consider the experimental procedures to be acceptable on ethical grounds for research involving human subjects.

12 May 2014

Date



Chair, IRB



Dean of Faculty

**Institutional Review Board Assurance Number: FWA 00004545**

**APPENDIX C**  
**CONSENT FORM**





## **POSITRON EMISSION TOMOGRAPHY (PET) & MAGNETIC RESONANCE IMAGING (MRI) CONSENT FORM**

*McConnell Brain Imaging Center, Departments of Nuclear Medicine & Neuroradiology*

### **Title of the Project:**

Clinical validation of the 18F-Fluoroethoxybenzovesamicol (FEOBV) as a reliable biomarker for Alzheimer's disease (AD).

### **Principal Investigators :**

Marc-André Bédard, PhD;  
Jean-Paul Soucy, MD, MSc;  
Pedro Rosa-Neto, MD, PhD

### **Co-Investigator:**

Serge Gauthier, MD

### **Sponsor :**

Fonds de Recherche du Québec en Santé (FRQS, Grant # 27303)

## **1. REASON FOR THE STUDY**

The aim of this study is to assess how effective a new Positron Emission Tomography (PET) imaging tracer is for improving the diagnosis and follow-up of Alzheimer's disease (AD). The new imaging tracer, called FEOBV, will be compared to two other PET tracers (FDG and NAV4694) more commonly used to assist in AD diagnosis.

The current document contains the information required to better understand the different steps and procedures involved in this study. You do not have to decide today whether or not you want to participate. Time will be set aside for you to review the document, ask questions, and discuss it with whomever you want.

## **2. PROCEDURES**

This study involves three different groups of 10 participants each: 1) Healthy volunteers; 2) Patients with a diagnosis of Alzheimer's Disease (AD); and 3) Patients with a diagnosis of Mild Cognitive Impairment (MCI).

You have been invited to take part in this study because you either have a diagnosis of AD, MCI, or you are considered a healthy research volunteer. If you choose to take part in this study, you will be asked to have a phone interview to confirm your eligibility. Thereafter, if you are eligible for this study, the brain imaging sessions will be scheduled. The imaging sessions will take place at the Montreal Neurological Institute (MNI).



## **2.1 Phone Interview**

During the phone interview, a series of questions will be asked about your past and current medical history as well as your previous involvement in other research projects on AD or MCI. This phone interview should last approximately 15 to 20 minutes.

## **2.2 Appointments at the Montreal Neurological Institute (MNI)**

If you are eligible to participate following the phone interview, you will be scheduled for a series of appointments at the MNI Brain Imaging Centre (BIC). During each of these appointments, PET imaging will be performed with one of the three compounds under study (FEOBV, FDG, and NAV4694). The mean duration of such PET imaging appointments is between 1 and 2 hours. However, another radiological technique called Magnetic Resonance Imaging (MRI) will be completed during the first appointment, as well as some questionnaires and memory tests, so that the total duration of that first appointment will rather be 3 hours.

Throughout the duration of this study, you will undergo a total of six PET scans: Three at the beginning of the study, and three others one year later. No more than one scan will be scheduled within the same week.

## **2.3 PET imaging Description**

PET is a nuclear medicine procedure involving the administration of very small amounts of a chemical called a tracer, and labeled with a radioactive atom of very short half-life (the time it takes for half of the radioactivity to disappear). When administered intravenously to a subject, this tracer circulates in the blood to reach its target where it will briefly stay before it decays. During this process, the tracer will emit a very small amount of radioactivity that can be detected by a sophisticated PET camera. With the help of high power computing, researchers are then able to study the distribution in brain of the chemical that has been administered. No effect of the tracer can be detected in a given individual, since it is always administered in very small amounts (tracer dose).

All PET imaging sessions scheduled as part of your participation will be supervised by a qualified nuclear medicine physician. On your arrival at the MNI PET unit, you will have to fill in routine questionnaires about your general physical condition. Then, you must lay on a couch, and a fine needle-catheter will be inserted into an arm vein. This needle-catheter will be used for the administration of one of the radioactive chemical substances used in the study (FEOBV, FDG and NAV4694). The couch will be moved into a cylindrical opening for the scanning process, which lasts approximately 30 minutes. The device is completely passive and has no electrical (or other) output that may be harmful.

## **2.4 MRI Description**

MRI is a non invasive technique used in radiology to investigate the anatomy of the body. MRI scanners use strong magnetic fields and radiowaves to form images of the body. The technique is widely used in hospitals for medical diagnosis. It will be used in the current study to obtain a detailed picture of your brain anatomy, in order to analyse the images obtained from the PET sessions.

You will be asked to lie on a couch that will be moved into a cylindrical opening where pictures of your head will be taken during a period of approximately 30 minutes. The MRI machine will not

produce any pain during the scan, but it is very noisy. To reduce the noise, you will be given earplugs. You will be able to communicate with the technician during the procedure.

### **3. CONTRAINDICATIONS**

#### **3.1 For the PET Studies**

The following conditions preclude participation to the PET scan : 1) Being under the age of 18; 2) Pregnancy or Breast Feeding; 3) Previous radiation doses received within the past year (12 months) that would lead - with the inclusion of the current study - to an total radiation absorbed dose exceeding 50 mSv.

#### **3.2 For the MRI Study**

The following conditions preclude participation to the MRI scan: 1) Pacemaker; 2) Aneurysm Clip; 3) Heart/Vascular Clip; 4) Prosthetic Valve; 5) Metal Prosthesis; 6) Claustrophobia; 7) Pregnancy; 8) Transdermal patches (if you need to have a patch on most of the time, you should bring one with you for application after the scanning session).

### **4. ADVANTAGES**

There is no direct advantage for your participation to this study. No aspect of this study may be considered as part of a medical treatment or management for your personal condition. However, it is hoped that the information obtained with your participation will help us improve the current methods of diagnosis and follow up of AD.

### **5. RISKS & DISADVANTAGES RELATED TO THE PET SCANS**

During the PET imaging sessions, you may feel a stinging sensation at the time of the needle-catheter insertion into the vein. Moreover, the reduced mobility during the scanning process may also be a source of restlessness and discomfort for some participants.

PET imaging involves the injection of specific agents (FEOBV, NAV4694, FDG) not normally present in your body. Like any other chemical or pharmaceutical compound, these agents have a potential to produce undesirable or allergic reactions. To date, there have been two adverse reactions reported in the world following the administration of NAV4694 : 1) Syncope (brief loss of consciousness), and 2) Allergic reaction. No other unfavourable drug reactions associated with the use of any of these three agents (FEOBV, NAV4694, FDG) have been identified until now.

Given that FEOBV, NAV4694 and FDG are radioactive compounds, this means that you will be exposed to a small dose of radiation (measured in milliSieverts, or mSv), above what one individual is usually exposed to in daily life (natural radiation in the environment, cosmic rays, ...), or for medical reasons (diagnostic X-rays, radiation therapy, ...). Most of the radioactivity will be gone from your body after a few hours. Nationally accepted limits of radiation doses administered for research purposes have been defined at 50 mSv/year. In order to ensure that the amount of radiation you receive does not exceed the annual limits, you must inform us of your participation in any research involving radiation exposure. Similarly, if you are participating in or thinking of participating in other research involving radiation exposure, you must inform the investigator of those studies of your participation in this study. The dose you are expected to receive for the 3 PET scans at the start of the study is estimated at 19 mSv. The same is expected for the 3 other ones performed one year later, for a total study dose of 38 mSv.



Most of the radioactivity you will receive will be gone from your body in a matter of hours (by 20 hours, it will be essentially undetectable). When people think of radiation exposure and risks, often the risk pertains to the development of cancer. It is known that radiation increases the risk of developing cancer when exposed to certain doses. The doses used for this PET imaging study are very small, and these small doses have not been associated with the development of cancer. The risk of developing some future cancer resulting from your participation in this study is very low, and might not even exist.

If you are or may become pregnant, please note that this research procedure may involve unforeseeable risks to the embryo or foetus. Enrolled participants must not be pregnant and should agree to contraception while on study.

Please note that FEOBV and NAV4694 are not currently approved for clinical use in Canada. However, their use for research purposes is allowed by Health Canada. As for the FDG, its usage is approved in Canada for both clinical and research purposes.

## **6. EFFECTS OF PARTICIPATION IN THIS STUDY ON YOUR TREATMENT**

Positron emission tomography or magnetic resonance spectroscopy do not interfere with any treatment or other diagnostic tests. Your participation to this research will not affect any part the current medical management of your condition. Moreover, in the event of any research-related injury or adverse event, an appropriate treatment will be put in place for you.

## **7. CONFIDENTIAL NATURE OF THIS STUDY**

The data collected in this study will be kept confidential. No personal information will be released to third parties without your written approval. Only the person directly involved in the research project will have access to these data. In case of dissemination of the study results, it will not be possible to identify the participating individuals. Your name, date of birth, address, telephone number and medical information collected for this study may have to be forwarded to Health Canada, upon request. Data will be kept for a 5-year duration after the end of the study (funding period) before being destroyed.

## **8. INCIDENTAL FINDINGS**

MRI/PET research scans are not subject to clinical review. However, incidental findings noted by the researcher may be communicated to you and, upon your request, to your physician.

## **9. DISCONTINUATION OF THE STUDY BY THE INVESTIGATOR**

At any time during testing, the investigators have the right to terminate the study for any reason such as technical, financial, scientific, or safety issues.

## **10. COMPENSATION**

Upon completion of the study you will qualify for a compensation for transport, time lost, and other inconveniences: 40.00\$ per session, for a total of \$240.00 (6 sessions).

If studies have to be terminated for any reason, compensation will be adjusted according to the fraction of the study completed.



## 11. WITHDRAWAL FROM THE STUDY

Your participation in this research project is voluntary. You may withdraw at any time, including during the procedure, without justification or prejudice to yourself or your treatment.

## 12. CONTACTS

At any time during this research project, you may be contacted by a member of the McGill Institutional Review Board, at the discretion of the board.

For any query regarding your participation into this research project, you may want to contact the coordinator, Ms **Meghmik Aghourian**, at the following number: (514) 769-9716

You may also contact one of the investigators involved in this study:

- Project as a whole and neuropsychological testing:
  - Dr M.A. Bédard, PhD (514) 987-3000, ext. 0220
  
- PET & MRI Imaging:
  - Dr J.P. Soucy, MD, MSc (514) 398-8515
  - Dr P. Rosa-Neto, MD, PhD (514) 766-2010
  
- Enrollment of participants:
  - Dr S. Gauthier, MD (514) 766-2010

## 13. COMPLAINTS

You may address any complaint related to this research project to the Montreal Neurological Hospital patient's committee at the following number (514) 398-5358



**POSITRON EMISSION TOMOGRAPHY (PET) & MAGNETIC RESONANCE IMAGING  
(MRI)  
CONSENT FORM**

*McConnell Brain Imaging Center, Departments of Nuclear Medicine & Neuroradiology*

**Title of the Project:**

Clinical validation of the 18F-Fluoroethoxybenzovesamicol (FEOBV) as a reliable biomarker for Alzheimer’s disease (AD).

**Principal Investigators :**

Marc-André Bédard, PhD;  
Jean-Paul Soucy, MD, MSc;  
Pedro Rosa-Neto, MD, PhD

**Co-Investigator:**

Serge Gauthier, MD

**Sponsor :**

Fonds de Recherche du Québec en Santé (FRQS, Grant # 27303)

**SUBJECT'S DECLARATION OF CONSENT**

I, \_\_\_\_\_, have read the above description with one  
of the above investigators, \_\_\_\_\_.

I fully understand the procedures, advantages and disadvantages of the study, which have been explained to me. I freely and voluntarily consent to participate in this study.

Further, I understand that I may seek information about any aspect of this research project, before, during, or after its realisation, that I am free to withdraw at any time if I desire, and that my personal information will be kept confidential.

I do not waive any of my legal rights by signing this consent form.

I will receive a signed copy of this consent form.

SIGNATURE \_\_\_\_\_  
SUBJECT

\_\_\_\_\_  
DATE

SIGNATURE \_\_\_\_\_  
INVESTIGATOR

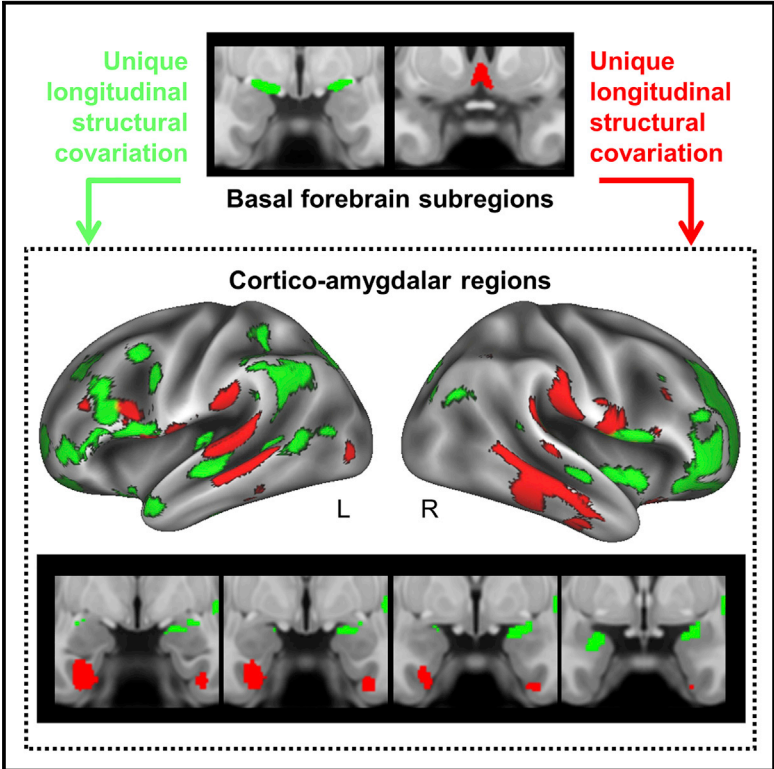
\_\_\_\_\_  
DATE

**APPENDIX D**

**REPRINT OF ARTICLE BY TAYLOR SCHMITZ AND COLLEAGUES 2018**

## Longitudinal Alzheimer’s Degeneration Reflects the Spatial Topography of Cholinergic Basal Forebrain Projections

### Graphical Abstract



### Authors

Taylor W. Schmitz, Marieke Mur, Meghmik Aghourian, Marc-Andre Bedard, R. Nathan Spreng, for the Alzheimer’s Disease Neuroimaging Initiative

### Correspondence

taylor.schmitz@gmail.com

### In Brief

Among older adults in prodromal stages of Alzheimer’s disease, Schmitz et al. show that longitudinal degeneration within sub-regions of the basal forebrain covaries with cortico-amygdalar topographies of both structural degeneration and cholinergic denervation. The findings support the view that loss of cortico-amygdalar cholinergic input is a pivotal event in AD progression.

### Highlights

- The basal forebrain degenerates substantially in early Alzheimer’s disease (AD)
- Longitudinal gray matter loss in the basal forebrain, cortex, and amygdalae covaries
- This covariation reflects the organization of the basal forebrain cholinergic projections
- This covariation also reflects [<sup>18</sup>F] FEOBV PET indices of cholinergic denervation





# Longitudinal Alzheimer's Degeneration Reflects the Spatial Topography of Cholinergic Basal Forebrain Projections

Taylor W. Schmitz,<sup>1,7,\*</sup> Marieke Mur,<sup>2</sup> Meghmik Aghourian,<sup>3,4,5</sup> Marc-Andre Bedard,<sup>3,4,5</sup> and R. Nathan Spreng,<sup>1,6</sup> for the Alzheimer's Disease Neuroimaging Initiative

<sup>1</sup>Department of Neurology and Neurosurgery, Montreal Neurological Institute, McGill University, Montreal, QC, Canada

<sup>2</sup>Medical Research Council Cognition and Brain Sciences Unit, University of Cambridge, Cambridge, UK

<sup>3</sup>Cognitive Pharmacology Research Unit, Université du Québec à Montréal (UQAM), Montreal, QC, Canada

<sup>4</sup>McConnell Brain Imaging Centre, Montreal Neurological Institute, Montreal, QC, Canada

<sup>5</sup>McGill Centre for Studies in Aging, Douglas Mental Health University Institute, Verdun, QC, Canada

<sup>6</sup>Department of Human Development, Human Neuroscience Institute, Cornell University, Ithaca, NY, USA

<sup>7</sup>Lead Contact

\*Correspondence: [taylor.schmitz@gmail.com](mailto:taylor.schmitz@gmail.com)

<https://doi.org/10.1016/j.celrep.2018.06.001>

## SUMMARY

The cholinergic neurons of the basal forebrain (BF) provide virtually all of the brain's cortical and amygdalar cholinergic input. They are particularly vulnerable to neuropathology in early Alzheimer's disease (AD) and may trigger the emergence of neuropathology in their cortico-amygdalar projection system through cholinergic denervation and *trans*-synaptic spreading of misfolded proteins. We examined whether longitudinal degeneration within the BF can explain longitudinal cortico-amygdalar degeneration in older human adults with abnormal cerebrospinal fluid biomarkers of AD neuropathology. We focused on two BF subregions, which are known to innervate cortico-amygdalar regions via two distinct macroscopic cholinergic projections. To further assess whether structural degeneration of these regions in AD reflects cholinergic denervation, we used the [<sup>18</sup>F] FEOBV radiotracer, which binds to cortico-amygdalar cholinergic terminals. We found that the two BF subregions explain spatially distinct patterns of cortico-amygdalar degeneration, which closely reflect their cholinergic projections, and overlap with [<sup>18</sup>F] FEOBV indices of cholinergic denervation.

## INTRODUCTION

The emergence of Alzheimer's disease (AD) neuropathologies, such as misfolded  $\beta$ -amyloid (A $\beta$ ) and Tau proteins, progresses in stages across anatomically and functionally connected regions of the brain, with certain brain regions affected before others (Braak and Braak, 1991; Braak and Del Tredici, 2015; Raj et al., 2012, 2015; Seeley et al., 2009). Why certain brain regions appear more vulnerable to AD pathology than others has

long remained a mystery. However, recent functional genomics research, using brain tissue in both human AD and non-human animal models of AD, has started to elucidate structural and functional cell characteristics that predict selective neuronal vulnerability to AD pathology. Vulnerable neurons typically have large axonal projections that extend relatively long distances, from one region of the brain to another. As a result, they require high metabolic expenditure to maintain trophic support—transporting materials over long distances and maintaining enormous cytoskeletal surface areas. These morphological properties increase vulnerability to oxidative stress and neuroinflammation, perturbed energy homeostasis, and accumulation of misfolded proteins (Lewis et al., 2010; Mattson and Magnus, 2006; Wang et al., 2010).

The magnocellular cholinergic neurons in the basal forebrain (BF) are known to have very large projections, targeting distal areas of the cortical mantle and amygdalae via multiple routes such as the cingulum bundle (Bloem et al., 2014; Chandler et al., 2013; Hecker and Mesulam, 1994; Kondo and Zaborszky, 2016; Mesulam et al., 1983a, 1986; Zaborszky et al., 2015). Precise estimates of their size have been difficult to obtain due to the complexity of their axonal branching. Recently, however, the complete morphology of individual cholinergic neurons was visualized in mice using a novel cell labeling technique (Wu et al., 2014). Extrapolating from their results, the authors estimated that cholinergic projections in humans approach  $\sim$ 100 m in length for a single cell when accounting for all axonal branches. As a result of their exceptional size, cholinergic neurons are therefore likely to exhibit selective neuronal vulnerability (SNV) to AD pathology.

Consistent with the SNV model, post-mortem histological evidence suggests that the cholinergic BF neurons accumulate both intraneuronal Tau, and, interestingly, intraneuronal A $\beta$  as early as the third decade of life, with profound accumulation observed 1 year after transition to mild cognitive impairment (MCI) (Arendt et al., 2015; Baker-Nigh et al., 2015; Braak and Braak, 1991; Braak and Del Tredici, 2015; Geula et al., 2008; Mesulam et al., 2004; Mesulam, 2013; Schliebs and Arendt, 2006, 2011). *In vivo* neuroimaging data have demonstrated that



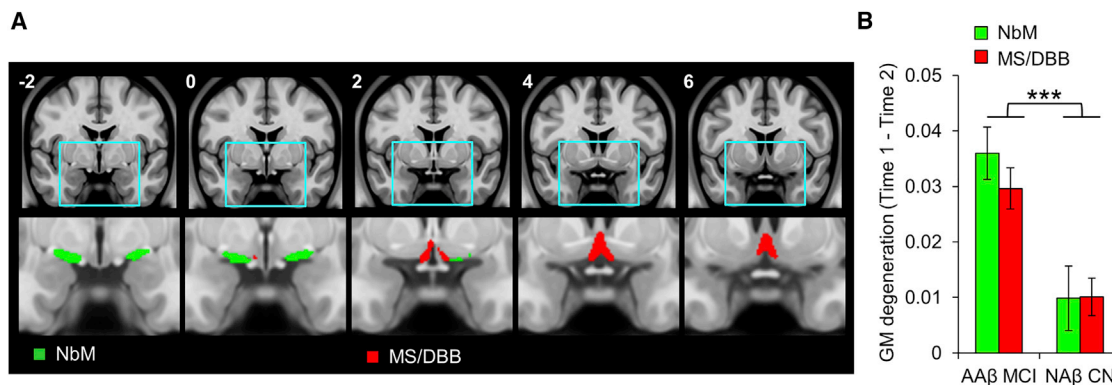


**Figure 1. Basal Forebrain Regions of Interest and Longitudinal Degeneration in Early AD**

(A) Regions of interest (ROIs) were defined from stereotaxic probabilistic maps of the human basal forebrain (Zaborszky et al., 2008). The nucleus basalis of Meynert (NbM) is displayed in green. The medial septal nucleus and diagonal band of Broca (MS/DBB) are displayed in red. The ROIs are projected on coronal slices in standard atlas space (MNI y coordinates are inset).

(B) Longitudinal degeneration (y axis) of both NbM and MS/DBB was elevated among individuals with abnormal cerebrospinal levels of the amyloid- $\beta$  biomarker and mild cognitive impairment (A $\beta$  MCI) relative to age-matched controls with normal A $\beta$  and cognitive function (NA $\beta$  CN). y axis units are averaged gray matter volume within each ROI  $\pm$  SEM.

cognitively normal (CN) older adults expressing abnormal cerebrospinal fluid (CSF) biomarkers of A $\beta$  accumulation, i.e., individuals in preclinical stages of AD, exhibit greater longitudinal degeneration in the BF compared to CN adults with normal CSF A $\beta$  (Schmitz and Spreng, 2016). Furthermore, total gray matter volume in the BF at baseline was found to predict subsequent longitudinal degeneration in the entorhinal cortex—a major target of cholinergic innervation (Kondo and Zaborszky, 2016)—and memory impairment. Competing models using baseline volume in entorhinal cortex to predict longitudinal degeneration in BF were not supported (Schmitz and Spreng, 2016). These findings suggest a potential interdependence between degeneration in the BF and the cholinergic cortical targets of its projection system.

Research in non-human animals strongly supports this possibility. In mice bred to express a genetic knockout or knockdown of the vesicular acetylcholine transporter (VAcHT, SLC18A3), a protein required for acetylcholine (ACh) release from cholinergic BF neurons (de Castro et al., 2009; Prado et al., 2013), long-term cholinergic deficiency leads to abnormal accumulation of A $\beta$  and Tau in cholinergic cortical neurons (Kolisnyk et al., 2016, 2017). These data suggest a role for cholinergic signaling in maintaining normal cell metabolism, including native biological functions related to the amyloid precursor and Tau proteins. In parallel to cholinergic denervation, intact but diseased cholinergic inputs might facilitate yet another mechanism of “seeding” the cortex with AD pathology, specifically through the *trans*-synaptic spread of misfolded Tau fragments (Clavaguera et al., 2009; de Calignon et al., 2012; Khan et al., 2014).

If the emergence of AD pathology in the cortex is caused by the loss of cortical cholinergic input or *trans*-synaptic spreading of Tau from cholinergic neurons, then the spatial topography of cortico-amygdalar degeneration should reflect the cholinergic projection system. The cholinergic BF projections exhibit topographical organization at multiple spatial scales (Ballinger et al., 2016; Bloem et al., 2014; Kondo and Zaborszky, 2016; Me-

sulam and Geula, 1988; Mesulam et al., 1983b, 1986; Zaborszky et al., 2015). To accommodate the spatial scale of high-resolution structural magnetic resonance imaging (MRI) data employed in the present study, we chose a topography that divides the BF into two segregated macroscopic projections (Zaborszky et al., 2008), the medial septal nucleus and diagonal band of Broca (MS/DBB) projection targeting medial temporal lobe, and the nucleus basalis of Meynert (NbM) projection targeting frontoparietal cortices and the amygdalae (Figures 1A and S1; Experimental Procedures). Structural properties such as gray matter volume are known to selectively co-vary between brain regions that are functionally and anatomically connected (Alexander-Bloch et al., 2013; Bassett et al., 2008; Cantero et al., 2017; Chen et al., 2008; Dupre and Spreng, 2017; He et al., 2007; Kilimann et al., 2017; Schmitz and Spreng, 2016; Spreng and Turner, 2013), enabling us to test the covariance in longitudinal structural degeneration between the BF and distinct targets of its cholinergic projections in the cortex and amygdalae.

Longitudinal voxel-based morphometry was used to measure changes in BF and cortico-amygdalar gray matter (GM) volume over a 2-year interval in older adults with mild cognitive impairment (MCI) and the CSF-A $\beta$  biomarker of central AD pathology (Shaw et al., 2009). These data were acquired from the Alzheimer’s Disease Neuroimaging Initiative (Mueller et al., 2005). Voxel-based morphometry was used to derive longitudinal indices of GM degeneration within the BF sub-regions (Grothe et al., 2018). We then performed a “seed-to-searchlight” analysis to determine whether the BF MS/DBB and NbM sub-regions (the “seeds”) exhibit unique patterns of covariation with regions of cortex (the “searchlights”). We then compared these maps against a direct *in vivo* assay of cortical cholinergic denervation using the positron emission tomography (PET) radiotracer [ $^{18}$ F] FEOBV, which exhibits high binding sensitivity and specificity to VAcHT (Aghourian et al., 2017). We show that in AD, topographies of longitudinal cortical degeneration covary with

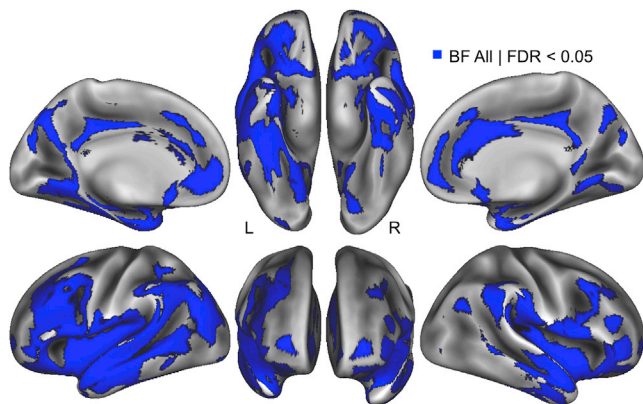


**Figure 2. Spatial Topography of Covariance between BF and Cortical Degeneration**

Seed-to-searchlight analysis tested whether BF degeneration (averaged over NbM and MS/DBB sub-regions) covaried with cortical degeneration within 6 mm radius spherical “searchlight” ROIs in the AA $\beta$  MCI group, controlling for age, sex, education, total intracranial volume, and longitudinal change in whole brain volume. Significant searchlights (blue overlay) were determined using a false discovery rate (FDR)-corrected  $p < 0.05$ . Results are projected on an inflated cortical surface in MNI atlas space.

longitudinal degeneration of the NbM and MS/DBB and closely reflect the known anatomical organization of the cortical cholinergic projection system, as well as the functional topographies of cortical cholinergic denervation assayed by [ $^{18}\text{F}$ ] FEOBV PET.

## RESULTS

### The BF Exhibits Severe Longitudinal Degeneration in Early AD

To ensure the presence of AD pathology in our sample of older adults, independent of longitudinal structural MRI, we used the cerebrospinal fluid amyloid- $\beta$  biomarker (CSF A $\beta_{1-42}$ ). Prior analyses of the ADNI core datasets (Shaw et al., 2009) have provided a cutpoint for CSF A $\beta_{1-42}$  concentration at which diagnostic sensitivity and specificity to AD is maximal (192 pg mL $^{-1}$ ), yielding correct detection of 96.4% (<192 pg mL $^{-1}$ ) and correct rejection of 95.2% (>192 pg mL $^{-1}$ ) (Experimental Procedures). Only individuals with abnormal CSF A $\beta_{1-42}$  values (AA $\beta$ ) falling below this cutpoint were included. Second, in order to ensure our sample was at a stage of AD characterized by longitudinal degeneration in amygdalar, allocortical, and neocortical areas (Grothe et al., 2013; Schmitz and Spreng, 2016), we further filtered individuals according to their neuropsychological status. Only individuals with a diagnosis of MCI based on the ADNI neuropsychological test battery were included. We included both MCI individuals who remained stable and converted to AD in the 2-year study interval. After triangulating AD pathology from CSF biomarker and neuropsychological measures, our final sample size of AA $\beta$  MCI adults was  $n = 80$  (mean  $\pm$  SD; CSF A $\beta_{1-42}$  concentration = 136.45  $\pm$  25.31, range = 81–190). See Table S1 for demographic and neuropsychological information, as well as CSF total Tau and phosphorylated Tau indices. See Table S2 for individual ADNI research identifier numbers, sMRI image identifier numbers, and A $\beta$  subgroup designation. Individ-

uals presenting MCI neuropsychological status but normal CSF A $\beta$  levels were excluded from all forthcoming analyses, as their cognitive symptoms are likely to be caused by non-AD pathology, for example, vascular dementia and hippocampal sclerosis. See Table S3 for excluded MCI participants.

We next confirmed that the AA $\beta$  MCI group exhibited abnormal longitudinal degeneration in the BF subregional ROIs: NbM and MS/DBB. To do so, we compared longitudinal GM changes (time 1 – time 2) in the AA $\beta$  MCI group against a control group of age-matched older adults with both normal CSF A $\beta_{1-42}$  values (NA $\beta$ ) and normal neuropsychological status (NA $\beta$  CN:  $n = 52$ , mean  $\pm$  SD; CSF A $\beta_{1-42}$  concentration = 242.46  $\pm$  25.55, range = 196–300). These groups also differed significantly in their CSF concentrations of total Tau and phosphorylated Tau (Tables S1 and S2). A 2 (group)  $\times$  2 (BF ROI) repeated-measures ANOVA revealed a significant main effect of group ( $F_{1,130} = 16.4$ ,  $p < 0.001$ ), driven by significant between group differences in both BF subregions (NbM:  $t_{130} = 3.5$ ,  $p < 0.001$ ; MS/DBB:  $t_{130} = 3.9$ ,  $p < 0.001$ ) (Figure 1B). We did not observe a main effect of ROI ( $F < 1$ ), or a group by ROI interaction ( $F = 1$ ). Consistent with existing work on longitudinal structural degeneration of the BF in MCI (Grothe et al., 2013; Schmitz and Spreng, 2016), our initial findings indicate that the presence of AD pathology yielded large increases in the magnitude of degeneration in both BF nuclei over a 2-year interval compared to normally aging older adults.

### Covariation of Longitudinal Degeneration between the BF and Cortico-Amygdalar Regions

Having confirmed abnormal BF degeneration in our MCI sample, we next conducted a regression-based seed-to-searchlight analysis using the entire BF (NbM and MS/DBB combined) as the seed region. Searchlight analyses test a statistical model in small spherical ROIs (“searchlights”) centered on every voxel, as opposed to the individual voxels themselves (Kriegeskorte et al., 2006). At each searchlight, a multiple linear regression model was performed with mean longitudinal degeneration (time 1 – time 2) within the BF as the predictor, and nuisance covariates for age, sex, education, total intracranial volume, and longitudinal change in whole brain volume. The dependent variable was mean degeneration (time 1 – time 2) within the cortical searchlight. A significant searchlight indicates a covariation in longitudinal degeneration between the BF and the local neighborhood of voxels within the searchlight region.

Across AA $\beta$  MCI individuals, we found that larger magnitudes of longitudinal BF degeneration covaried with larger magnitudes of cortical degeneration in the frontal, temporal, and parietal cortices. The data were corrected for multiple comparisons using a false discovery (FDR) rate  $p < 0.05$  (Figure 2). Spatial foci within these cortical areas are in close agreement with prior work showing preferential vulnerability to AD pathology in anterior medial temporal cortex, cingulate cortex, and lateral frontoparietal cortices (Buckner et al., 2005). We also observed significant covariation bilaterally in the amygdalae.

We conducted a second seed-to-searchlight analysis in the NA $\beta$  CN group, using the same model specifications as in the AA $\beta$  MCI group. However, this model failed to detect supra-threshold cortical degeneration after correction for multiple



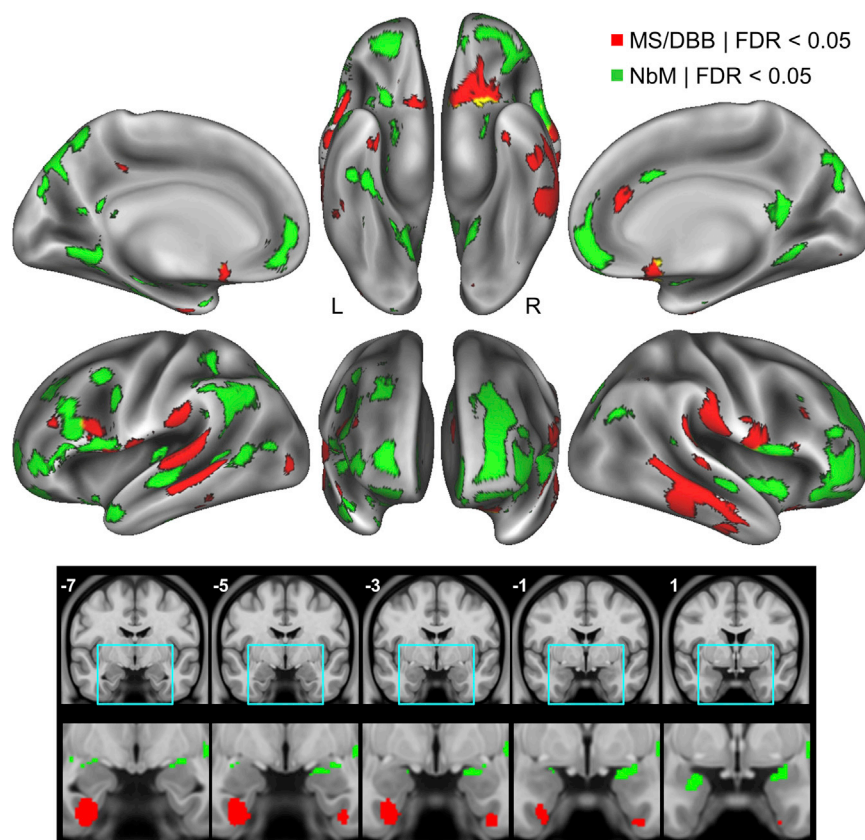


**Figure 3. Degeneration within BF NbM and MS/DBB Nuclei Covaries with Distinct Spatial Topographies of Degeneration in Their Cortical Targets**

Seed-to-searchlight analysis tested whether the NbM or MS/DBB BF subregions selectively covaried with cortical degeneration in the A $\beta$  MCI group, controlling for degeneration in the opposing BF subregion (MS/DBB and NbM, respectively). The NbM selectively covaried with degeneration (green overlays) in distributed areas of frontal, parietal, and occipital cortex (top), as well as in the amygdalae (bottom). The MS/DBB selectively covaried with degeneration (red overlays) in more circumscribed areas of temporal cortex including the middle temporal gyrus (cortical surfaces), and the entorhinal cortices (bottom). Additional areas included the temporo-parietal and left inferior frontal cortices. Significant searchlights were determined using a FDR-corrected  $p < 0.05$ . Top: results are projected on an inflated cortical surface in MNI atlas space. Bottom: results are displayed on coronal slices in MNI atlas space (y coordinates are inset).

comparisons. Hence, these patterns do not appear to reflect normal age-related patterns of covariance between BF and cortical degeneration.

### Cortico-Amygdalar Covariation with BF Subregions Reflects the Cholinergic BF Projections

Many of the spatial foci identified by this initial analysis are also known to be strongly innervated by the ascending cholinergic projections, including the entorhinal cortex, hippocampus, amygdalae, and medial prefrontal cortex (Bloem et al., 2014; Chandler et al., 2013; Hecker and Mesulam, 1994; Kondo and Zaborszky, 2016; Mesulam et al., 1986, 1983a; Zaborszky et al., 2015). However, the observed spatial topography may merely reflect coincidental degeneration of the BF, cortex, and amygdalae; A $\beta$  MCI individuals with larger magnitudes of BF degeneration may tend to exhibit larger magnitudes of cortico-amygdalar degeneration due to parallel independent events. If this were the case, we would not expect degeneration within subregions of the BF to exhibit distinct patterns of covariation with degeneration in the cortex and amygdalae. Alternatively, if pathological events within the cholinergic BF subregions and their cortico-amygdalar targets are linked, longitudinal degeneration in NbM and MS/DBB should exhibit a pattern of cortico-amygdalar interdependence reflecting the distinct topography of their projections.

To adjudicate these competing alternatives, we conducted two modified seed-to-searchlight analyses on each BF subre-

gion—NbM and MS/DBB—that are known to form segregated macroscopic projections to distinct areas of cortex and amygdalae. Each analysis examined whether mean longitudinal degeneration (time 1 – time 2) within either the NbM or MS/DBB ROI selectively covaried with

mean degeneration within the cortical searchlights, while controlling for degeneration in the opposing subregion. As before, additional covariates included age, sex, education, total intracranial volume, and longitudinal change in whole brain volume. Across A $\beta$  MCI individuals, we observed that NbM and MS/DBB selectively covaried with distinct topographies of cortical degeneration that closely align with the segregated organization of their cholinergic projections (Figure 3). Higher magnitudes of NbM degeneration selectively covaried with higher magnitudes of degeneration in a more distributed topography reflecting its widespread cholinergic innervations of the frontal, parietal, and occipital cortices (Bloem et al., 2014; Mesulam and Geula, 1988; Mesulam et al., 1986, 1983a). The NbM also selectively covaried with higher focal degeneration in the amygdalae, an area which is densely innervated by its cholinergic projections (Hecker and Mesulam, 1994).

By contrast, the MS/DBB selectively covaried with higher magnitudes of degeneration in a more circumscribed topography. Degeneration within the temporal lobe, including the entorhinal cortex and extending laterally into the middle temporal gyri, are areas known to receive cholinergic innervations from the medial septal nucleus (MS) and vertical band of the DBB (Kondo and Zaborszky, 2016). Areas of MS/DBB covariation outside of the temporal cortex included the olfactory cortex, an area known to receive cholinergic projections from the horizontal band of the DBB (Mesulam et al., 1983a, 1986). Our longitudinal findings are consistent with cross-sectional studies

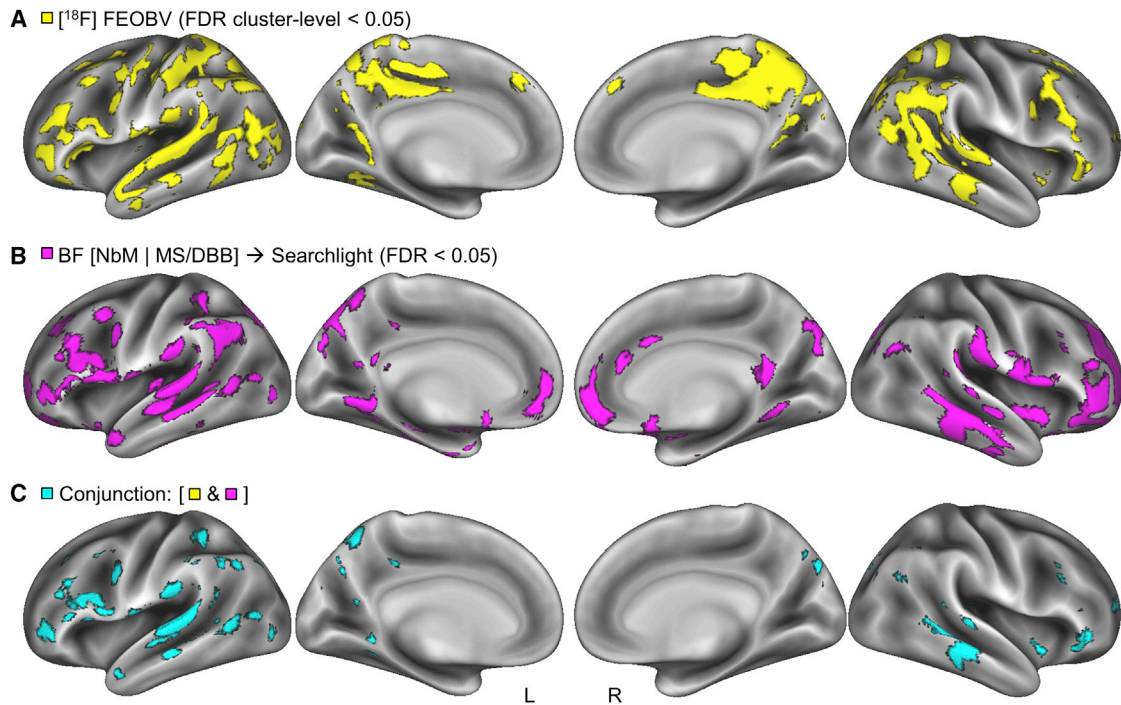


**Figure 4. Spatial Convergence across Multimodal Indices of Cortical Cholinergic Degeneration**

(A) A map of cortical cholinergic degeneration assayed by between group comparison of [ $^{18}\text{F}$ ] FEOBV binding in cognitively normal versus AD adults (primary cluster forming threshold  $p$  uncorrected  $<0.001$ , secondary FDR cluster level threshold  $<0.05$ ).

(B) A composite of the seed-to-searchlight maps for each BF subregion (Figure 3) was generated using a logical OR operation.

(C) A conjunction analysis (logical AND) was then applied to the FDR-corrected maps in (A) and (B). Results are projected on an inflated cortical surface in MNI atlas space.

demonstrating stronger inter-regional covariation of MS/DBB with hippocampal and amygdalar gray matter, and NbM with cingulate gray matter, in MCI compared to CN older adults (Cantero et al., 2017; Kilimann et al., 2017).

The subregional NbM and MS/DBB searchlight topographies were more spatially restricted than the searchlight topography observed in the initial analysis (both NbM and MS/DBB combined; Figure 2), especially in the cortical midline, indicating that the NbM and MS/DBB share common variance in these searchlight locations.

### Convergent Structural and Functional Topographies of Cholinergic Degeneration

Our seed-to-searchlight structural degeneration maps suggest an interdependence between AD pathology within the BF projection system and its cortico-amygdalar targets. However, by itself, sMRI cannot determine whether the observed structural interdependencies (Figure 3) are specific to cortical cholinergic innervations. We therefore adopted a multimodal imaging strategy using the [ $^{18}\text{F}$ ] FEOBV PET radiotracer, which exhibits a very high binding affinity and an excellent specificity for the vesicular acetylcholine transporter (VAChT), a glycoprotein found on the membrane of synaptic vesicles of cholinergic neurons (Aghourian et al., 2017; Cyr et al., 2014; Parent et al., 2012) (Figure S2; Table S4; Supplemental Experimental Procedures). The [ $^{18}\text{F}$ ] FEOBV tracer provides an estimate of presynaptic neuronal

integrity and is thought to remain unaffected by the post-synaptic activity of enzymes such as acetylcholinesterase (ACHE), although this has yet to be demonstrated *in vivo*. Cortical cholinergic denervation, whether induced experimentally via selective lesions of the BF nuclei in rats (Cyr et al., 2014; Parent et al., 2012), or due to AD pathology in humans (Aghourian et al., 2017), both alter regionally specific patterns of [ $^{18}\text{F}$ ] FEOBV binding.

We first compared cognitively normal ( $n = 6$ ) and AD ( $n = 6$ ) older adults with indices of [ $^{18}\text{F}$ ] FEOBV PET, collected as part of a prior study (Aghourian et al., 2017), to identify areas of significant cholinergic denervation. A two-sample  $t$  test controlling for age (Table S4; Experimental Procedures) revealed lower [ $^{18}\text{F}$ ] FEOBV binding in the AD group spanning lateral fronto-parietal and temporal cortical areas. Due to the smaller sample sizes, we first imposed a cluster-forming threshold with an uncorrected  $p < 0.001$ , followed a cluster-level FDR-corrected  $p < 0.05$  (Woo et al., 2014) (Figure 4A). We note that no differences were observed in the thalamus, medial temporal lobe, or amygdalar areas at the FDR-corrected threshold.

We next examined the precise areas of spatial convergence between the [ $^{18}\text{F}$ ] FEOBV assay of cholinergic denervation (Figure 4A) and our seed-to-searchlight assay of BF-dependent structural degeneration (Figure 4B). To do so, a logical AND operation was performed on the FDR-corrected maps from each imaging modality (Nichols et al., 2005). The resulting

conjunction revealed tight correspondence in virtually all cortical areas of the left hemisphere. The right hemisphere exhibited lower spatial overlap, due in part to weaker effect sizes of clusters in these areas in the [ $^{18}\text{F}$ ] FEOBV group comparison (Figure 4C). Taken together, these findings indicate that spatial topographies of cortical degeneration in AD reflect the anatomical topography of the cholinergic projection system, and thus suggest the loss of cortical cholinergic input from the BF might play a major role in the emergence of cortico-amygdalar gray matter degeneration.

## DISCUSSION

We demonstrated that the MS/DBB and NbM subregions of the basal forebrain covary with segregated topographies of cortical degeneration (Figure 3). These topographies align closely with the known anatomical segregation between the cholinergic projections of the MS/DBB and NbM subregions (Bloem et al., 2014; Hecker and Mesulam, 1994; Kondo and Zaborszky, 2016; Mesulam et al., 1983a, 1986; Zaborszky et al., 2015). We then used [ $^{18}\text{F}$ ] FEOBV PET indices of binding with the vesicular acetylcholine transporter (VACHT) to demonstrate that cortical cholinergic denervation in AD exhibits spatial correspondence with our BF-dependent structural degeneration maps (Figure 4).

If the cholinergic BF neurons are selectively vulnerable to perturbed energy homeostasis, oxidative stress, and neuroinflammation due to their large axons (Lewis et al., 2010; Mattson and Magnus, 2006; Wang et al., 2010; Wu et al., 2014), they might lose the capacity to maintain full trophic support of these large axons over the course of aging. Lending support to this hypothesis, the number of cholinergic fibers per BF neuron reduces in early middle age, and especially in the transition from preclinical to MCI stages of AD, against a background of accumulating intraneuronal A $\beta$ , hyper-phosphorylated Tau, and neurofibrillary tangles (Arendt et al., 2015; Baker-Nigh et al., 2015; Braak and Braak, 1991; Braak and Del Tredici, 2015; Geula et al., 2008; Mesulam et al., 2004; Mesulam, 2013; Schliebs and Arendt, 2006, 2011). As a result, the cortex and amygdalae might become progressively denuded of cholinergic input, with genetic AD risk factors such as the APOE  $\epsilon$ 4 allele (Poirier et al., 1995) and reduced metabolism (Rivera et al., 2005) contributing to differentiate normal age-related from AD trajectories of cholinergic loss.

Work in non-human animals indicates that cortico-amygdalar cholinergic denervation is a pivotal event in the AD pathophysiological cascade. Among mice bred to express a deficiency in VACHT (SLC18A3) capacity, the consequent reduction in cholinergic tone across the lifespan is, by itself, sufficient to induce aggregation of A $\beta$  and hyper-phosphorylated Tau within brain areas receiving BF cholinergic projections, such as the hippocampus (Kolisnyk et al., 2016, 2017). Under this scenario, loss of cholinergic BF projections might “seed” pathophysiological changes in their cortical and amygdalar targets due to loss of cholinergic signaling. In parallel to the loss of cholinergic input, intact but diseased cholinergic projections might also transmit Tau *trans*-synaptically to cholinoreceptive cortico-amygdalar neurons. *Trans*-synaptic spread of Tau has been reported for glutamatergic neurons in the entorhinal and hippocampal cortices (Clavaguera et al., 2009; de Calignon et al., 2012;

Khan et al., 2014), however, the findings imply a general mechanism by which AD pathology can spread from diseased neurons to functionally and anatomically connected healthy neurons. In either scenario, degeneration within cortico-amygdalar targets of cholinergic BF projections should reflect the topography of the cholinergic projections themselves. We provide additional support for this hypothesis with longitudinal structural MRI.

In humans, cholinergic hypofunction correlates with the formation of A $\beta$  plaques, tangles containing hyper-phosphorylated Tau and clinical severity of AD (Auld et al., 2002; Fisher, 2012). We observed that in addition to abnormal CSF A $\beta$  concentration (that was used as a grouping variable), both CSF phosphorylated Tau and total Tau were significantly elevated in the AA $\beta$  MCI compared to the NA $\beta$  CN group (Table S1). Although we cannot infer from CSF data where and how these biomarkers are distributed in the brain, our findings demonstrate that in the MCI group longitudinal gray matter degeneration within the cortico-amygdalar cholinergic BF projection system, as well as cognitive decline, occurred against a biomolecular background of significant neuropathology. Nevertheless, in humans, stronger connections are needed to link the progression of cortical cholinergic denervation to its potentially very early roles in driving cortical neuropathology and altering cortical functions important for cognition, such as selective attention (Romberg et al., 2013; Schmitz et al., 2010, 2014; Schmitz and Duncan, 2018).

Standard T1-weighted sMRI measures of gray matter volume cannot distinguish different cell types. Hence, we cannot infer from our sMRI data alone whether longitudinal reductions in gray matter within the BF reflect a selective loss of cholinergic cell bodies, or some combination of cholinergic, GABAergic, and glutamatergic neurons known to co-populate its MS/DBB and NbM subregions (Henny and Jones, 2008; Lin et al., 2015). The [ $^{18}\text{F}$ ] FEOBV PET radiotracer obviates this limitation. Unlike FDG and amyloid radiotracers, [ $^{18}\text{F}$ ] FEOBV provides a highly sensitive and selective biomarker of central cholinergic integrity—VACHT binding (Aghourian et al., 2017). In the present study, we did not have access to longitudinal structural MRI and [ $^{18}\text{F}$ ] FEOBV PET within the same individuals. Although we assessed the spatial convergence between imaging modalities using conjunction analysis in MNI template space, the accuracy of co-registration between modalities can be further improved by acquiring high-resolution PET and structural MRI within the same individuals. Finally, we note that [ $^{18}\text{F}$ ] FEOBV PET was acquired in AD participants who were actively taking ACHE inhibitors to treat cognitive symptoms. Systematic investigation is required to determine whether these drugs might influence [ $^{18}\text{F}$ ] FEOBV binding.

Future work will benefit from a within-subjects multimodal imaging strategy combining longitudinal [ $^{18}\text{F}$ ] FEOBV PET with structural MRI, as well as direct evaluation of how pharmacological intervention with ACHE inhibitors influences these measures. Nevertheless, our present findings underscore the need for *in vivo* measures of cell-type-specific degeneration of the cholinergic system. Longitudinal monitoring of [ $^{18}\text{F}$ ] FEOBV binding in cohorts of cognitively normal APOE  $\epsilon$ 4 carriers and non-carriers, in combination with CSF biomarker indices of neuropathology, will provide novel insights into the differential trajectories of the neurotypical and preclinical aging brain.



## EXPERIMENTAL PROCEDURES

### Structural MRI

Data used in the preparation of this article were obtained from the Alzheimer's Disease Neuroimaging Initiative (ADNI) database (<http://adni.loni.usc.edu>). The ADNI was launched in 2003 as a public-private partnership, led by Principal Investigator Michael W. Weiner, MD. The primary goal of ADNI has been to test whether serial magnetic resonance imaging (MRI), positron emission tomography (PET), cerebrospinal fluid (CSF) biomarkers, and clinical and neuropsychological assessment can be combined to measure the progression of mild cognitive impairment (MCI) and early Alzheimer's disease (AD).

Methodological steps for group classification (cognitively normal and early AD), structural MRI preprocessing, and definition of basal forebrain ROIs are in the [Supplemental Information](#).

### Seed-to-Searchlight Analyses

Longitudinal differences in GM were computed for the combined BF (NbM, MS/DBB) ROI and the NbM and MS/DBB sub-region ROIs, for each subject. These values were entered into multiple linear regression models (either combined BF only, or both NbM and MD/DBB) as the predictor "seeds." In both cases, additional covariates included: age, sex, education, total intracranial volume, and longitudinal change in whole brain volume. The dependent measure was the longitudinal difference in GM within a 6-mm radius spherical searchlight ROI. Over successive iterations, the searchlight was positioned at every voxel constrained within the population-average gray matter mask, producing a seed-to-searchlight map. At each searchlight the multiple linear regression was computed with the robust fitting method (i.e., robust regression) (Wilcox, 2004) to reduce potential outlier effects. Code for the seed-to-searchlight analyses was adapted from the freely available RSA Toolbox (Nili et al., 2014). Statistical significance on the searchlight maps was determined at a FDR-corrected  $p < 0.05$ .

### <sup>18</sup>[F] FEOBV PET

The [<sup>18</sup>F] FEOBV PET radiotracer was acquired in 12 participants: six patients diagnosed with probable AD and six age-matched healthy volunteers (Table S4). These sample sizes are similar to those of previous rodent studies comparing FEOBV binding between an experimental group with induced mild cholinergic lesions and controls (Cyr et al., 2014; Parent et al., 2012). All participants were recruited at the McGill Centre for Studies in Aging (MCSA) and assessed at the McConnell Brain Imaging Unit (BIC) of the Montreal Neurological Institute (MNI). The original study protocol was approved by "Université du Québec à Montréal" (UQAM), and McGill University Research Ethics Boards. Informed consent was obtained from all subjects prior to participation in the study.

Methodological steps for group classification (cognitively normal and early AD) and [<sup>18</sup>F] FEOBV PET preprocessing are in the [Supplemental Information](#).

### ANCOVA Model

We used SPM12 (<http://www.fil.ion.ucl.ac.uk/spm/software/spm12/>) to conduct a between groups analysis (CN versus AD). The parameters for the general linear model specification were as follows: threshold masking = relative (0.8), global calculation = mean voxel value, global normalization = overall grand mean scaling (50); normalization = ANCOVA. Other parameter fields were set to default values. Age was modeled as a covariate of non-interest in the model. Statistical significance on the between group contrast (CN > AD) was determined at a cluster-level FDR-corrected  $p < 0.05$ .

## SUPPLEMENTAL INFORMATION

Supplemental Information includes Supplemental Experimental Procedures, two figures, and four tables and can be found with this article online at <https://doi.org/10.1016/j.celrep.2018.06.001>.

## ACKNOWLEDGMENTS

Data collection and sharing for this project were funded by the Alzheimer's Disease Neuroimaging Initiative (ADNI) (NIH grant U01 AG024904) and DOD ADNI (Department of Defense award number W81XWH-12-2-0012). ADNI is funded

by the National Institute on Aging, the National Institute of Biomedical Imaging and Bioengineering, and through generous contributions from the following: AbbVie, Alzheimer's Association; Alzheimer's Drug Discovery Foundation; Araclon Biotech; BioClinica; Biogen; Bristol-Myers Squibb Company; CereSpir; Eisai; Elan Pharmaceuticals; Eli Lilly and Company; EuroImmun; F. Hoffmann-La Roche Ltd and its affiliated company Genentech; Fujirebio; GE Healthcare; IXICO; Janssen Alzheimer Immunotherapy Research & Development, LLC.; Johnson & Johnson Pharmaceutical Research & Development, LLC.; Lumosity; Lundbeck; Merck & Co.; Meso Scale Diagnostics, LLC.; NeuroRx Research; Neurotrack Technologies; Novartis Pharmaceuticals Corporation; Pfizer; Piramal Imaging; Servier; Takeda Pharmaceutical Company; and Transition Therapeutics. The Canadian Institutes of Health Research is providing funds to support ADNI clinical sites in Canada. Private sector contributions are facilitated by the Foundation for the National Institutes of Health (<https://fnih.org>). The grantee organization is the Northern California Institute for Research and Education, and the study is coordinated by the Alzheimer's disease Cooperative Study at the University of California, San Diego. ADNI data are disseminated by the Laboratory for Neuro Imaging at the University of Southern California. This work was supported in part by a grant from the NIA (R03 RAG060263A) (T.W.S. and R.N.S.), the Canada First Research Excellence Fund (T.W.S. and R.N.S.), and the British Academy Postdoctoral Fellowship PS140117 (M.M.).

Data used in preparation of this article were obtained from the Alzheimer's Disease Neuroimaging Initiative (ADNI) database (<http://adni.loni.usc.edu>). As such, the investigators within the ADNI contributed to the design and implementation of ADNI and/or provided data but did not participate in analysis or writing of this report. A complete listing of ADNI investigators can be found at: [http://adni.loni.usc.edu/wp-content/uploads/how\\_to\\_apply/ADNI\\_Acknowledgement\\_List.pdf](http://adni.loni.usc.edu/wp-content/uploads/how_to_apply/ADNI_Acknowledgement_List.pdf).

## AUTHOR CONTRIBUTIONS

ADNI collected all data, with the exception of the [<sup>18</sup>F] FEOBV PET experiments, which were collected by M.A. and M.-A.B. The ADNI data were preprocessed by R.N.S. The [<sup>18</sup>F] FEOBV PET data were preprocessed by M.A. and M.-A.B. All additional analyses on the ADNI and [<sup>18</sup>F] FEOBV PET data were conducted by T.W.S. and M.M. T.W.S. and R.N.S. wrote the paper, with the exception of the [<sup>18</sup>F] FEOBV PET methods (M.A. and M.-A.B.).

## DECLARATION OF INTERESTS

The authors declare no competing interests.

Received: November 14, 2017

Revised: April 9, 2018

Accepted: May 30, 2018

Published: July 3, 2018

## REFERENCES

- Aghourian, M., Legault-Denis, C., Soucy, J.P., Rosa-Neto, P., Gauthier, S., Kostikov, A., Gravel, P., and Bédard, M.A. (2017). Quantification of brain cholinergic denervation in Alzheimer's disease using PET imaging with [<sup>18</sup>F]-FEOBV. *Mol. Psychiatry* 22, 1531–1538.
- Alexander-Bloch, A., Giedd, J.N., and Bullmore, E. (2013). Imaging structural co-variance between human brain regions. *Nat. Rev. Neurosci.* 14, 322–336.
- Arendt, T., Brückner, M.K., Morawski, M., Jäger, C., and Gertz, H.J. (2015). Early neuron loss in Alzheimer's disease: cortical or subcortical? *Acta Neuropathol. Commun.* 3, 10.
- Auld, D.S., Kornecook, T.J., Bastianetto, S., and Quirion, R. (2002). Alzheimer's disease and the basal forebrain cholinergic system: relations to beta-amyloid peptides, cognition, and treatment strategies. *Prog. Neurobiol.* 68, 209–245.
- Baker-Nigh, A., Vahedi, S., Davis, E.G., Weintraub, S., Bigio, E.H., Klein, W.L., and Geula, C. (2015). Neuronal amyloid- $\beta$  accumulation within cholinergic basal forebrain in ageing and Alzheimer's disease. *Brain* 138, 1722–1737.

- Ballinger, E.C., Ananth, M., Talmage, D.A., and Role, L.W. (2016). Basal forebrain cholinergic circuits and signaling in cognition and cognitive decline. *Neuron* 97, 1199–1218.
- Bassett, D.S., Bullmore, E., Verchinski, B.A., Mattay, V.S., Weinberger, D.R., and Meyer-Lindenberg, A. (2008). Hierarchical organization of human cortical networks in health and schizophrenia. *J. Neurosci.* 28, 9239–9248.
- Bloem, B., Schoppink, L., Rotaru, D.C., Faiz, A., Hendriks, P., Mansvelde, H.D., van de Berg, W.D., and Wouterlood, F.G. (2014). Topographic mapping between basal forebrain cholinergic neurons and the medial prefrontal cortex in mice. *J. Neurosci.* 34, 16234–16246.
- Braak, H., and Braak, E. (1991). Neuropathological staging of Alzheimer-related changes. *Acta Neuropathol.* 82, 239–259.
- Braak, H., and Del Tredici, K. (2015). The preclinical phase of the pathological process underlying sporadic Alzheimer's disease. *Brain* 138, 2814–2833.
- Buckner, R.L., Snyder, A.Z., Shannon, B.J., LaRossa, G., Sachs, R., Fotenos, A.F., Sheline, Y.I., Klunk, W.E., Mathis, C.A., Morris, J.C., and Mintun, M.A. (2005). Molecular, structural, and functional characterization of Alzheimer's disease: evidence for a relationship between default activity, amyloid, and memory. *J. Neurosci.* 25, 7709–7717.
- Cantero, J.L., Zaborszky, L., and Atienza, M. (2017). Volume loss of the nucleus basalis of Meynert is associated with atrophy of innervated regions in mild cognitive impairment. *Cereb. Cortex* 27, 3881–3889.
- Chandler, D.J., Lamperski, C.S., and Waterhouse, B.D. (2013). Identification and distribution of projections from monoaminergic and cholinergic nuclei to functionally differentiated subregions of prefrontal cortex. *Brain Res.* 1522, 38–58.
- Chen, Z.J., He, Y., Rosa-Neto, P., Germann, J., and Evans, A.C. (2008). Revealing modular architecture of human brain structural networks by using cortical thickness from MRI. *Cereb. Cortex* 18, 2374–2381.
- Clavaguera, F., Bolmont, T., Crowther, R.A., Abramowski, D., Frank, S., Probst, A., Fraser, G., Stalder, A.K., Beibel, M., Staufenbiel, M., et al. (2009). Transmission and spreading of tauopathy in transgenic mouse brain. *Nat. Cell Biol.* 11, 909–913.
- Cyr, M., Parent, M.J., Mechawar, N., Rosa-Neto, P., Soucy, J.P., Aliaga, A., Kostikov, A., Maclaren, D.A., Clark, S.D., and Bedard, M.A. (2014). PET imaging with [<sup>18</sup>F]fluoroethoxybenzovesamicol ([<sup>18</sup>F]FEOBV) following selective lesion of cholinergic pedunculopontine tegmental neurons in rat. *Nucl. Med. Biol.* 41, 96–101.
- de Calignon, A., Polydoro, M., Suárez-Calvet, M., William, C., Adamowicz, D.H., Kopeikina, K.J., Pittstick, R., Sahara, N., Ashe, K.H., Carlson, G.A., et al. (2012). Propagation of tau pathology in a model of early Alzheimer's disease. *Neuron* 73, 685–697.
- de Castro, B.M., De Jaeger, X., Martins-Silva, C., Lima, R.D., Amaral, E., Mezezes, C., Lima, P., Neves, C.M., Pires, R.G., Gould, T.W., et al. (2009). The vesicular acetylcholine transporter is required for neuromuscular development and function. *Mol. Cell. Biol.* 29, 5238–5250.
- Dupre, E., and Spreng, R.N. (2017). Structural covariance networks across the lifespan, from 6 to 94 years of age. *Netw. Neurosci.* 1, 302–323.
- Fisher, A. (2012). Cholinergic modulation of amyloid precursor protein processing with emphasis on M1 muscarinic receptor: perspectives and challenges in treatment of Alzheimer's disease. *J. Neurochem.* 120 (Suppl 1), 22–33.
- Geula, C., Nagykerly, N., Nicholas, A., and Wu, C.K. (2008). Cholinergic neuronal and axonal abnormalities are present early in aging and in Alzheimer disease. *J. Neuropathol. Exp. Neurol.* 67, 309–318.
- Grothe, M., Heinsen, H., and Teipel, S. (2013). Longitudinal measures of cholinergic forebrain atrophy in the transition from healthy aging to Alzheimer's disease. *Neurobiol. Aging* 34, 1210–1220.
- Grothe, M., Kilimann, I., Grinberg, L., Heinsen, H., and Teipel, S. (2018). In vivo volumetry of the cholinergic basal forebrain. *Neuroinformatics*, 213–232.
- He, Y., Chen, Z.J., and Evans, A.C. (2007). Small-world anatomical networks in the human brain revealed by cortical thickness from MRI. *Cereb. Cortex* 17, 2407–2419.
- Hecker, S., and Mesulam, M.M. (1994). Two types of cholinergic projections to the rat amygdala. *Neuroscience* 60, 383–397.
- Henny, P., and Jones, B.E. (2008). Projections from basal forebrain to prefrontal cortex comprise cholinergic, GABAergic and glutamatergic inputs to pyramidal cells or interneurons. *Eur. J. Neurosci.* 27, 654–670.
- Khan, U.A., Liu, L., Provenzano, F.A., Berman, D.E., Profaci, C.P., Sloan, R., Mayeux, R., Duff, K.E., and Small, S.A. (2014). Molecular drivers and cortical spread of lateral entorhinal cortex dysfunction in preclinical Alzheimer's disease. *Nat. Neurosci.* 17, 304–311.
- Kilimann, I., Hausner, L., Fellgiebel, A., Filippi, M., Würdemann, T.J., Heinsen, H., and Teipel, S.J. (2017). Parallel atrophy of cortex and basal forebrain cholinergic system in mild cognitive impairment. *Cereb. Cortex* 27, 1841–1848.
- Kolisnyk, B., Al-Onaizi, M., Soreq, L., Barbash, S., Bekenstein, U., Haberman, N., Hanin, G., Kish, M.T., Souza da Silva, J., Fahnestock, M., et al. (2017). Cholinergic surveillance over hippocampal RNA metabolism and Alzheimer's-like pathology. *Cereb. Cortex* 27, 3553–3567.
- Kolisnyk, B., Al-Onaizi, M.A., Xu, J., Parfitt, G.M., Ostapchenko, V.G., Hanin, G., Soreq, H., Prado, M.A., and Prado, V.F. (2016). Cholinergic regulation of hnRNP2/B1 translation by M1 muscarinic receptors. *J. Neurosci.* 36, 6287–6296.
- Kondo, H., and Zaborszky, L. (2016). Topographic organization of the basal forebrain projections to the perirhinal, postrhinal, and entorhinal cortex in rats. *J. Comp. Neurol.* 524, 2503–2515.
- Kriegeskorte, N., Goebel, R., and Bandettini, P. (2006). Information-based functional brain mapping. *Proc. Natl. Acad. Sci. USA* 103, 3863–3868.
- Lewis, N.E., Schramm, G., Bordbar, A., Schellenberger, J., Andersen, M.P., Cheng, J.K., Patel, N., Yee, A., Lewis, R.A., Eils, R., et al. (2010). Large-scale in silico modeling of metabolic interactions between cell types in the human brain. *Nat. Biotechnol.* 28, 1279–1285.
- Lin, S.C., Brown, R.E., Hussain Shuler, M.G., Petersen, C.C., and Kepecs, A. (2015). Optogenetic dissection of the basal forebrain neuromodulatory control of cortical activation, plasticity, and cognition. *J. Neurosci.* 35, 13896–13903.
- Mattson, M.P., and Magnus, T. (2006). Ageing and neuronal vulnerability. *Nat. Rev. Neurosci.* 7, 278–294.
- Mesulam, M.M. (2013). Cholinergic circuitry of the human nucleus basalis and its fate in Alzheimer's disease. *J. Comp. Neurol.* 521, 4124–4144.
- Mesulam, M.M., and Geula, C. (1988). Nucleus basalis (Ch4) and cortical cholinergic innervation in the human brain: observations based on the distribution of acetylcholinesterase and choline acetyltransferase. *J. Comp. Neurol.* 275, 216–240.
- Mesulam, M.M., Mufson, E.J., Levey, A.I., and Wainer, B.H. (1983a). Cholinergic innervation of cortex by the basal forebrain: cytochemistry and cortical connections of the septal area, diagonal band nuclei, nucleus basalis (substantia innominata), and hypothalamus in the rhesus monkey. *J. Comp. Neurol.* 214, 170–197.
- Mesulam, M.M., Mufson, E.J., Wainer, B.H., and Levey, A.I. (1983b). Central cholinergic pathways in the rat: an overview based on an alternative nomenclature (Ch1-Ch6). *Neuroscience* 10, 1185–1201.
- Mesulam, M.M., Mufson, E.J., and Wainer, B.H. (1986). Three-dimensional representation and cortical projection topography of the nucleus basalis (Ch4) in the macaque: concurrent demonstration of choline acetyltransferase and retrograde transport with a stabilized tetramethylbenzidine method for horseradish peroxidase. *Brain Res.* 367, 301–308.
- Mesulam, M., Shaw, P., Mash, D., and Weintraub, S. (2004). Cholinergic nucleus basalis tauopathy emerges early in the aging-MCI-AD continuum. *Ann. Neurol.* 55, 815–828.
- Mueller, S.G., Weiner, M.W., Thal, L.J., Petersen, R.C., Jack, C.R., Jagust, W., Trojanowski, J.Q., Toga, A.W., and Beckett, L. (2005). Ways toward an early diagnosis in Alzheimer's disease: the Alzheimer's Disease Neuroimaging Initiative (ADNI). *Alzheimers Dement.* 1, 55–66.
- Nichols, T., Brett, M., Andersson, J., Wager, T., and Poline, J.B. (2005). Valid conjunction inference with the minimum statistic. *Neuroimage* 25, 653–660.



- Nili, H., Wingfield, C., Walther, A., Su, L., Marslen-Wilson, W., and Kriegeskorte, N. (2014). A toolbox for representational similarity analysis. *PLoS Comput. Biol.* *10*, e1003553.
- Parent, M., Bedard, M.A., Aliaga, A., Soucy, J.P., Landry St-Pierre, E., Cyr, M., Kostikov, A., Schirmacher, E., Massarweh, G., and Rosa-Neto, P. (2012). PET imaging of cholinergic deficits in rats using [<sup>18</sup>F]fluoroethoxybenzovesamicol ([<sup>18</sup>F]FEOBV). *Neuroimage* *62*, 555–561.
- Poirier, J., Delisle, M.C., Quirion, R., Aubert, I., Farlow, M., Lahiri, D., Hui, S., Bertrand, P., Nalbantoglu, J., Gilfix, B.M., and Gauthier, S. (1995). Apolipoprotein E4 allele as a predictor of cholinergic deficits and treatment outcome in Alzheimer disease. *Proc. Natl. Acad. Sci. USA* *92*, 12260–12264.
- Prado, V.F., Roy, A., Kolisnyk, B., Gros, R., and Prado, M.A. (2013). Regulation of cholinergic activity by the vesicular acetylcholine transporter. *Biochem. J.* *450*, 265–274.
- Raj, A., Kuceyeski, A., and Weiner, M. (2012). A network diffusion model of disease progression in dementia. *Neuron* *73*, 1204–1215.
- Raj, A., LoCastro, E., Kuceyeski, A., Tosun, D., Relkin, N., and Weiner, M.; for the Alzheimer's Disease Neuroimaging Initiative (ADNI) (2015). Network diffusion model of progression predicts longitudinal patterns of atrophy and metabolism in Alzheimer's disease. *Cell Rep.* Published online January 14, 2015. <https://doi.org/10.1016/j.celrep.2014.12.034>.
- Rivera, E.J., Goldin, A., Fulmer, N., Tavares, R., Wands, J.R., and de la Monte, S.M. (2005). Insulin and insulin-like growth factor expression and function deteriorate with progression of Alzheimer's disease: link to brain reductions in acetylcholine. *J. Alzheimers Dis.* *8*, 247–268.
- Romberg, C., Bussey, T.J., and Saksida, L.M. (2013). Paying more attention to attention: towards more comprehensive cognitive translation using mouse models of Alzheimer's disease. *Brain Res. Bull.* *92*, 49–55.
- Schliebs, R., and Arendt, T. (2006). The significance of the cholinergic system in the brain during aging and in Alzheimer's disease. *J. Neural Transm. (Vienna)* *113*, 1625–1644.
- Schliebs, R., and Arendt, T. (2011). The cholinergic system in aging and neuronal degeneration. *Behav. Brain Res.* *221*, 555–563.
- Schmitz, T.W., and Duncan, J. (2018). Normalization and the cholinergic microcircuit: a unified basis for attention. *Trends Cogn. Sci.* *22*, 422–437.
- Schmitz, T.W., Cheng, F.H., and De Rosa, E. (2010). Failing to ignore: paradoxical neural effects of perceptual load on early attentional selection in normal aging. *J. Neurosci.* *30*, 14750–14758.
- Schmitz, T.W., Dixon, M.L., Anderson, A.K., and De Rosa, E. (2014). Distinguishing attentional gain and tuning in young and older adults. *Neurobiol. Aging* *35*, 2514–2525.
- Schmitz, T.W., and Spreng, R.N.; Alzheimer's Disease Neuroimaging Initiative (2016). Basal forebrain degeneration precedes and predicts the cortical spread of Alzheimer's pathology. *Nat. Commun.* *7*, 13249.
- Seeley, W.W., Crawford, R.K., Zhou, J., Miller, B.L., and Greicius, M.D. (2009). Neurodegenerative diseases target large-scale human brain networks. *Neuron* *62*, 42–52.
- Shaw, L.M., Vanderstichele, H., Knapiak-Czajka, M., Clark, C.M., Aisen, P.S., Petersen, R.C., Blennow, K., Soares, H., Simon, A., Lewczuk, P., et al.; Alzheimer's Disease Neuroimaging Initiative (2009). Cerebrospinal fluid biomarker signature in Alzheimer's disease neuroimaging initiative subjects. *Ann. Neurol.* *65*, 403–413.
- Spreng, R.N., and Turner, G.R. (2013). Structural covariance of the default network in healthy and pathological aging. *J. Neurosci.* *33*, 15226–15234.
- Wang, X., Michaelis, M.L., and Michaelis, E.K. (2010). Functional genomics of brain aging and Alzheimer's disease: focus on selective neuronal vulnerability. *Curr. Genomics* *11*, 618–633.
- Wilcox, R. (2004). *Introduction to Robust Estimation and Hypothesis Testing*, Second Edition (Academic Press).
- Woo, C.W., Krishnan, A., and Wager, T.D. (2014). Cluster-extent based thresholding in fMRI analyses: pitfalls and recommendations. *Neuroimage* *91*, 412–419.
- Wu, H., Williams, J., and Nathans, J. (2014). Complete morphologies of basal forebrain cholinergic neurons in the mouse. *eLife* *3*, e02444.
- Zaborszky, L., Hoemke, L., Mohlberg, H., Schleicher, A., Amunts, K., and Zilles, K. (2008). Stereotaxic probabilistic maps of the magnocellular cell groups in human basal forebrain. *Neuroimage* *42*, 1127–1141.
- Zaborszky, L., Csordas, A., Mosca, K., Kim, J., Gielow, M.R., Vadasz, C., and Nadasdy, Z. (2015). Neurons in the basal forebrain project to the cortex in a complex topographic organization that reflects corticocortical connectivity patterns: an experimental study based on retrograde tracing and 3D reconstruction. *Cereb. Cortex* *25*, 118–137.

## REFERENCES

- Aghourian, M., Legault-Denis, C., Soucy, J. P., Rosa-Neto, P., Gauthier, S., Kostikov, A., ... & Bedard, M. A. (2017). Quantification of brain cholinergic denervation in Alzheimer's disease using PET imaging with [18 F]-FEOBV. *Molecular psychiatry*, 22(11), 1531-1538.
- Aizenstein, H. J., Nebes, R. D., Saxton, J. A., Price, J. C., Mathis, C. A., Tsopelas, N. D., ... & Klunk, W. E. (2008). Frequent amyloid deposition without significant cognitive impairment among the elderly. *Archives of neurology*, 65(11), 1509-1517.
- Albert, M. S., DeKosky, S. T., Dickson, D., Dubois, B., Feldman, H. H., Fox, N. C., ... & Phelps, C. H. (2011). The diagnosis of mild cognitive impairment due to Alzheimer's disease: recommendations from the National Institute on Aging-Alzheimer's Association workgroups on diagnostic guidelines for Alzheimer's disease. *Alzheimer's & dementia*, 7(3), 270-279.
- Albin, R. L., Bohnen, N. I., Muller, M. L., Dauer, W. T., Sarter, M., Frey, K. A., & Koeppe, R. A. (2018). Regional vesicular acetylcholine transporter distribution in human brain: a [18F] fluoroethoxybenzovesamicol positron emission tomography study. *Journal of Comparative Neurology*, 526(17), 2884-2897.
- Alonso, A. D. C., Zaidi, T., Grundke-Iqbal, I., & Iqbal, K. (1994). Role of abnormally phosphorylated tau in the breakdown of microtubules in Alzheimer disease. *Proceedings of the National Academy of Sciences*, 91(12), 5562-5566.
- Altar, C. A., & Marien, M. R. (1988). [3H]vesamicol binding in brain: autoradiographic distribution, pharmacology, and effects of cholinergic lesions. *Synapse*, 2(5), 486-493. doi: 10.1002/syn.890020504
- American Psychiatric Association. (2013). Diagnostic and statistical manual of mental disorders: 5<sup>th</sup> Edition (DSM-5). American Psychiatric Association.
- Araujo, D. M., Lapchak, P. A., Robitaille, Y., Gauthier, S., & Quirion, R. (1988). Differential alteration of various cholinergic markers in cortical and subcortical regions of human brain in Alzheimer's disease. *Journal of neurochemistry*, 50(6), 1914-1923.
- Arendt, T., Brückner, M. K., Morawski, M., Jäger, C., & Gertz, H. J. (2015). Early neurone loss in Alzheimer's disease: cortical or subcortical?. *Acta neuropathologica communications*, 3(1), 1-11.
- Baker, J. E., Lim, Y. Y., Jaeger, J., Ames, D., Lautenschlager, N. T., Robertson, J., ... & Maruff, P. (2018). Episodic memory and learning dysfunction over an 18-month period in preclinical and prodromal Alzheimer's disease. *Journal of Alzheimer's Disease*, 65(3), 977-988.
- Ballinger, E. C., Ananth, M., Talmage, D. A., & Role, L. W. (2016). Basal forebrain cholinergic circuits and signaling in cognition and cognitive decline. *Neuron*, 91(6), 1199-1218.
- Baratti, C. M., Opezzo, J. W., & Kopf, S. R. (1993). Facilitation of memory storage by the acetylcholine M2 muscarinic receptor antagonist AF-DX 116. *Behavioral and neural biology*, 60(1), 69-74.

- Bartus, R. T., Dean, R. 3., Beer, B., & Lipka, A. S. (1982). The cholinergic hypothesis of geriatric memory dysfunction. *Science*, 217(4558), 408-414.
- Becker, G., Dammicco, S., Bahri, M. A., & Salmon, E. (2020). The rise of synaptic density PET imaging. *Molecules*, 25(10), 2303.
- Bierer, L. M., Haroutunian, V., Gabriel, S., Knott, P. J., Carlin, L. S., Purohit, D. P., ... & Davis, K. L. (1995). Neurochemical correlates of dementia severity in Alzheimer's disease: relative importance of the cholinergic deficits. *Journal of neurochemistry*, 64(2), 749-760.
- Bohnen, N. I., Kaufer, D. I., Hendrickson, R., Ivanco, L. S., Lopresti, B. J., Koeppe, R. A., ... & Moore, R. Y. (2005). Degree of inhibition of cortical acetylcholinesterase activity and cognitive effects by donepezil treatment in Alzheimer's disease. *Journal of Neurology, Neurosurgery & Psychiatry*, 76(3), 315-319.
- Bohnen, N. I., Djang, D. S., Herholz, K., Anzai, Y., & Minoshima, S. (2012). Effectiveness and safety of 18F-FDG PET in the evaluation of dementia: a review of the recent literature. *Journal of Nuclear Medicine*, 53(1), 59-71.
- Borgaonkar, D., Schmidt, L., Martin, S. E., Kanzer, M., Edelson, L., Growdon, J., & Farrer, L. (1993). Linkage of late-onset Alzheimer's disease with apolipoprotein E type 4 on chromosome 19. *Lancet (London, England)*, 342(8871), 625-625.
- Bourgade, K., Garneau, H., Giroux, G., Le Page, A. Y., Bocti, C., Dupuis, G., ... & Fülöp, T. (2015).  $\beta$ -Amyloid peptides display protective activity against the human Alzheimer's disease-associated herpes simplex virus-1. *Biogerontology*, 16(1), 85-98.
- Bowen, D. M., Smith, C. B., White, P. & Davison, A. N. (1976). Neurotransmitter-related enzymes and indices of hypoxia in senile dementia and other abiotrophies. *Brain: a journal of neurology*, 99(3), 459-496.
- Braak, H., & Braak, E. (1991). Neuropathological staging of Alzheimer-related changes. *Acta neuropathologica*, 82(4), 239-259.
- Braak, H., & Del Tredici, K. (2011). The pathological process underlying Alzheimer's disease in individuals under thirty. *Acta neuropathologica*, 121(2), 171-181.
- Braak, H., & Del Tredici, K. (2018). Spreading of tau pathology in sporadic Alzheimer's disease along cortico-cortical top-down connections. *Cerebral Cortex*, 28(9), 3372-3384.
- Brown, R. K., Bohnen, N. I., Wong, K. K., Minoshima, S., & Frey, K. A. (2014). Brain PET in suspected dementia: patterns of altered FDG metabolism. *Radiographics*, 34(3), 684-701.
- Buerger, K., Ewers, M., Pirttilä, T., Zinkowski, R., Alafuzoff, I., Teipel, S. J., ... & Hampel, H. (2006). CSF phosphorylated tau protein correlates with neocortical neurofibrillary pathology in Alzheimer's disease. *Brain*, 129(11), 3035-3041.
- Burton, E. J., Mukaetova-Ladinska, E. B., Perry, R. H., Jaros, E., Barber, R., & O'Brien, J. T. (2012). Quantitative neurodegenerative pathology does not explain the degree of hippocampal atrophy

- on MRI in degenerative dementia. *International journal of geriatric psychiatry*, 27(12), 1267-1274.
- Canas, P. M., Duarte, J. M., Rodrigues, R. J., Köfalvi, A., & Cunha, R. A. (2009). Modification upon aging of the density of presynaptic modulation systems in the hippocampus. *Neurobiology of aging*, 30(11), 1877-1884.
- Cantero, J. L., Atienza, M., Lage, C., Zaborszky, L., Vilaplana, E., Lopez-Garcia, S., ... & Alzheimer's Disease Neuroimaging Initiative. (2020). Atrophy of basal forebrain initiates with tau pathology in individuals at risk for Alzheimer's disease. *Cerebral Cortex*, 30(4), 2083-2098.
- Caricasole, A., Copani, A., Caruso, A., Caraci, F., Iacovelli, L., Sortino, M. A., ... & Nicoletti, F. (2003). The Wnt pathway, cell-cycle activation and  $\beta$ -amyloid: novel therapeutic strategies in Alzheimer's disease?. *Trends in pharmacological sciences*, 24(5), 233-238.
- Carson, R. E., Naganawa, M., Toyonaga, T., Koohsari, S., Yang, Y., Chen, M. K., ... & Finnema, S. J. (2022). Imaging of synaptic density in neurodegenerative disorders. *Journal of Nuclear Medicine*, 63(Supplement 1), 60S-67S.
- Caulfield, M. P., & Birdsall, N. J. (1998). International Union of Pharmacology. XVII. Classification of muscarinic acetylcholine receptors. *Pharmacological reviews*, 50(2), 279-290.
- Chen, M. K., Mecca, A. P., Naganawa, M., Finnema, S. J., Toyonaga, T., Lin, S. F., ... & van Dyck, C. H. (2018). Assessing synaptic density in Alzheimer disease with synaptic vesicle glycoprotein 2A positron emission tomographic imaging. *JAMA neurology*, 75(10), 1215-1224.
- Chen, M. K., Mecca, A. P., Naganawa, M., Gallezot, J. D., Toyonaga, T., Mondal, J., ... & Carson, R. E. (2021). Comparison of [11C] UCB-J and [18F] FDG PET in Alzheimer's disease: A tracer kinetic modeling study. *Journal of Cerebral Blood Flow & Metabolism*, 0271678X211004312.
- Chen, X. Q., & Mobley, W. C. (2019). Exploring the pathogenesis of Alzheimer disease in basal forebrain cholinergic neurons: converging insights from alternative hypotheses. *Frontiers in neuroscience*, 13, 446.
- Chételat, G., Desgranges, B., De La Sayette, V., Viader, F., Eustache, F., & Baron, J. C. (2003). Mild cognitive impairment Can FDG-PET predict who is to rapidly convert to Alzheimer's disease?. *Neurology*, 60(8), 1374-1377.
- Chételat, G., Arbizu, J., Barthel, H., Garibotto, V., Law, I., Morbelli, S., ... & Drzezga, A. (2020). Amyloid-PET and 18F-FDG-PET in the diagnostic investigation of Alzheimer's disease and other dementias. *The Lancet Neurology*, 19(11), 951-962.
- Chiotis, K., Saint-Aubert, L., Savitcheva, I., Jelic, V., Andersen, P., Jonasson, M., ... & Nordberg, A. (2016). Imaging in-vivo tau pathology in Alzheimer's disease with THK5317 PET in a multimodal paradigm. *European journal of nuclear medicine and molecular imaging*, 43(9), 1686-1699.
- Colangelo, C., Shichkova, P., Keller, D., Markram, H., & Ramaswamy, S. (2019). Cellular, synaptic and network effects of acetylcholine in the neocortex. *Frontiers in neural circuits*, 13, 24.

- Costa, A. S., Reich, A., Fimm, B., Ketteler, S. T., Schulz, J. B., & Reetz, K. (2014). Evidence of the sensitivity of the MoCA alternate forms in monitoring cognitive change in early Alzheimer's disease. *Dementia and geriatric cognitive disorders*, *37*(1-2), 95-103.
- Coughlin, J. M., Du, Y., Rosenthal, H. B., Slania, S., Koo, S. M., Park, A., ... & Pomper, M. G. (2018). The distribution of the  $\alpha 7$  nicotinic acetylcholine receptor in healthy aging: an in vivo positron emission tomography study with [18F] ASEM. *Neuroimage*, *165*, 118-124.
- Coughlin, J. M., Rubin, L. H., Du, Y., Rowe, S. P., Crawford, J. L., Rosenthal, H. B., ... & Pomper, M. G. (2020). High availability of the  $\alpha 7$ -nicotinic acetylcholine receptor in brains of individuals with mild cognitive impairment: a pilot study using 18F-ASEM PET. *Journal of Nuclear Medicine*, *61*(3), 423-426.
- Cover, K. S., van Schijndel, R. A., Versteeg, A., Leung, K. K., Mulder, E. R., Jong, R. A., ... & Alzheimer's Disease Neuroimaging Initiative. (2016). Reproducibility of hippocampal atrophy rates measured with manual, FreeSurfer, AdaBoost, FSL/FIRST and the MAPS-HBSI methods in Alzheimer's disease. *Psychiatry Research: Neuroimaging*, *252*, 26-35.
- Crow, T. J., & Grove-White, I. G. (1973). An analysis of the learning deficit following hyoscine administration to man. *British Journal of Pharmacology*, *49*(2), 322-327.
- Crous-Bou, M., Minguillón, C., Gramunt, N., & Molinuevo, J. L. (2017). Alzheimer's disease prevention: from risk factors to early intervention. *Alzheimer's research & therapy*, *9*(1), 1-9.
- Cselényi, Z., Jönhagen, M. E., Forsberg, A., Halldin, C., Julin, P., Schou, M., ... & Farde, L. (2012). Clinical validation of 18F-AZD4694, an amyloid- $\beta$ -specific PET radioligand. *Journal of Nuclear Medicine*, *53*(3), 415-424.
- Cyr, M., Parent, M. J., Mechawar, N., Rosa-Neto, P., Soucy, J. P., Aliaga, A., ... & Bedard, M. A. (2014). PET imaging with [18F] fluoroethoxybenzovesamicol ([18F] FEOBV) following selective lesion of cholinergic pedunculopontine tegmental neurons in rat. *Nuclear medicine and biology*, *41*(1), 96-101.
- Cyr, M., Parent, M. J., Mechawar, N., Rosa-Neto, P., Soucy, J. P., Clark, S. D., ... & Bedard, M. A. (2015). Deficit in sustained attention following selective cholinergic lesion of the pedunculopontine tegmental nucleus in rat, as measured with both post-mortem immunocytochemistry and in vivo PET imaging with [18F] fluoroethoxybenzovesamicol. *Behavioural brain research*, *278*, 107-114.
- Cuello, A. C., Pentz, R., & Hall, H. (2019). The brain NGF metabolic pathway in health and in Alzheimer's pathology. *Frontiers in neuroscience*, *13*, 62.
- DeKosky, S. T., Scheff, S. W., & Styren, S. D. (1996). Structural correlates of cognition in dementia: quantification and assessment of synapse change. *Neurodegeneration*, *5*(4), 417-421.
- De Leon, M. J., DeSanti, S., Zinkowski, R., Mehta, P. D., Pratico, D., Segal, S., ... & Davies, P. (2006). Longitudinal CSF and MRI biomarkers improve the diagnosis of mild cognitive impairment. *Neurobiology of aging*, *27*(3), 394-401.

- Dournaud, P., Delaere, P., Hauw, J. J., & Epelbaum, J. (1995). Differential correlation between neurochemical deficits, neuropathology, and cognitive status in Alzheimer's disease. *Neurobiology of aging*, *16*(5), 817-823.
- Drachman, D. A., & Leavitt, J. (1974). Human memory and the cholinergic system: a relationship to aging?. *Archives of neurology*, *30*(2), 113-121.
- Drachman, D. A. (2014). The amyloid hypothesis, time to move on: amyloid is the downstream result, not cause, of Alzheimer's disease. *Alzheimer's & Dementia*, *10*(3), 372-380.
- de Bruijn, R. F., & Ikram, M. A. (2014). Cardiovascular risk factors and future risk of Alzheimer's disease. *BMC medicine*, *12*(1), 1-9.
- Dournaud, P., Delaere, P., Hauw, J. J., & Epelbaum, J. (1995). Differential correlation between neurochemical deficits, neuropathology, and cognitive status in Alzheimer's disease. *Neurobiology of aging*, *16*(5), 817-823.
- Dringenberg, H. C. (2000). Alzheimer's disease: more than a 'cholinergic disorder'—evidence that cholinergic–monoaminergic interactions contribute to EEG slowing and dementia. *Behavioural brain research*, *115*(2), 235-249
- Dringenberg, H. C. (2000). Alzheimer's disease: more than a 'cholinergic disorder'—evidence that cholinergic–monoaminergic interactions contribute to EEG slowing and dementia. *Behavioural brain research*, *115*(2), 235-249.
- Dubois, B., Feldman, H. H., Jacova, C., DeKosky, S. T., Barberger-Gateau, P., Cummings, J., ... & Scheltens, P. (2007). Research criteria for the diagnosis of Alzheimer's disease: revising the NINCDS–ADRDA criteria. *The Lancet Neurology*, *6*(8), 734-746.
- Eglen, R. M. (2006). Muscarinic receptor subtypes in neuronal and non-neuronal cholinergic function. *Autonomic and Autacoid Pharmacology*, *26*(3), 219-233.
- Elder, G. J., Mactier, K., Colloby, S. J., Watson, R., Blamire, A. M., O'Brien, J. T., & Taylor, J. P. (2017). The influence of hippocampal atrophy on the cognitive phenotype of dementia with Lewy bodies. *International journal of geriatric psychiatry*, *32*(11), 1182-1189.
- Efange, S. M., Mach, R. H., Khare, A., Michelson, R. H., Nowak, P. A., & Evora, P. H. (1994). p-[<sup>18</sup>F]fluorobenzyltrozamicol ([<sup>18</sup>F]FBT): molecular decomposition- reconstitution approach to vesamicol receptor radioligands for positron emission tomography. *Applied radiation and isotopes : including data, instrumentation and methods for use in agriculture, industry and medicine*, *45*(4), 465-472.
- Efange, S. M., Langason, R. B., Khare, A. B., & Low, W. C. (1996). The vesamicol receptor ligand (+)-meta-[<sup>125</sup>I]iodobenzyltrozamicol [(+)-[<sup>125</sup>I]-MIBT] reveals blunting of the striatal cholinergic response to dopamine D2 receptor blockade in the 6-hydroxydopamine (6-OHDA)-lesioned rat: possible implications for Parkinson's disease. *Life Sci*, *58*(16), 1367-1374.
- Efange, S. M., Nader, M. A., Ehrenkaufer, R. L., Khare, A. B., Smith, C. R., Morton, T. E., & Mach, R. H. (1999). (+)-p-([<sup>18</sup>F]fluorobenzyl)spirotrozamicol [(+)-[<sup>18</sup>F]spiro-FBT]: synthesis and biological

- evaluation of a high-affinity ligand for the vesicular acetylcholine transporter (VACHT). *Nuclear medicine and biology*, 26(2), 189-192.
- Efange, S. M. (2000). In vivo imaging of the vesicular acetylcholine transporter and the vesicular monoamine transporter. *The FASEB journal : official publication of the Federation of American Societies for Experimental Biology*, 14(15), 2401-2413.
- Everitt, B. J., & Robbins, T. W. (1997). Central cholinergic systems and cognition. *Annual review of psychology*, 48(1), 649-684.
- Fahnestock, M., & Shekari, A. (2019). ProNGF and neurodegeneration in Alzheimer's disease. *Frontiers in neuroscience*, 13, 129.
- Farrer, L. A., Cupples, L. A., Haines, J. L., Hyman, B., Kukull, W. A., Mayeux, R., ... & Van Duijn, C. M. (1997). Effects of age, sex, and ethnicity on the association between apolipoprotein E genotype and Alzheimer disease: a meta-analysis. *Jama*, 278(16), 1349-1356.
- Fayed, N., Modrego, P. J., García-Martí, G., Sanz-Requena, R., & Marti-Bonmatí, L. (2017). Magnetic resonance spectroscopy and brain volumetry in mild cognitive impairment. A prospective study. *Magnetic resonance imaging*, 38, 27-32.
- Fernández-Cabello, S., Kronbichler, M., Van Dijk, K. R., Goodman, J. A., Spreng, R. N., Schmitz, T. W., & Alzheimer's Disease Neuroimaging Initiative. (2020). Basal forebrain volume reliably predicts the cortical spread of Alzheimer's degeneration. *Brain*, 143(3), 993-1009.
- Fibiger, H. C. (1991). Cholinergic mechanisms in learning, memory and dementia: a review of recent evidence. *Trends in neurosciences*, 14(6), 220-223.
- Flynn, D. D., Ferrari-DiLeo, G., Mash, D. C., & Levey, A. I. (1995). Differential regulation of molecular subtypes of muscarinic receptors in Alzheimer's disease. *Journal of neurochemistry*, 64(4), 1888-1891.
- Folstein, M. F., Folstein, S. E., & McHugh, P. R. (1975). "Mini-mental state": a practical method for grading the cognitive state of patients for the clinician. *Journal of psychiatric research*, 12(3), 189-198.
- Fontanilla, D., Johannessen, M., Hajipour, A. R., Cozzi, N. V., Jackson, M. B., Ruoho, A. E. (2009). The hallucinogen N,N-dimethyltryptamine (DMT) is an endogenous sigma-1 receptor regulator. *Science* 323 (5916), 934–937. doi: 10.1126/science.1166127
- Foster, N. L., Heidebrink, J. L., Clark, C. M., Jagust, W. J., Arnold, S. E., Barbas, N. R., ... & Minoshima, S. (2007). FDG-PET improves accuracy in distinguishing frontotemporal dementia and Alzheimer's disease. *Brain*, 130(10), 2616-2635.
- Francis, P. T., Ramírez, M. J., & Lai, M. K. (2010). Neurochemical basis for symptomatic treatment of Alzheimer's disease. *Neuropharmacology*, 59(4-5), 221-229.

- Freitas, S., Simões, M. R., Alves, L., & Santana, I. (2013). Montreal cognitive assessment: validation study for mild cognitive impairment and Alzheimer disease. *Alzheimer Disease & Associated Disorders*, 27(1), 37-43.
- Frisoni, G. B., Fox, N. C., Jack, C. R., Scheltens, P., & Thompson, P. M. (2010). The clinical use of structural MRI in Alzheimer disease. *Nature Reviews Neurology*, 6(2), 67-77.
- Fritz, H. J., Ray, N., Dyrba, M., Sorg, C., Teipel, S. et Grothe, M. J. (2019). The corticotopic organization of the human basal forebrain as revealed by regionally selective functional connectivity profiles. *Human Brain Mapping*, 40(3), 868-878. doi: 10.1002/hbm.24417
- Fujishiro, H., Umegaki, H., Isojima, D., Akatsu, H., Iguchi, A., & Kosaka, K. (2006). Depletion of cholinergic neurons in the nucleus of the medial septum and the vertical limb of the diagonal band in dementia with Lewy bodies. *Acta neuropathologica*, 111(2), 109-114.
- Gage, H. D., Voytko, M. L., Ehrenkaufer, R. L., Tobin, J. R., Efange, S. M., & Mach, R. H. (2000). Reproducibility of repeated measures of cholinergic terminal density using. *Journal of nuclear medicine : official publication, Society of Nuclear Medicine*, 41(12), 2069-2076.
- Garcia-Alloza, M., Gil-Bea, F. J., Diez-Ariza, M., Chen, C. H., Francis, P. T., Lasheras, B., & Ramirez, M. J. (2005). Cholinergic-serotonergic imbalance contributes to cognitive and behavioral symptoms in Alzheimer's disease. *Neuropsychologia*, 43(3), 442-449.
- Gaubert, S., Raimondo, F., Houot, M., Corsi, M. C., Naccache, L., Diego Sitt, J., ... & Alzheimer's Disease Neuroimaging Initiative. (2019). EEG evidence of compensatory mechanisms in preclinical Alzheimer's disease. *Brain*, 142(7), 2096-2112.
- Geula, C., & Mesulam, M. M. (1996). Systematic regional variations in the loss of cortical cholinergic fibers in Alzheimer's disease. *Cerebral Cortex*, 6(2), 165-177.
- Geula, C., & Mesulam, M. M. (1999). Cholinergic systems in Alzheimer disease. In R. D. Terry, R. Katzman, K. L. Bick, & S. S. Sisodia (Eds.), *Alzheimer Disease*, Vol. 2 (pp. 269-292). Lippincott Williams and Wilkins.
- Geula, C., Dunlop, S. R., Ayala, I., Kawles, A. S., Flanagan, M. E., Gefen, T., & Mesulam, M. M. (2021). Basal forebrain cholinergic system in the dementias: Vulnerability, resilience, and resistance. *Journal of neurochemistry*, 158(6), 1394-1411.
- Giboureau, N., Emond, P., Fulton, R. R., Henderson, D. J., Chalon, S., Garreau, L., ... & Kassiou, M. (2007). Ex vivo and in vivo evaluation of (2R, 3R)-5-[18F]-fluoroethoxy-and fluoropropoxy-benzovesamicol, as PET radioligands for the vesicular acetylcholine transporter. *Synapse*, 61(12), 962-970.
- Gil-Bea, F. J., García-Alloza, M., Domínguez, J., Marcos, B., & Ramírez, M. J. (2005). Evaluation of cholinergic markers in Alzheimer's disease and in a model of cholinergic deficit. *Neuroscience letters*, 375(1), 37-41.



- Gilmor, M. L., Nash, N. R., Roghani, A., Edwards, R. H., Yi, H., Hersch, S. M., & Levey, A. I. (1996). Expression of the putative vesicular acetylcholine transporter in rat brain and localization in cholinergic synaptic vesicles. *Journal of Neuroscience*, *16*(7), 2179-2190.
- Gilmor, M. L., Erickson, J. D., Varoqui, H., Hersh, L. B., Bennett, D. A., Cochran, E. J., ... & Levey, A. I. (1999). Preservation of nucleus basalis neurons containing choline acetyltransferase and the vesicular acetylcholine transporter in the elderly with mild cognitive impairment and early Alzheimer's disease. *Journal of Comparative Neurology*, *411*(4), 693-704.
- Giuffrida, M. L., Caraci, F., Pignataro, B., Cataldo, S., De Bona, P., Bruno, V., ... & Copani, A. (2009).  $\beta$ -amyloid monomers are neuroprotective. *Journal of Neuroscience*, *29*(34), 10582-10587.
- Glodzik, L., Sollberger, M., Gass, A., Gokhale, A., Rusinek, H., Babb, J., ... & Gonen, O. (2015). Global N-acetylaspartate in normal subjects, mild cognitive impairment and Alzheimer's disease patients. *Journal of Alzheimer's Disease*, *43*(3), 939-947.
- González, M. M., Suárez-Sanmartín, E., García, C., Martínez-Cambor, P., Westman, E., & Simmons, A. (2016). Manual planimetry of the medial temporal lobe versus automated volumetry of the hippocampus in the diagnosis of Alzheimer's disease. *Cureus*, *8*(3).
- Goodman, Y., & Mattson, M. P. (1994). Secreted forms of  $\beta$ -amyloid precursor protein protect hippocampal neurons against amyloid  $\beta$ -peptide-induced oxidative injury. *Experimental neurology*, *128*(1), 1-12.
- Gordon, B. A., Blazey, T., Su, Y., Fagan, A. M., Holtzman, D. M., Morris, J. C., & Benzinger, T. L. (2016). Longitudinal  $\beta$ -amyloid deposition and hippocampal volume in preclinical Alzheimer disease and suspected non-Alzheimer disease pathophysiology. *JAMA neurology*, *73*(10), 1192-1200.
- Gosztyla, M. L., Brothers, H. M., & Robinson, S. R. (2018). Alzheimer's Amyloid- $\beta$  is an Antimicrobial Peptide: A Review of the Evidence. *Journal of Alzheimer's Disease*, *62*(4), 1495-1506.
- Graff-Radford, J., & Kantarci, K. (2013). Magnetic resonance spectroscopy in Alzheimer's disease. *Neuropsychiatric disease and treatment*, *9*, 687.
- Gratwicke, J., Kahan, J., Zrinzo, L., Hariz, M., Limousin, P., Foltynie, T. et al. Jahanshahi, M. (2013). The nucleus basalis of Meynert: A new target for deep brain stimulation in dementia?. *Neuroscience & Biobehavioral Reviews*, *37*(10), 2676-2688. doi: 10.1016/j.neubiorev.2013.09.003
- Grothe, M., Zaborszky, L., Atienza, M., Gil-Neciga, E., Rodriguez-Romero, R., Teipel, S. J., ... & Cantero, J. L. (2010). Reduction of basal forebrain cholinergic system parallels cognitive impairment in patients at high risk of developing Alzheimer's disease. *Cerebral Cortex*, *20*(7), 1685-1695.
- Grothe, M., Heinsen, H., & Teipel, S. J. (2012). Atrophy of the cholinergic basal forebrain over the adult age range and in early stages of Alzheimer's disease. *Biological psychiatry*, *71*(9), 805-813.
- Grothe, M., Heinsen, H., & Teipel, S. (2013). Longitudinal measures of cholinergic forebrain atrophy in the transition from healthy aging to Alzheimer's disease. *Neurobiology of aging*, *34*(4), 1210-1220.

- Grothe, M. J., Schuster, C., Bauer, F., Heinsen, H., Prudlo, J., & Teipel, S. J. (2014). Atrophy of the cholinergic basal forebrain in dementia with Lewy bodies and Alzheimer's disease dementia. *Journal of neurology*, 261(10), 1939-1948.
- Grothe, M. J., Kilimann, I., Grinberg, L., Heinsen, H., & Teipel, S. (2018). In vivo Volumetry of the cholinergic basal forebrain. In *Biomarkers for Preclinical Alzheimer's Disease* (pp. 213-232). Humana Press, New York, NY.
- Grottick, A. J., & Higgins, G. A. (2000). Effect of subtype selective nicotinic compounds on attention as assessed by the five-choice serial reaction time task. *Behavioural brain research*, 117(1-2), 197-208.
- Grudzien, A., Shaw, P., Weintraub, S., Bigio, E., Mash, D. C., & Mesulam, M. M. (2007). Locus coeruleus neurofibrillary degeneration in aging, mild cognitive impairment and early Alzheimer's disease. *Neurobiology of aging*, 28(3), 327-335.
- Geula, C., Dunlop, S. R., Ayala, I., Kawles, A. S., Flanagan, M. E., Gefen, T., & Mesulam, M. M. (2021). Basal forebrain cholinergic system in the dementias: Vulnerability, resilience, and resistance. *Journal of neurochemistry*, 158(6), 1394-1411.
- Haense, C., Kalbe, E., Herholz, K., Hohmann, C., Neumaier, B., Kraiss, R., & Heiss, W. D. (2012). Cholinergic system function and cognition in mild cognitive impairment. *Neurobiology of aging*, 33(5), 867-877.
- Hempel, H., Mesulam, M. M., Cuellar, A. C., Farlow, M. R., Giacobini, E., Grossberg, G. T., ... & Khachaturian, Z. S. (2018). The cholinergic system in the pathophysiology and treatment of Alzheimer's disease. *Brain*, 141(7), 1917-1933.
- Hempel, H., Hardy, J., Blennow, K., Chen, C., Perry, G., Kim, S. H., ... & Vergallo, A. (2021). The amyloid- $\beta$  pathway in Alzheimer's disease. *Molecular Psychiatry*, 26(10), 5481-5503.
- Hansson, O., Mikulskis, A., Fagan, A. M., Teunissen, C., Zetterberg, H., Vanderstichele, H., ... & Blennow, K. (2018). The impact of preanalytical variables on measuring cerebrospinal fluid biomarkers for Alzheimer's disease diagnosis: a review. *Alzheimer's & Dementia*, 14(10), 1313-1333.
- Hanyu, H., Asano, T., Sakurai, H., Tanaka, Y., Takasaki, M., & Abe, K. (2002). MR analysis of the substantia innominata in normal aging, Alzheimer disease, and other types of dementia. *American Journal of Neuroradiology*, 23(1), 27-32.
- Hardy, J. A., & Higgins, G. A. (1992). Alzheimer's disease: the amyloid cascade hypothesis. *Science*, 256(5054), 184-186.
- Hardy, J., & Selkoe, D. J. (2002). The amyloid hypothesis of Alzheimer's disease: progress and problems on the road to therapeutics. *science*, 297(5580), 353-356.
- Harper, L., Fumagalli, G. G., Barkhof, F., Scheltens, P., O'Brien, J. T., Bouwman, F., ... & Schott, J. M. (2016). MRI visual rating scales in the diagnosis of dementia: evaluation in 184 post-mortem confirmed cases. *Brain*, 139(4), 1211-1225.

- Hashimoto, M., Kitagaki, H., Imamura, T., Hirono, N., Shimomura, T., Kazui, H., ... & Mori, E. (1998). Medial temporal and whole-brain atrophy in dementia with Lewy bodies: a volumetric MRI study. *Neurology*, *51*(2), 357-362.
- Hasselmo, M. E., & Sarter, M. (2011). Modes and models of forebrain cholinergic neuromodulation of cognition. *Neuropsychopharmacology*, *36*(1), 52-73.
- Hatashita, S., & Wakebe, D. (2017). Amyloid- $\beta$  deposition and long-term progression in mild cognitive impairment due to Alzheimer's disease defined with amyloid PET imaging. *Journal of Alzheimer's Disease*, *57*(3), 765-773.
- Hebert, L. E., Beckett, L. A., Scherr, P. A., & Evans, D. A. (2001). Annual incidence of Alzheimer disease in the United States projected to the years 2000 through 2050. *Alzheimer Disease & Associated Disorders*, *15*(4), 169-173.
- Hebert, L. E., Scherr, P. A., Bienias, J. L., Bennett, D. A., & Evans, D. A. (2003). Alzheimer disease in the US population: prevalence estimates using the 2000 census. *Archives of neurology*, *60*(8), 1119-1122.
- Helbert H, Wenzel B, Deuther-Conrad W, Luurtsema G, Szymanski W, Brust P, Feringa B, Dierckx R, Elsinga P. (2019). Pd catalyzed cross-coupling of [11C]MeLi and its application in the synthesis and evaluation of a potential PET tracer for the vesicular acetylcholine transporter (VACHT). *J Label Compd Radiopharm* *62*, S238-S239.
- Hernandez, C., & T Dineley, K. (2012).  $\alpha 7$  Nicotinic acetylcholine receptors in Alzheimer's disease: neuroprotective, neurotrophic or both?. *Current drug targets*, *13*(5), 613-622.
- Herrmann, N., Harimoto, T., Balshaw, R., Lanctôt, K. L., & Canadian Outcomes Study in Dementia (COSID) Investigators (members) 5. (2015). Risk factors for progression of Alzheimer disease in a Canadian population: the Canadian Outcomes Study in Dementia (COSID). *The Canadian Journal of Psychiatry*, *60*(4), 189-199.
- Hilker, R., Thomas, A. V., Klein, J. C., Weisenbach, S., Kalbe, E., Burghaus, L., ... & Heiss, W. D. (2005). Dementia in Parkinson disease: functional imaging of cholinergic and dopaminergic pathways. *Neurology*, *65*(11), 1716-1722.
- Hillmer, A. T., Wooten, D. W., Slesarev, M. S., Ahlers, E. O., Barnhart, T. E., Murali, D., . . . Christian, B. T. (2012). PET imaging of alpha4beta2\* nicotinic acetylcholine receptors: quantitative analysis of 18F-nifene kinetics in the nonhuman primate. *Journal of nuclear medicine : official publication, Society of Nuclear Medicine*, *53*(9), 1471-1480. doi: 10.2967/jnumed.112.103846
- Hirano, S., Shinotoh, H., Shimada, H., Ota, T., Sato, K., Tanaka, N., ... & Suhara, T. (2018). Voxel-based acetylcholinesterase PET study in early and late onset Alzheimer's disease. *Journal of Alzheimer's Disease*, *62*(4), 1539-1548.
- Huang, L. K., Chao, S. P., & Hu, C. J. (2020). Clinical trials of new drugs for Alzheimer disease. *Journal of biomedical science*, *27*(1), 1-13.

- Husain, M. A., Laurent, B., & Plourde, M. (2021). APOE and Alzheimer's disease: from lipid transport to physiopathology and therapeutics. *Frontiers in Neuroscience*, *15*, 630502.
- Hyman, B. T., Van Hoesen, G. W., & Damasio, A. R. (1987). Alzheimer's disease: glutamate depletion in the hippocampal perforant pathway zone. *Annals of neurology*, *22*(1), 37-40.
- Ikonomovic, M. D., Klunk, W. E., Abrahamson, E. E., Mathis, C. A., Price, J. C., Tsopelas, N. D., ... & DeKosky, S. T. (2008). Post-mortem correlates of in vivo PiB-PET amyloid imaging in a typical case of Alzheimer's disease. *Brain*, *131*(6), 1630-1645.
- Insel, P. S., Weiner, M., Mackin, R. S., Mormino, E., Lim, Y. Y., Stomrud, E., ... & Mattsson, N. (2019). Determining clinically meaningful decline in preclinical Alzheimer disease. *Neurology*, *93*(4), e322-e333.
- Iqbal, M., Pumford, N. R., Tang, Z. X., Lassiter, K., Ojano-Dirain, C., Wing, T., ... & Bottje, W. (2005). Compromised liver mitochondrial function and complex activity in low feed efficient broilers are associated with higher oxidative stress and differential protein expression. *Poultry science*, *84*(6), 933-941.
- Iqbal, K., Liu, F., Gong, C. X., & Grundke-Iqbal, I. (2010). Tau in Alzheimer disease and related tauopathies. *Current Alzheimer Research*, *7*(8), 656-664.
- Irie, T., Fukushi, K., Akimoto, Y., Tamagami, H., & Nozaki, T. (1994). Design and evaluation of radioactive acetylcholine analogs for mapping brain acetylcholinesterase (AChE) in vivo. *Nuclear medicine and biology*, *21*(6), 801-808.
- Irwin, D. J., & Hurtig, H. I. (2018). The contribution of tau, amyloid-beta and alpha-synuclein pathology to dementia in Lewy body disorders. *Journal of Alzheimer's disease & Parkinsonism*, *8*(4).
- Jack, C. R., Petersen, R. C., Xu, Y. C., O'Brien, P. C., Smith, G. E., Ivnik, R. J., ... & Kokmen, E. (1999). Prediction of AD with MRI-based hippocampal volume in mild cognitive impairment. *Neurology*, *52*(7), 1397-1397.
- Jack, C. R., Dickson, D. W., Parisi, J. E., Xu, Y. C., Cha, R. H., O'Brien, P. C., ... & Petersen, R. C. (2002). Antemortem MRI findings correlate with hippocampal neuropathology in typical aging and dementia. *Neurology*, *58*(5), 750-757.
- Jack Jr, C. R., Knopman, D. S., Jagust, W. J., Shaw, L. M., Aisen, P. S., Weiner, M. W., ... & Trojanowski, J. Q. (2010). Hypothetical model of dynamic biomarkers of the Alzheimer's pathological cascade. *The Lancet Neurology*, *9*(1), 119-128.
- Jack Jr, C. R., & Holtzman, D. M. (2013). Biomarker modeling of Alzheimer's disease. *Neuron*, *80*(6), 1347-1358.
- Jack Jr, C. R., Bennett, D. A., Blennow, K., Carrillo, M. C., Dunn, B., Haeberlein, S. B., ... & Silverberg, N. (2018). NIA-AA research framework: toward a biological definition of Alzheimer's disease. *Alzheimer's & Dementia*, *14*(4), 535-562.

- Jagust, W. M. R. B., Reed, B., Mungas, D., Ellis, W., & DeCarli, C. (2007). What does fluorodeoxyglucose PET imaging add to a clinical diagnosis of dementia?. *Neurology*, *69*(9), 871-877.
- Jones, B. E., & Cuello, A. C. (1989). Afferents to the basal forebrain cholinergic cell area from pontomesencephalic—catecholamine, serotonin, and acetylcholine—neurons. *Neuroscience*, *31*(1), 37-61.
- Josephs, K. A., Dickson, D. W., Tosakulwong, N., Weigand, S. D., Murray, M. E., Petrucelli, L., ... & Whitwell, J. L. (2017). Rates of hippocampal atrophy and presence of post-mortem TDP-43 in patients with Alzheimer's disease: a longitudinal retrospective study. *The Lancet Neurology*, *16*(11), 917-924.
- Kagan, B. L. (2012). Membrane pores in the pathogenesis of neurodegenerative disease. *Progress in molecular biology and translational science*, *107*, 295-325.
- Kametani, F., & Hasegawa, M. (2018). Reconsideration of amyloid hypothesis and tau hypothesis in Alzheimer's disease. *Frontiers in neuroscience*, *25*
- Kanel, P., Bedard, M. A., Aghourian, M., Rosa-Neto, P., Soucy, J. P., Albin, R. L., & Bohnen, N. I. (2021). Molecular Imaging of the Cholinergic System in Alzheimer and Lewy Body Dementias: Expanding Views. *Current Neurology and Neuroscience Reports*, *21*(10), 1-9.
- Kantarci, K. J. C. J., Jack, C. R., Xu, Y. C., Campeau, N. G., O'Brien, P. C., Smith, G. E., ... & Petersen, R. C. (2000). Regional metabolic patterns in mild cognitive impairment and Alzheimer's disease: a 1H MRS study. *Neurology*, *55*(2), 210-217.
- Kantarci, K., Petersen, R. C., Boeve, B. F., Knopman, D. S., Weigand, S. D., O'Brien, P. C., ... & Jack, C. R. (2005). DWI predicts future progression to Alzheimer disease in amnesic mild cognitive impairment. *Neurology*, *64*(5), 902-904.
- Kato, T., Inui, Y., Nakamura, A., & Ito, K. (2016). Brain fluorodeoxyglucose (FDG) PET in dementia. *Ageing research reviews*, *30*, 73-84.
- Kawamura, K., Shiba, K., Tsukada, H., Nishiyama, S., Mori, H., & Ishiwata, K. (2006). Synthesis and evaluation of vesamicol analog (-)-O-[11C]methylvesamicol as a PET ligand for vesicular acetylcholine transporter. *Annals of nuclear medicine*, *20*(6), 417-424.
- Kemppainen, N. M., Aalto, S., Wilson, I. A., Någren, K., Helin, S., Brück, A., ... & Rinne, J. O. (2007). PET amyloid ligand [11C] PIB uptake is increased in mild cognitive impairment. *Neurology*, *68*(19), 1603-1606.
- Khan, W., Westman, E., Jones, N., Wahlund, L. O., Mecocci, P., Vellas, B., ... & Simmons, A. (2015). Automated hippocampal subfield measures as predictors of conversion from mild cognitive impairment to Alzheimer's disease in two independent cohorts. *Brain topography*, *28*(5), 746-759.
- Khatoon, S., Grundke-Iqbal, I., & Iqbal, K. (1992). Brain levels of microtubule-associated protein  $\tau$  are elevated in Alzheimer's disease: A radioimmuno-slot-blot assay for nanograms of the protein. *Journal of neurochemistry*, *59*(2), 750-753.

- Kilbourn, M. R., Jung, Y. W., Haka, M. S., Gildersleeve, D. L., Kuhl, D. E., & Wieland, D. M. (1990). Mouse brain distribution of a carbon-11 labeled vesamicol derivative: presynaptic marker of cholinergic neurons. *Life Sci*, 47(21), 1955-1963.
- Kilbourn, M. R., Hockley, B., Lee, L., Sherman, P., Quesada, C., Frey, K. A., & Koeppe, R. A. (2009). Positron emission tomography imaging of (2R, 3R)-5-[18F] fluoroethoxybenzovesamicol in rat and monkey brain: a radioligand for the vesicular acetylcholine transporter. *Nuclear medicine and biology*, 36(5), 489-493.
- Kilimann, I., Grothe, M., Heinsen, H., Alho, E. J. L., Grinberg, L., Amaro Jr, E., Teipel, S. J. (2014). Subregional basal forebrain atrophy in Alzheimer's disease: a multicenter study. *Journal of Alzheimer's Disease*, 40(3), 687-700.
- Klinkenberg, I., Sambeth, A., & Blokland, A. (2011). Acetylcholine and attention. *Behavioural brain research*, 221(2), 430-442.
- Klunk, W. E., Engler, H., Nordberg, A., Wang, Y., Blomqvist, G., Holt, D. P., ... & Långström, B. (2004). Imaging brain amyloid in Alzheimer's disease with Pittsburgh Compound-B. *Annals of Neurology: Official Journal of the American Neurological Association and the Child Neurology Society*, 55(3), 306-319.
- Kolb, H. C., & Andrés, J. I. (2017). Tau positron emission tomography imaging. *Cold Spring Harbor perspectives in biology*, 9(5), a023721.
- Kotagal, V., Müller, M. L., Kaufer, D. I., Koeppe, R. A., & Bohnen, N. I. (2012). Thalamic cholinergic innervation is spared in Alzheimer disease compared to parkinsonian disorders. *Neuroscience letters*, 514(2), 169-172.
- Kuhl, D. E., Koeppe, R. A., Fessler, J. A., Minoshima, S., Ackermann, R. J., Carey, J. E., . . . Wieland, D. M. (1994). In vivo mapping of cholinergic neurons in the human brain using SPECT and IBVM. *Journal of nuclear medicine : official publication, Society of Nuclear Medicine*, 35(3), 405-410.
- Kuhl, D. E., Koeppe, R. A., Minoshima, S., Snyder, S. E., Ficarò, E. P., Foster, N. L., ... & Kilbourn, M. R. (1999). In vivo mapping of cerebral acetylcholinesterase activity in aging and Alzheimer's disease. *Neurology*, 52(4), 691-691.
- Laakso, M. P., Partanen, K., Riekkinen, P., Lehtovirta, M., Helkala, E. L., Hallikainen, M., ... & Soininen, H. (1996). Hippocampal volumes in Alzheimer's disease, Parkinson's disease with and without dementia, and in vascular dementia: An MRI study. *Neurology*, 46(3), 678-681.
- Lai, M. K., Tsang, S. W., Francis, P. T., Keene, J., Hope, T., Esiri, M. M., ... & Chen, C. P. H. (2002). Postmortem serotonergic correlates of cognitive decline in Alzheimer's disease. *Neuroreport*, 13(9), 1175-1178.
- Landau, S. M., Mintun, M. A., Joshi, A. D., Koeppe, R. A., Petersen, R. C., Aisen, P. S., ... & Alzheimer's Disease Neuroimaging Initiative. (2012). Amyloid deposition, hypometabolism, and longitudinal cognitive decline. *Annals of neurology*, 72(4), 578-586.

- a Landry, E., Rosa-Neto, P., Massarweh, G., Aliaga, A., Mzengeza, S., Bedard, M. A., & Soucy, J. P. (2008). Distribution of [18F]-FEOBV in rat: a promising tracer for imaging cholinergic innervation densities. *Can J Neurol Sci*, *35*, S46.
- b Landry, E., Rosa-Neto, P., Massarweh, G., Aliaga, A., Mzengeza, F., Bedard, M. A., & Soucy, J. P. (2008). Plasma chromatographic profile of [18F]-FEOBV in rat: results and implications for clinical applications. *Can J Neurol Sci*, *35*, S46.
- Lehéricy, S., Hirsch, É. C., Cervera-Piérot, P., Hersh, L. B., Bakchine, S., Piette, F., ... & Agid, Y. (1993). Heterogeneity and selectivity of the degeneration of cholinergic neurons in the basal forebrain of patients with Alzheimer's disease. *Journal of Comparative Neurology*, *330*(1), 15-31.
- Lemoine, L., Leuzy, A., Chiotis, K., Rodriguez-Vieitez, E., & Nordberg, A. (2018). Tau positron emission tomography imaging in tauopathies: the added hurdle of off-target binding. *Alzheimer's & Dementia: Diagnosis, Assessment & Disease Monitoring*, *10*, 232-236.
- Lindsay, J., Laurin, D., Verreault, R., Hébert, R., Helliwell, B., Hill, G. B., & McDowell, I. (2002). Risk factors for Alzheimer's disease: a prospective analysis from the Canadian Study of Health and Aging. *American journal of epidemiology*, *156*(5), 445-453.
- Lindwall, G., & Cole, R. D. (1984). Phosphorylation affects the ability of tau protein to promote microtubule assembly. *Journal of Biological Chemistry*, *259*(8), 5301-5305.
- Iizuka, T., & Kameyama, M. (2017). Cholinergic enhancement increases regional cerebral blood flow to the posterior cingulate cortex in mild Alzheimer's disease. *Geriatrics & gerontology international*, *17*(6), 951-958.
- Liu, C. C., Kanekiyo, T., Xu, H., & Bu, G. (2013). Apolipoprotein E and Alzheimer disease: risk, mechanisms and therapy. *Nature Reviews Neurology*, *9*(2), 106-118.
- Liu, A. K. L., Chang, R. C. C., Pearce, R. K., & Gentleman, S. M. (2015). Nucleus basalis of Meynert revisited: anatomy, history and differential involvement in Alzheimer's and Parkinson's disease. *Acta neuropathologica*, *129*(4), 527-540.
- Long, J. M., & Holtzman, D. M. (2019). Alzheimer disease: an update on pathobiology and treatment strategies. *Cell*, *179*(2), 312-339.
- Lonie, J. A., Tierney, K. M., & Ebmeier, K. P. (2009). Screening for mild cognitive impairment: a systematic review. *International Journal of Geriatric Psychiatry: A journal of the psychiatry of late life and allied sciences*, *24*(9), 902-915.
- Lowe, V. J., Curran, G., Fang, P., Liesinger, A. M., Josephs, K. A., Parisi, J. E., ... & Murray, M. E. (2016). An autoradiographic evaluation of AV-1451 Tau PET in dementia. *Acta neuropathologica communications*, *4*(1), 1-19.
- Lustbader, J. W., Cirilli, M., Lin, C., Xu, H. W., Takuma, K., Wang, N., ... & Wu, H. (2004). Aβ directly links Aβ to mitochondrial toxicity in Alzheimer's disease. *Science*, *304*(5669), 448-452.

- Mach, R. H., Voytko, M. L., Ehrenkaufner, R. L., Nader, M. A., Tobin, J. R., Efange, S. M., . . . Morton, T. E. (1997). Imaging of cholinergic terminals using the radiotracer [<sup>18</sup>F](+)-4-fluorobenzyltrozamicol: in vitro binding studies and positron emission tomography studies in nonhuman primates. *Synapse*, 25(4), 368-380. doi: 10.1002/(SICI)1098-2396(199704)25:4<368::AID-SYN8>3.0.CO;2-8
- Martorana, A., Assogna, M., Motta, C., Bonomi, C. G., Bernocchi, F., MG, D. D., & Koch, G. (2021). Cognitive reserve and Alzheimer's biological continuum: clues for prediction and prevention of dementia. *Minerva Medica*.
- Matej, R., Tesar, A., & Rusina, R. (2019). Alzheimer's disease and other neurodegenerative dementias in comorbidity: a clinical and neuropathological overview. *Clinical biochemistry*, 73, 26-31.
- Mathotaarachchi, S., Wang, S., Shin, M., Pascoal, T. A., Benedet, A. L., Kang, M. S., ... & Rosa-Neto, P. (2016). VoxelStats: a MATLAB package for multi-modal voxel-wise brain image analysis. *Frontiers in neuroinformatics*, 10, 20.
- Mazère, J., Meissner, W. G., Mayo, W., Sibon, I., Lamare, F., Guilloteau, D., ... & Allard, M. (2012). Progressive supranuclear palsy: in vivo SPECT imaging of presynaptic vesicular acetylcholine transporter with [<sup>123</sup>I]-iodobenzovesamicol. *Radiology*, 265(2), 537-543.
- Mazère, J., Meissner, W. G., Sibon, I., Lamare, F., Tison, F., Allard, M., & Mayo, W. (2013). [(<sup>123</sup>I)]-IBVM SPECT imaging of cholinergic systems in multiple system atrophy: A specific alteration of the ponto-thalamic cholinergic pathways (Ch5-Ch6). *Neuroimage Clin*, 3, 212-217. doi: 10.1016/j.nicl.2013.07.012
- McCluskey, S. P., Plisson, C., Rabiner, E. A., & Howes, O. (2020). Advances in CNS PET: the state-of-the-art for new imaging targets for pathophysiology and drug development. *European journal of nuclear medicine and molecular imaging*, 47(2), 451-489.
- McKeith, I. G., Boeve, B. F., Dickson, D. W., Halliday, G., Taylor, J. P., Weintraub, D., ... & Kosaka, K. (2017). Diagnosis and management of dementia with Lewy bodies: Fourth consensus report of the DLB Consortium. *Neurology*, 89(1), 88-100.
- McKhann, G. M., Knopman, D. S., Chertkow, H., Hyman, B. T., Jack Jr, C. R., Kawas, C. H., ... & Phelps, C. H. (2011). The diagnosis of dementia due to Alzheimer's disease: recommendations from the National Institute on Aging-Alzheimer's Association workgroups on diagnostic guidelines for Alzheimer's disease. *Alzheimer's & dementia*, 7(3), 263-269.
- Mecca, A. P., Chen, M. K., O'Dell, R. S., Naganawa, M., Toyonaga, T., Godek, T. A., ... & van Dyck, C. H. (2020). In vivo measurement of widespread synaptic loss in Alzheimer's disease with SV2A PET. *Alzheimer's & Dementia*, 16(7), 974-982.
- Mecca, A. P., O'Dell, R. S., Sharp, E. S., Banks, E. R., Bartlett, H. H., Zhao, W., ... & van Dyck, C. H. (2022). Synaptic density and cognitive performance in Alzheimer's disease: A PET imaging study with [<sup>11</sup>C] UCB-J. *Alzheimer's & Dementia*.
- Mesulam, M.-M., Mufson, E. J., Levey, A. I. et Wainer, B. H. (1983). Cholinergic innervation of cortex by the basal forebrain: Cytochemistry and cortical connections of the septal area, diagonal band



- nuclei, nucleus basalis (Substantia innominata), and hypothalamus in the rhesus monkey. *The Journal of Comparative Neurology*, 214(2), 170-197.
- Mesulam, M. M. et Geula, C. (1988). Nucleus basalis (Ch4) and cortical cholinergic innervation in the human brain: Observations based on the distribution of acetylcholinesterase and choline acetyltransferase. *The Journal of Comparative Neurology*, 275(2), 216-240.
- Mesulam, M. M. (1990). Human brain cholinergic pathways. *Progress in brain research*, 84, 231-241.
- Mesulam, M. M., & Geula, C. (1992). Overlap between acetylcholinesterase-rich and choline acetyltransferase-positive (cholinergic) axons in human cerebral cortex. *Brain research*, 577(1), 112-120.
- Mesulam, M. M. (2004). The cholinergic innervation of the human cerebral cortex. *Progress in brain research*, 145, 67-78.
- Mesulam, M., Shaw, P., Mash, D., & Weintraub, S. (2004). Cholinergic nucleus basalis tauopathy emerges early in the aging-MCI-AD continuum. *Annals of Neurology: Official Journal of the American Neurological Association and the Child Neurology Society*, 55(6), 815-828.
- Mesulam, M. M. (2013). Cholinergic circuitry of the human nucleus basalis and its fate in Alzheimer's disease. *Journal of Comparative Neurology*, 521(18), 4124-4144.
- Mesulam, M. M., Lalehzari, N., Rahmani, F., Ohm, D., Shahidehpour, R., Kim, G., ... & Geula, C. (2019). Cortical cholinergic denervation in primary progressive aphasia with Alzheimer pathology. *Neurology*, 92(14), e1580-e1588.
- Meziane, H., Dodart, J. C., Mathis, C., Little, S., Clemens, J., Paul, S. M., & Ungerer, A. (1998). Memory-enhancing effects of secreted forms of the  $\beta$ -amyloid precursor protein in normal and amnesic mice. *Proceedings of the national academy of sciences*, 95(21), 12683-12688.
- Minoshima, S., Frey, K. A., Koeppe, R. A., Foster, N. L., & Kuhl, D. E. (1995). A diagnostic approach in Alzheimer's disease using three-dimensional stereotactic surface projections of fluorine-18-FDG PET. *Journal of Nuclear Medicine*, 36(7), 1238-1248.
- Minoshima, S., Foster, N. L., Sima, A. A., Frey, K. A., Albin, R. L., & Kuhl, D. E. (2001). Alzheimer's disease versus dementia with Lewy bodies: cerebral metabolic distinction with autopsy confirmation. *Annals of Neurology: Official Journal of the American Neurological Association and the Child Neurology Society*, 50(3), 358-365.
- Modrego, P. J., Pina, M. A., Fayed, N., & Díaz, M. (2006). Changes in metabolite ratios after treatment with rivastigmine in Alzheimer's disease. *CNS drugs*, 20(10), 867-877.
- Mohammed, A. H. (1993). Effects of cholinesterase inhibitors on learning and memory in rats: a brief review with special reference to THA. *Acta Neurologica Scandinavica*, 88(S149), 13-15
- Molinuevo, J. L., Ayton, S., Batrla, R., Bednar, M. M., Bittner, T., Cummings, J., ... & Blennow, K. (2018). Current state of Alzheimer's fluid biomarkers. *Acta neuropathologica*, 136(6), 821-853.

- Mosconi, L. (2005). Brain glucose metabolism in the early and specific diagnosis of Alzheimer's disease. *European journal of nuclear medicine and molecular imaging*, 32(4), 486-510.
- Mosconi, L., Tsui, W. H., Herholz, K., Pupi, A., Drzezga, A., Lucignani, G., ... & De Leon, M. J. (2008). Multicenter standardized 18F-FDG PET diagnosis of mild cognitive impairment, Alzheimer's disease, and other dementias. *Journal of nuclear medicine*, 49(3), 390-398.
- Mosconi, L., Andrews, R. D., Matthews, D. C., & Alzheimer's Disease Neuroimaging Initiative (ADNI). (2013). Comparing brain amyloid deposition, glucose metabolism, and atrophy in mild cognitive impairment with and without a family history of dementia. *Journal of Alzheimer's disease*, 35(3), 509-524.
- Mufson, E. J., Cochran, E., Benzing, W., & Kordower, J. H. (1993). Galaninergic innervation of the cholinergic vertical limb of the diagonal band (Ch2) and bed nucleus of the Stria terminalis in aging, Alzheimer's disease and down's syndrome (Part 1 of 2). *Dementia and Geriatric Cognitive Disorders*, 4(5), 237-243.
- Mufson, E. J., Bothwell, M., & Kordower, J. H. (1989). Loss of nerve growth factor receptor-containing neurons in Alzheimer's disease: a quantitative analysis across subregions of the basal forebrain. *Experimental neurology*, 105(3), 221-232.
- Mufson, E. J., Ginsberg, S. D., Ikonovic, M. D., & DeKosky, S. T. (2003). Human cholinergic basal forebrain: chemoanatomy and neurologic dysfunction. *Journal of chemical neuroanatomy*, 26(4), 233-242.
- Mufson, E. J., Counts, S. E., Fahnstock, M., & Ginsberg, S. D. (2007). Cholinergic molecular substrates of mild cognitive impairment in the elderly. *Current Alzheimer Research*, 4(4), 340-350.
- Mufson, E. J., Ikonovic, M. D., Counts, S. E., Perez, S. E., Malek-Ahmadi, M., Scheff, S. W., & Ginsberg, S. D. (2016). Molecular and cellular pathophysiology of preclinical Alzheimer's disease. *Behavioural brain research*, 311, 54-69.
- Mullane, K., & Williams, M. (2013). Alzheimer's therapeutics: continued clinical failures question the validity of the amyloid hypothesis—but what lies beyond?. *Biochemical pharmacology*, 85(3), 289-305.
- Mullane, K., & Williams, M. (2018). Alzheimer's disease (AD) therapeutics—1: Repeated clinical failures continue to question the amyloid hypothesis of AD and the current understanding of AD causality. *Biochemical pharmacology*, 158, 359-375.
- Mulholland, G. Keith, Yong-Woon Jung, Donald M. Wieland, Michael R. Kilbourn, and David E. Kuhl. (1993). Synthesis of [18F] fluoroethoxy-benzovesamicol, a radiotracer for cholinergic neurons. *Journal of Labelled Compounds and Radiopharmaceuticals*, 33 (7): 583-591.
- Mulholland, G. K., Wieland, D. M., Kilbourn, M. R., Frey, K. A., Sherman, P. S., Carey, J. E., & Kuhl, D. E. (1998). [18F] fluoroethoxy-benzovesamicol, a PET radiotracer for the vesicular acetylcholine transporter and cholinergic synapses. *Synapse*, 30(3), 263-274.

- Mufson, E. J., Ginsberg, S. D., Ikonovic, M. D., & DeKosky, S. T. (2003). Human cholinergic basal forebrain: chemoanatomy and neurologic dysfunction. *Journal of chemical neuroanatomy*, 26(4), 233-242.
- Muth, K., Schönmeier, R., Matura, S., Haenschel, C., Schröder, J., & Pantel, J. (2010). Mild cognitive impairment in the elderly is associated with volume loss of the cholinergic basal forebrain region. *Biological psychiatry*, 67(6), 588-591.
- Mzengeza, S., Massarweh, G., Rosa-Neto, P., Soucy, J. P., & Bedard, M. A. (2007). Radiosynthesis of [18F]FEOBV and in vivo PET imaging of acetylcholine vesicular transporter in the rat. *J. Cereb. Blood Flow Metab*, 27, 10-17U.
- Nabulsi, N. B., Mercier, J., Holden, D., Carré, S., Najafzadeh, S., Vandergeten, M. C., ... & Huang, Y. (2016). Synthesis and preclinical evaluation of 11C-UCB-J as a PET tracer for imaging the synaptic vesicle glycoprotein 2A in the brain. *Journal of Nuclear Medicine*, 57(5), 777-784.
- Naganawa, M., Nabulsi, N., Henry, S., Matuskey, D., Lin, S. F., Sliker, L., ... & Huang, Y. (2021). First-in-human assessment of 11C-LSN3172176, an M1 muscarinic acetylcholine receptor PET radiotracer. *Journal of Nuclear Medicine*, 62(4), 553-560.
- Naseri, N. N., Wang, H., Guo, J., Sharma, M., & Luo, W. (2019). The complexity of tau in Alzheimer's disease. *Neuroscience letters*, 705, 183-194.
- Nasreddine, Z. S., Phillips, N. A., Bédirian, V., Charbonneau, S., Whitehead, V., Collin, I., ... & Chertkow, H. (2005). The Montreal Cognitive Assessment, MoCA: a brief screening tool for mild cognitive impairment. *Journal of the American Geriatrics Society*, 53(4), 695-699.
- Nazarali, A. J., & Reynolds, G. P. (1992). Monoamine neurotransmitters and their metabolites in brain regions in Alzheimer's disease: a postmortem study. *Cellular and molecular neurobiology*, 12(6), 581-587.
- Nejad-Davarani, S., Koeppe, R. A., Albin, R. L., Frey, K. A., Müller, M. L., & Bohnen, N. I. (2019). Quantification of brain cholinergic denervation in dementia with Lewy bodies using PET imaging with [18 F]-FEOBV. *Molecular psychiatry*, 24(3), 322-327.
- Newman, E., Gupta, K., Climer, J., Monaghan, C., and Hasselmo, M. (2012). Cholinergic modulation of cognitive processing: insights drawn from computational models. *Front. Behav. Neurosci.* 6:24. doi : 10.3389/fnbeh.2012.00024
- O'Brien, J. T., Firbank, M. J., Davison, C., Barnett, N., Bamford, C., Donaldson, C., ... & Lloyd, J. (2014). 18F-FDG PET and perfusion SPECT in the diagnosis of Alzheimer and Lewy body dementias. *Journal of Nuclear Medicine*, 55(12), 1959-1965.
- Odawara, T., Shiozaki, K., Iseki, E., Hino, H., & Kosaka, K. (2003). Alterations of muscarinic acetylcholine receptors in atypical Pick's disease without Pick bodies. *Journal of Neurology, Neurosurgery & Psychiatry*, 74(7), 965-967.

- Overk, C. R., Felder, C. C., Tu, Y., Schober, D. A., Bales, K. R., Wu, J., & Mufson, E. J. (2010). Cortical M1 receptor concentration increases without a concomitant change in function in Alzheimer's disease. *Journal of chemical neuroanatomy*, *40*(1), 63-70.
- Pagani, M., Nobili, F., Morbelli, S., Arnaldi, D., Giuliani, A., Öberg, J., ... & Piva, R. (2017). Early identification of MCI converting to AD: a FDG PET study. *European Journal of Nuclear Medicine and Molecular Imaging*, *44*(12), 2042-2052.
- Palmqvist, S., Zetterberg, H., Mattsson, N., Johansson, P., Minthon, L., Blennow, K., ... & Swedish BioFINDER Study Group. (2015). Detailed comparison of amyloid PET and CSF biomarkers for identifying early Alzheimer disease. *Neurology*, *85*(14), 1240-1249.
- Pappata, S., Tavitian, B., Traykov, L., Jobert, A., Dalger, A., Mangin, J. F., . . . DiGiambardino, L. (1996). In vivo imaging of human cerebral acetylcholinesterase. *J Neurochem*, *67*(2), 876-879.
- Parent, M., Bédard, M. A., Rosa-Neto, P., Davoli, M. A., Mechawar, N., Aliaga, A., & Soucy, J. P. (2011). Reliability and sensitivity to detect cortical cholinergic denervation in rats using PET imaging with [18F] Fluoroethoxybenzovesamicol. *Alzheimer's & Dementia: The Journal of the Alzheimer's Association*, *4*(7), S34.
- Parent, M., Bedard, M. A., Aliaga, A., Soucy, J. P., St-Pierre, E. L., Cyr, M., ... & Rosa-Neto, P. (2012). PET imaging of cholinergic deficits in rats using [18F] fluoroethoxybenzovesamicol ([18F] FEOBV). *Neuroimage*, *62*(1), 555-561.
- Parent, M. J., Bedard, M. A., Aliaga, A., Minuzzi, L., Mechawar, N., Soucy, J. P., ... & Rosa-Neto, P. (2013). Cholinergic depletion in Alzheimer's disease shown by [18F] FEOBV autoradiography. *International journal of molecular imaging*, *2013*.
- Pascoal, T. A., Mathotaarachchi, S., Mohades, S., Benedet, A. L., Chung, C. O., Shin, M., ... & Rosa-Neto, P. (2017). Amyloid- $\beta$  and hyperphosphorylated tau synergy drives metabolic decline in preclinical Alzheimer's disease. *Molecular psychiatry*, *22*(2), 306-311.
- Patel, R., Stebbins, G., Bernard, B., & Goldman, J. (2017). Hippocampal and entorhinal cortex atrophy across the Parkinson's disease cognitive impairment spectrum (S39. 004). *Neurology*, *88*(16 Supplement), S39-004.
- Pei, J. J., Braak, E., Braak, H., Grundke-Iqbal, I., Iqbal, K., Winblad, B., & Cowburn, R. F. (1999). Distribution of active glycogen synthase kinase 3 $\beta$  (GSK-3 $\beta$ ) in brains staged for Alzheimer disease neurofibrillary changes. *Journal of neuropathology and experimental neurology*, *58*(9), 1010-1019.
- Perrin, R. J., Fagan, A. M., & Holtzman, D. M. (2009). Multimodal techniques for diagnosis and prognosis of Alzheimer's disease. *Nature*, *461*(7266), 916-922.
- Perry, E. K., Tomlinson, B. E., Blessed, G., Bergmann, K., Gibson, P. H., & Perry, R. H. (1978). Correlation of cholinergic abnormalities with senile plaques and mental test scores in senile dementia. *Br Med J*, *2*(6150), 1457-1459.

- Petrou, M., Frey, K. A., Kilbourn, M. R., Scott, P. J., Raffel, D. M., Bohnen, N. I., ... & Koeppe, R. A. (2014). In vivo imaging of human cholinergic nerve terminals with (-)-5-18F-Fluoroethoxybenzovesamicol: Biodistribution, dosimetry, and tracer kinetic analyses. *Journal of Nuclear Medicine*, *55*(3), 396-404.
- Pike, C. J. (2017). Sex and the development of Alzheimer's disease. *Journal of neuroscience research*, *95*(1-2), 671-680.
- Rascovsky, K., Hodges, J. R., Knopman, D., Mendez, M. F., Kramer, J. H., Neuhaus, J., ... & Miller, B. L. (2011). Sensitivity of revised diagnostic criteria for the behavioural variant of frontotemporal dementia. *Brain*, *134*(9), 2456-2477.
- Ravasi, L., Tokugawa, J., Nakayama, T., Seidel, J., Sokoloff, L., Eckelman, W. C., & Kiesewetter, D. O. (2012). Imaging of the muscarinic acetylcholine neuroreceptor in rats with the M2 selective agonist [18F]FP-TZTP. *Nuclear medicine and biology*, *39*(1), 45-55. doi: 10.1016/j.nucmedbio.2011.06.003
- Reed, B. R., Mungas, D. M., Kramer, J. H., Ellis, W., Vinters, H. V., Zarow, C., ... & Chui, H. C. (2007). Profiles of neuropsychological impairment in autopsy-defined Alzheimer's disease and cerebrovascular disease. *Brain*, *130*(3), 731-739.
- Richter, N., Beckers, N., Onur, O. A., Dietlein, M., Tittgemeyer, M., Kracht, L., ... & Kukolja, J. (2018). Effect of cholinergic treatment depends on cholinergic integrity in early Alzheimer's disease. *Brain*, *141*(3), 903-915.
- Richter, N., David, L. S., Grothe, M. J., Teipel, S., Dietlein, M., Tittgemeyer, M., ... & Kukolja, J. (2022). Age and Anterior Basal Forebrain Volume Predict the Cholinergic Deficit in Patients with Mild Cognitive Impairment due to Alzheimer's Disease. *Journal of Alzheimer's Disease*, (Preprint), 1-16.
- Rinne, J. O., Kaasinen, V., Järvenpää, T., Någren, K., Roivainen, A., Yu, M., ... & Kurki, T. (2003). Brain acetylcholinesterase activity in mild cognitive impairment and early Alzheimer's disease. *Journal of Neurology, Neurosurgery & Psychiatry*, *74*(1), 113-115.
- Roch, J. M., Masliah, E., Roch-Levecq, A. C., Sundsmo, M. P., Otero, D. A., Veinbergs, I., & Saitoh, T. (1994). Increase of synaptic density and memory retention by a peptide representing the trophic domain of the amyloid beta/A4 protein precursor. *Proceedings of the National Academy of Sciences*, *91*(16), 7450-7454.
- Rocher, A. B., Chapon, F., Blaizot, X., Baron, J. C., & Chavoix, C. (2003). Resting-state brain glucose utilization as measured by PET is directly related to regional synaptophysin levels: a study in baboons. *Neuroimage*, *20*(3), 1894-1898.
- Rogers, G. A., Stone-Elander, S., Ingvar, M., Eriksson, L., Parsons, S. M., & Widén, L. (1994). 18F-labelled vesamicol derivatives: syntheses and preliminary in vivo small animal positron emission tomography evaluation. *Nuclear medicine and biology*, *21*(2), 219-230.

- Rosa-Neto P, Alliaga A, Mzengeza S, Massarweh G et al. (2007) Imaging vesicular acetylcholine transporter in rodents using [ $^{18}\text{F}$ ]fluoroethoxy-benzovesamicol and microPET; *Journal of Cerebral Blood Flow & Metabolism*; 27, 1S, 3-7M.
- Rowe, C. C., Pejoska, S., Mulligan, R. S., Jones, G., Chan, J. G., Svensson, S., ... & Villemagne, V. L. (2013). Head-to-head comparison of 11C-PiB and 18F-AZD4694 (NAV4694) for  $\beta$ -amyloid imaging in aging and dementia. *Journal of Nuclear Medicine*, 54(6), 880-886.
- Rowe, C. C., & Villemagne, V. L. (2013). Brain amyloid imaging. *Journal of nuclear medicine technology*, 41(1), 11-18.
- Roy, R., Niccolini, F., Pagano, G., & Politis, M. (2016). Cholinergic imaging in dementia spectrum disorders. *European journal of nuclear medicine and molecular imaging*, 43(7), 1376-1386.
- Russchen, F. T., Amaral, D. G., & Price, J. L. (1985). The afferent connections of the substantia innominata in the monkey, *Macaca fascicularis*. *Journal of Comparative Neurology*, 242(1), 1-27.
- Ryu, E. K., & Chen, X. (2008). Development of Alzheimer's disease imaging agents for clinical studies. *Front Biosci*, 13, 777-789.
- Sabri, O., Meyer, P. M., Gräf, S., Hesse, S., Wilke, S., Becker, G. A., ... & Brust, P. (2018). Cognitive correlates of  $\alpha 4\beta 2$  nicotinic acetylcholine receptors in mild Alzheimer's dementia. *Brain*, 141(6), 1840-1854.
- Sahakian, B. J., & Coull, J. T. (1994). Nicotine and tetrahydroaminoacradine: Evidence for improved attention in patients with dementia of the Alzheimer type. *Drug Development Research*, 31(1), 80-88.
- Saint-Aubert, L., Lemoine, L., Chiotis, K., Leuzy, A., Rodriguez-Vieitez, E., & Nordberg, A. (2017). Tau PET imaging: present and future directions. *Molecular neurodegeneration*, 12(1), 1-21.
- Sando, S. B., Melquist, S., Cannon, A., Hutton, M. L., Sletvold, O., Saltvedt, I., ... & Aasly, J. O. (2008). APOE  $\epsilon 4$  lowers age at onset and is a high risk factor for Alzheimer's disease; A case control study from central Norway. *BMC neurology*, 8(1), 1-7.
- Santangelo, R., Masserini, F., Agosta, F., Sala, A., Caminiti, S. P., Cecchetti, G., ... & Filippi, M. (2020). CSF p-tau/A $\beta$ 42 ratio and brain FDG-PET may reliably detect MCI "imminent" converters to AD. *European Journal of Nuclear Medicine and Molecular Imaging*, 47(13), 3152-3164.
- Seo, S. W., Ayakta, N., Grinberg, L. T., Villeneuve, S., Lehmann, M., Reed, B., ... & Rabinovici, G. D. (2017). Regional correlations between [11C] PIB PET and post-mortem burden of amyloid-beta pathology in a diverse neuropathological cohort. *NeuroImage: Clinical*, 13, 130-137.
- Sarter, M., & Bruno, J. P. (1999). Cortical cholinergic inputs mediating arousal, attentional processing and dreaming: differential afferent regulation of the basal forebrain by telencephalic and brainstem afferents. *Neuroscience*, 95(4), 933-952.

- Schaefferbeke, J., Evenepoel, C., Bruffaerts, R., Van Laere, K., Bormans, G., Dries, E., ... & Vandenberghe, R. (2017). Cholinergic depletion and basal forebrain volume in primary progressive aphasia. *Neuroimage: Clinical*, *13*, 271-279.
- Scheff, S. W., Neltner, J. H., & Nelson, P. T. (2014). Is synaptic loss a unique hallmark of Alzheimer's disease?. *Biochemical pharmacology*, *88*(4), 517-528.
- Schliebs, R., & Arendt, T. (2011). The cholinergic system in aging and neuronal degeneration. *Behavioural brain research*, *221*(2), 555-563.
- Schmeichel, A. M., Buchhalter, L. C., Low, P. A., Parisi, J. E., Boeve, B. W., Sandroni, P., & Benarroch, E. E. (2008). Mesopontine cholinergic neuron involvement in Lewy body dementia and multiple system atrophy. *Neurology*, *70*(5), 368-373.
- Schmitz, T. W., & Spreng, R. N. (2016). Basal forebrain degeneration precedes and predicts the cortical spread of Alzheimer's pathology. *Nature communications*, *7*(1), 1-13.
- Schmitz, T. W., Mur, M., Aghourian, M., Bedard, M. A., Spreng, R. N., & Alzheimer's Disease Neuroimaging Initiative. (2018). Longitudinal Alzheimer's degeneration reflects the spatial topography of cholinergic basal forebrain projections. *Cell reports*, *24*(1), 38-46.
- Schmitz, T. W., Soreq, H., Poirier, J., & Spreng, R. N. (2020). Longitudinal Basal Forebrain Degeneration Interacts with TREM2/C3 Biomarkers of Inflammation in Presymptomatic Alzheimer's Disease. *Journal of Neuroscience*, *40*(9), 1931-1942.
- Seeley, W. W., Menon, V., Schatzberg, A. F., Keller, J., Glover, G. H., Kenna, H., ... & Greicius, M. D. (2007). Dissociable intrinsic connectivity networks for salience processing and executive control. *Journal of Neuroscience*, *27*(9), 2349-2356.
- Seo, S. W., Ayakta, N., Grinberg, L. T., Villeneuve, S., Lehmann, M., Reed, B., ... & Rabinovici, G. D. (2017). Regional correlations between [11C] PIB PET and post-mortem burden of amyloid-beta pathology in a diverse neuropathological cohort. *NeuroImage: Clinical*, *13*, 130-137.
- Seshadri, S., Wolf, P. A., Beiser, A., Au, R., McNulty, K., White, R., & D'agostino, R. B. (1997). Lifetime risk of dementia and Alzheimer's disease: the impact of mortality on risk estimates in the Framingham Study. *Neurology*, *49*(6), 1498-1504.
- Shekari, A., & Fahnstock, M. (2019). Retrograde axonal transport of BDNF and proNGF diminishes with age in basal forebrain cholinergic neurons. *Neurobiology of aging*, *84*, 131-140.
- Shiba, K., Ogawa, K., Ishiwata, K., Yajima, K., & Mori, H. (2006). Synthesis and binding affinities of methylvesamicol analogs for the acetylcholine transporter and sigma receptor. *Bioorganic & medicinal chemistry*, *14*(8), 2620-2626. doi: 10.1016/j.bmc.2005.11.044
- Shiba, K., Nishiyama, S., Tsukada, H., Ishiwata, K., Kawamura, K., Ogawa, K., & Mori, H. (2009). The potential of (-)-o-[11C]methylvesamicol for diagnosing cholinergic deficit dementia. *Synapse*, *63*(2), 167-171. doi: 10.1002/syn.20590

- Shinotoh, H., Namba, H., Fukushi, K., Nagatsuka, S. I., Tanaka, N., Aotsuka, A., ... & Irie, T. (2000). Progressive loss of cortical acetylcholinesterase activity in association with cognitive decline in Alzheimer's disease: a positron emission tomography study. *Annals of Neurology: Official Journal of the American Neurological Association and the Child Neurology Society*, 48(2), 194-200.
- Shinotoh, H., Fukushi, K., Nagatsuka, S. I., & Irie, T. (2004). Acetylcholinesterase imaging: its use in therapy evaluation and drug design. *Current pharmaceutical design*, 10(13), 1505-1517.
- Šimić, G., Leko, M. B., Wray, S., Harrington, C. R., Delalle, I., Jovanov-Milošević, N., ... & Hof, P. R. (2017). Monoaminergic neuropathology in Alzheimer's disease. *Progress in neurobiology*, 151, 101-138.
- Sorger, D., Scheunemann, M., Grossmann, U., Fischer, S., Vercouille, J., Hiller, A., . . . Steinbach, J. (2008). A new 18F-labeled fluoroacetylmorpholino derivative of vesamicol for neuroimaging of the vesicular acetylcholine transporter. *Nuclear medicine and biology*, 35(2), 185-195. doi: 10.1016/j.nucmedbio.2007.10.004
- Sorger, D., Scheunemann, M., Vercouillie, J., Grossmann, U., Fischer, S., Hiller, A., . . . Sabri, O. (2009). Neuroimaging of the vesicular acetylcholine transporter by a novel 4-[18F]fluoro-benzoyl derivative of 7-hydroxy-6-(4-phenyl-piperidin-1-yl)-octahydro-benzo[1,4]oxazines. *Nuclear medicine and biology*, 36(1), 17-27. doi: 10.1016/j.nucmedbio.2008.10.006
- Soscia, S. J., Kirby, J. E., Washicosky, K. J., Tucker, S. M., Ingelsson, M., Hyman, B., ... & Moir, R. D. (2010). The Alzheimer's disease-associated amyloid  $\beta$ -protein is an antimicrobial peptide. *PLoS one*, 5(3), e9505.
- Soucy J-P, Rosa-Neto, P, Massarweh G, Aliaga A, et al., (2010) Imaging of cholinergic terminals in the non-human primate brain using 18F-FEOBV PET : Development of a tool to assess cholinergic losses in Alzheimer's disease. *Alzheimer's Disease & Associated Disorders*; 6(1), S-286.
- Sperling, R. A., Aisen, P. S., Beckett, L. A., Bennett, D. A., Craft, S., Fagan, A. M., ... & Phelps, C. H. (2011). Toward defining the preclinical stages of Alzheimer's disease: recommendations from the National Institute on Aging-Alzheimer's Association workgroups on diagnostic guidelines for Alzheimer's disease. *Alzheimer's & dementia*, 7(3), 280-292.
- Stern, Y. (2012). Cognitive reserve in ageing and Alzheimer's disease. *The Lancet Neurology*, 11(11), 1006-1012.
- Stockburger, C., Miano, D., Baeumlisberger, M., Pallas, T., Arrey, T. N., Karas, M., ... & Müller, W. E. (2016). A mitochondrial role of SV2a protein in aging and Alzheimer's disease: studies with levetiracetam. *Journal of Alzheimer's Disease*, 50(1), 201-215.
- Stomrud, E., Minthon, L., Zetterberg, H., Blennow, K., & Hansson, O. (2015). Longitudinal cerebrospinal fluid biomarker measurements in preclinical sporadic Alzheimer's disease: A prospective 9-year study. *Alzheimer's & Dementia: Diagnosis, Assessment & Disease Monitoring*, 1(4), 403-411.
- Stratmann, K., Heinsen, H., Korf, H. W., Del Turco, D., Ghebremedhin, E., Seidel, K., ... & Rüb, U. (2016). Precortical phase of Alzheimer's disease (AD)-related tau cytoskeletal pathology. *Brain pathology*, 26(3), 371-386.



- Strozyk, D., Blennow, K., White, L. R., & Launer, L. J. (2003). CSF A $\beta$  42 levels correlate with amyloid-neuropathology in a population-based autopsy study. *Neurology*, *60*(4), 652-656.
- Sunderland, T., Tariot, P. N., Cohen, R. M., Weingartner, H., Mueller, E. A., & Murphy, D. L. (1987). Anticholinergic sensitivity in patients with dementia of the Alzheimer type and age-matched controls: a dose-response study. *Archives of General Psychiatry*, *44*(5), 418-426.
- Szutowicz, A., Bielarczyk, H., Ronowska, A., Gul-Hinc, S., Klimaszewska-Łata, J., Dyś, A., ... & Pawełczyk, T. (2014). Intracellular redistribution of acetyl-CoA, the pivotal point in differential susceptibility of cholinergic neurons and glial cells to neurodegenerative signals. *Biochemical Society Transactions*, *42*(4), 1101-1106.
- Tan, J. Z. A., & Gleeson, P. A. (2019). The role of membrane trafficking in the processing of amyloid precursor protein and production of amyloid peptides in Alzheimer's disease. *Biochimica et Biophysica Acta (BBA)-Biomembranes*, *1861*(4), 697-712.
- Tanaka, Y., & Bachman, D. L. (2002). Pharmacotherapy of aphasia. In *Neurobehavior of Language and Cognition* (pp. 159-176). Springer, Boston, MA.
- Teipel, S. J., Meindl, T., Grinberg, L., Grothe, M., Cantero, J. L., Reiser, M. F., ... & Hampel, H. (2011). The cholinergic system in mild cognitive impairment and Alzheimer's disease: an in vivo MRI and DTI study. *Human brain mapping*, *32*(9), 1349-1362.
- Teipel, S., Raiser, T., Riedl, L., Riederer, I., Schroeter, M. L., Bisenius, S., ... & FTLDc Study Group. (2016). Atrophy and structural covariance of the cholinergic basal forebrain in primary progressive aphasia. *cortex*, *83*, 124-135. 2018
- Teipel, S. J., Cavado, E., Hampel, H., Grothe, M. J., Alzheimer's Disease Neuroimaging Initiative, & Alzheimer Precision Medicine Initiative. (2018). Basal forebrain volume, but not hippocampal volume, is a predictor of global cognitive decline in patients with Alzheimer's disease treated with cholinesterase inhibitors. *Frontiers in neurology*, *9*, 642.
- Terry, A. V., & Buccafusco, J. J. (2003). The cholinergic hypothesis of age and Alzheimer's disease-related cognitive deficits: recent challenges and their implications for novel drug development. *Journal of Pharmacology and Experimental Therapeutics*, *306*(3), 821-827.
- Thomas, B. A., Erlandsson, K., Modat, M., Thurfjell, L., Vandenberghe, R., Ourselin, S., & Hutton, B. F. (2011). The importance of appropriate partial volume correction for PET quantification in Alzheimer's disease. *European journal of nuclear medicine and molecular imaging*, *38*(6), 1104-1119.
- Tiepolt, S., Patt, M., Aghakhanyan, G., Meyer, P. M., Hesse, S., Barthel, H., & Sabri, O. (2019). Current radiotracers to image neurodegenerative diseases. *EJNMMI radiopharmacy and chemistry*, *4*(1), 1-23.
- Tiepolt, S., Meyer, P. M., Patt, M., Deuther-Conrad, W., Hesse, S., Barthel, H., & Sabri, O. (2022). PET imaging of cholinergic neurotransmission in neurodegenerative disorders. *Journal of Nuclear Medicine*, *63*(Supplement 1), 33S-44S.

- aTiernan, C. T., Mufson, E. J., Kanaan, N. M., & Counts, S. E. (2018). Tau oligomer pathology in nucleus basalis neurons during the progression of Alzheimer disease. *Journal of Neuropathology & Experimental Neurology*, 77(3), 246-259.
- bTiernan, C. T., Ginsberg, S. D., He, B., Ward, S. M., Guillozet-Bongaarts, A. L., Kanaan, N. M., ... & Counts, S. E. (2018). Pretangle pathology within cholinergic nucleus basalis neurons coincides with neurotrophic and neurotransmitter receptor gene dysregulation during the progression of Alzheimer's disease. *Neurobiology of disease*, 117, 125-136.
- van der Zee, S., Müller, M. L., Kanel, P., van Laar, T., & Bohnen, N. I. (2021). Cholinergic denervation patterns across cognitive domains in Parkinson's disease. *Movement Disorders*, 36(3), 642-650.
- van Dort, M. E., Jung, Y. W., Gildersleeve, D. L., Hagen, C. A., Kuhl, D. E., & Wieland, D. M. (1993). Synthesis of the 123I- and 125I-labeled cholinergic nerve marker (-)-5-iodobenzovesamicol. *Nuclear medicine and biology*, 20(8), 929-937.
- van Waarde, A., Marcolini, S., De Deyn, P. P., & Dierckx, R. A. (2021, May). PET agents in dementia: an overview. In *Seminars in Nuclear Medicine* (Vol. 51, No. 3, pp. 196-229). WB Saunders.
- Wang, H., Tan, L., Wang, H. F., Liu, Y., Yin, R. H., Wang, W. Y., ... & Yu, J. T. (2015). Magnetic resonance spectroscopy in Alzheimer's disease: systematic review and meta-analysis. *Journal of Alzheimer's Disease*, 46(4), 1049-1070.
- Wang, L. Y., Shofer, J. B., Rohde, K., Hart, K. L., Hoff, D. J., McFall, Y. H., ... & Peskind, E. R. (2009). Prazosin for the treatment of behavioral symptoms in patients with Alzheimer disease with agitation and aggression. *The American Journal of Geriatric Psychiatry*, 17(9), 744-751.
- Warren, N. M., Piggott, M. A., Perry, E. K., & Burn, D. J. (2005). Cholinergic systems in progressive supranuclear palsy. *Brain*, 128(2), 239-249.
- Warren, N. M., Piggott, M. A., Lees, A. J., & Burn, D. J. (2007). The basal ganglia cholinergic neurochemistry of progressive supranuclear palsy and other neurodegenerative diseases. *Journal of Neurology, Neurosurgery & Psychiatry*, 78(6), 571-575.
- Weintraub, S., Wicklund, A. H., & Salmon, D. P. (2012). The neuropsychological profile of Alzheimer disease. *Cold Spring Harbor perspectives in medicine*, 2(4), a006171.
- Wenzel, B., Deuther-Conrad, W., Scheunemann, M., & Brust, P. (2021). Radioligand development for PET imaging of the vesicular acetylcholine transporter (VACHT) in the brain. In *PET and SPECT of Neurobiological Systems*. Springer, Cham.
- Wernick, M. N., & Aarsvold, J. N. (2004). *Emission tomography: the fundamentals of PET and SPECT*. Elsevier.
- aWestman, E., Simmons, A., Zhang, Y., Muehlboeck, J. S., Tunnard, C., Liu, Y., ... & AddNeuroMed Consortium. (2011). Multivariate analysis of MRI data for Alzheimer's disease, mild cognitive impairment and healthy controls. *Neuroimage*, 54(2), 1178-1187.

- bWestman, E., Wahlund, L. O., Foy, C., Poppe, M., Cooper, A., Murphy, D., ... & Simmons, A. (2011). Magnetic resonance imaging and magnetic resonance spectroscopy for detection of early Alzheimer's disease. *Journal of Alzheimer's Disease*, *26*(s3), 307-319.
- Whitehouse, P. J., Price, D. L., Struble, R. G., Clark, A. W., Coyle, J. T., & Delon, M. R. (1982). Alzheimer's disease and senile dementia: loss of neurons in the basal forebrain. *Science*, *215*(4537), 1237-1239.
- Widen, L., Eriksson, L., Ingvar, M., Parsons, S. M., Rogers, G. A., & Stone-Elander, S. (1992). Positron emission tomographic studies of central cholinergic nerve terminals. *Neurosci Lett*, *136*(1), 1-4.
- Wiley RG. 1992. Neural lesioning with ribosome-inactivating proteins: suicide transport and immunolesioning. *Trends Neurosci*, *15*, 285-90.
- Wortmann, M. (2012). Dementia: a global health priority-highlights from an ADI and World Health Organization report. *Alzheimer's research & therapy*, *4*(5), 1-3.
- Wu, H., Williams, J., & Nathans, J. (2014). Complete morphologies of basal forebrain cholinergic neurons in the mouse. *Elife*, *3*, e02444.
- Xia, Y., Eeles, E., Fripp, J., Pinsker, D., Thomas, P., Latter, M., ... & Rose, S. (2022). Reduced cortical cholinergic innervation measured using [18F]-FEOBV PET imaging correlates with cognitive decline in mild cognitive impairment. *NeuroImage: Clinical*, *34*, 102992.
- Yan, Huanhuan, Pei Pang, Wenqi Chen, Houze Zhu, K. A. Henok, Hao Li, Zuoze Wu et al. "The lesion analysis of cholinergic neurons in 5XFAD mouse model in the three-dimensional level of whole brain." *Molecular neurobiology* 55, no. 5 (2018): 4115-4125.
- Yesavage, J. A., Brink, T. L., Rose, T. L., Lum, O., Huang, V., Adey, M., & Leirer, V. O. (1982). Development and validation of a geriatric depression screening scale: a preliminary report. *Journal of psychiatric research*, *17*(1), 37-49.
- Zhang, W., Arteaga, J., Cashion, D. K., Chen, G., Gangadharmath, U., Gomez, L. F., ... & Kolb, H. C. (2012). A highly selective and specific PET tracer for imaging of tau pathologies. *Journal of Alzheimer's Disease*, *31*(3), 601-612.
- Zhao, L., Mao, Z., Woody, S. K., & Brinton, R. D. (2016). Sex differences in metabolic aging of the brain: insights into female susceptibility to Alzheimer's disease. *Neurobiology of aging*, *42*, 69-79.
- Zimmer, E. R., Leuzy, A., Gauthier, S., & Rosa-Neto, P. (2014). Developments in tau PET imaging. *Canadian Journal of Neurological Sciences*, *41*(5), 547-553.
- Zimmer, E. R., Parent, M. J., Souza, D. G., Leuzy, A., Lecrux, C., Kim, H. I., ... & Rosa-Neto, P. (2017). [18 F] FDG PET signal is driven by astroglial glutamate transport. *Nature neuroscience*, *20*(3), 393-395.